Using Lignin Biomarkers and ^{14}C, of both River DOC and POC, and Permafrost Soils, to Characterize the Impacts of Climate Warming and Permafrost Degradation on the Organic Carbon Budget of the Hudson Bay, Canada.

By

Pamela Godin

A Thesis Submitted to the Faculty of Graduate Studies of

The University of Manitoba

in partial fulfillment of the requirements of the degree of

MASTER OF SCIENCE

Department of Environment and Geography

Centre for Earth Observation Science

University of Manitoba

Winnipeg

Copyright © 2014 by Pamela Godin

Table of Contents

Abstract

This study looks at characterizing the terrigenous OC sources, like permafrost, of POC and DOC through 17 rivers and six soils of the Hudson Bay (HB) using lignin biomarkers, and $\Delta^{14}C$. Our findings show the dominance of the OC flux (89%) from the southwest Hudson Bay Rivers, especially from DOC (93%), shedding light on the sources and fate of OC in HB sediments. With warming, organic cryosols, with high OC content in the Cz horizon, have the potential to release as much as 1.5 gOC/m^2 for every cm increase in active layer depth. The [Ad/Al] ratios, when combined with ^{14}C ages of DOM, show that older SOC is being released in some rivers and is fresher than expected due to its preservation within permafrost. S/V and C/V ratios, are well correlated to latitude in DOM, reflecting the vegetation in their drainage basins and can be used to indicate OC sources.

Acknowledgements

Thank you so very much to Gary Stern and Robie Macdonald, my supervisors, for giving me the opportunity to do research and for their patience, guidance and advice in making this thesis a reality. Thank you to my committee, Peter Outridge and Tee Boon Goh, for their advice throughout my research program and helping to improve the quality of this thesis. A special thanks goes out to Zou Zou Kuzyk for her many hours helping me with the interpretation of lignin reaction products and helping me to create a PCA analysis for my conclusion chapter and the countless other times I have not forgotten. Thank you to my parents for their support of my dreams, financially as well as emotionally, and to Jonathon for giving me the final push to get me through the last few pages.

I would like to thank the crew of the CCGS Amundsen, especially the late Serge Arsenault, who made it possible to reach so many remote locations by helicopter with such a restricted amount of time and fuel. Thank you to Joanne DeLaronde, Joscelyn Bailey, Greg McCullough and Allison MacHutchon for their assistance in the field and back at the Freshwater Institute of Fisheries and Oceans Canada in Winnipeg, Manitoba, Canada. Thanks also to Miguel Goni, Yvan Alleau and Sheanna Steingass of the College of Earth, Ocean, and Atmospheric Sciences (CEOAS) lab at Oregon State University for training and analytical help with bulk measurements, lignin biomarker analysis and prepping samples for NOSAMS. This study was made possible by funding from ArcticNet, a Network Centre of Excellence (http://www.arcticnet.ulaval.ca/).

List of Tables

List of Figures

List of Appendices

Chapter 1: Introduction

1.1 PREAMBLE

It is well documented that the Arctic has undergone significant climatic change over the last several decades (ACIA, 2005; Prowse et al., 2006b). Climate-induced impacts to the cryosphere include rapid warming above the global average, decreased snow cover, permafrost degradation, reduction in sea ice extent and duration as well as an increase in summer and winter precipitation events (Prowse et al., 2006a; Stieglitz et al., 2003; Dery et al., 2005). These changes impact river runoff and freshwater discharge into Arctic coastal regions influencing the release and transport of soil organic carbon (SOC) and sediments from sources such as permafrost (Peterson et al., 2002; Guo et al., 2007). The increase in SOC being released by degrading permafrost will result in more dissolved and particulate organic carbon (DOC, POC) entering into Arctic rivers. With increased warming, the ^{14}C age of OC is expected to increase as old SOC is released from deeper soil horizons as active layer thickness (ALT) increases and soil temperatures warm (Guo et al., 2007; Woo et al, 2008; Margesin, 2009).

The Hudson Bay System, which lies at the southern margin of the Arctic and is strongly affected by its drainage basin, may provide an early indication of how polar ocean systems will be affected by permafrost degradation as seen through change in the influx of organic carbon from land. The Hudson Bay region is projected to respond dramatically to climatic change, especially in its southern latitudes, due to the large terrestrial influence (ACIA, 2005). The composition and age of OC in the dissolved and particulate phase is likely to provide incisive information on current and future OC sources and inputs into the Hudson Bay carbon cycle. This thesis seeks connections

between permafrost SOC and Hudson Bay riverine DOC and POC, using lignin biomarkers and ^{14}C as pathway tracers for carbon released from permafrost sources.

1.1.1 Hudson Bay and Study Area

Hudson Bay is a semi-enclosed bay-estuarine system, located in the most southern extent of the Arctic, and spans 14 degrees latitude of coastline, which includes three provinces, and two territories (Kuzyk et al., 2008). Its mean depth is 125 m with a shoreline ranging from rocky coastal cliffs in the northeast to emergent tidal flats in the southwest. Isostatic rebound, estimated at approximately 1cm/year (Tsuji et al, 2009), strongly influences drainage patterns and the discharge of freshwater into the Bay. This region is unique due to its southern extent while still maintaining a complete annual sea-ice cover, and its large input of freshwater from over 40 Hudson Bay Rivers (HBRs) (Kuzyk et al., 2009). Meteorological forcing from Arctic (AO), North Atlantic (NAO), and Pacific Decadal (PDO) oscillations influence the region creating intra-seasonal and interannual variability in sea level pressure (SLP), which affects regional weather and atmospheric circulation (Carmack et al., 2006; Thompson and Wallace, 2001).

The climate in the Hudson Bay region follows a north to south gradient and dictates the distribution of vegetation, the location of the treeline and permafrost zonation creating a complex biogeographical system (Figure 1.1). Vegetation shifts from Taiga forest in the south to tundra and barren landscape in the north. Permafrost is distributed from continuous in the north and southwest coastline to isolated patches in the south and is influenced by both local and regional factors such as topography, drainage patterns and soil type (Figure 1.2).

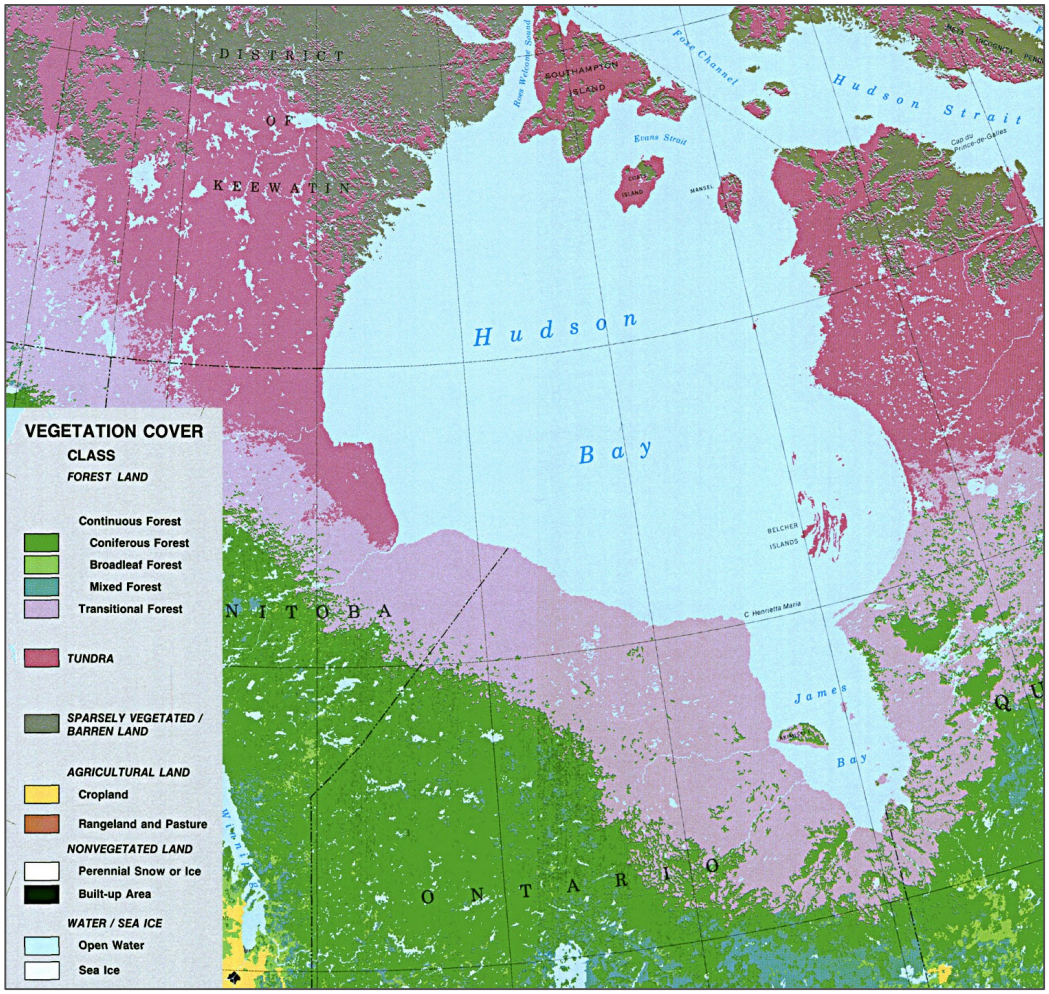

Figure 1.1: Map of the Hudson Bay region and its Vegetation Cover (Natural Resources Canada, 1995).

1.1.2 Freshwater - Marine Coupling in Hudson Bay

Hudson Bay, which is essentially a shallow, coastal shelf sea, holds a large freshwater inventory controlled by river discharge, annual freeze/thaw cycles and direct precipitation/evaporation at the surface (Dery et al., 2010). River inflow dominates freshwater inputs into Hudson Bay carrying with it large amounts of particulate and dissolved materials, much of which are deposited on coastal shelves thence to be redistributed by resuspension and transported by ocean circulation (Kuzyk et al., 2009).

Freshwater discharge is controlled by air temperature, permafrost degradation and thaw, depth and duration of snow cover as well as precipitation events (Dery et al., 2005).

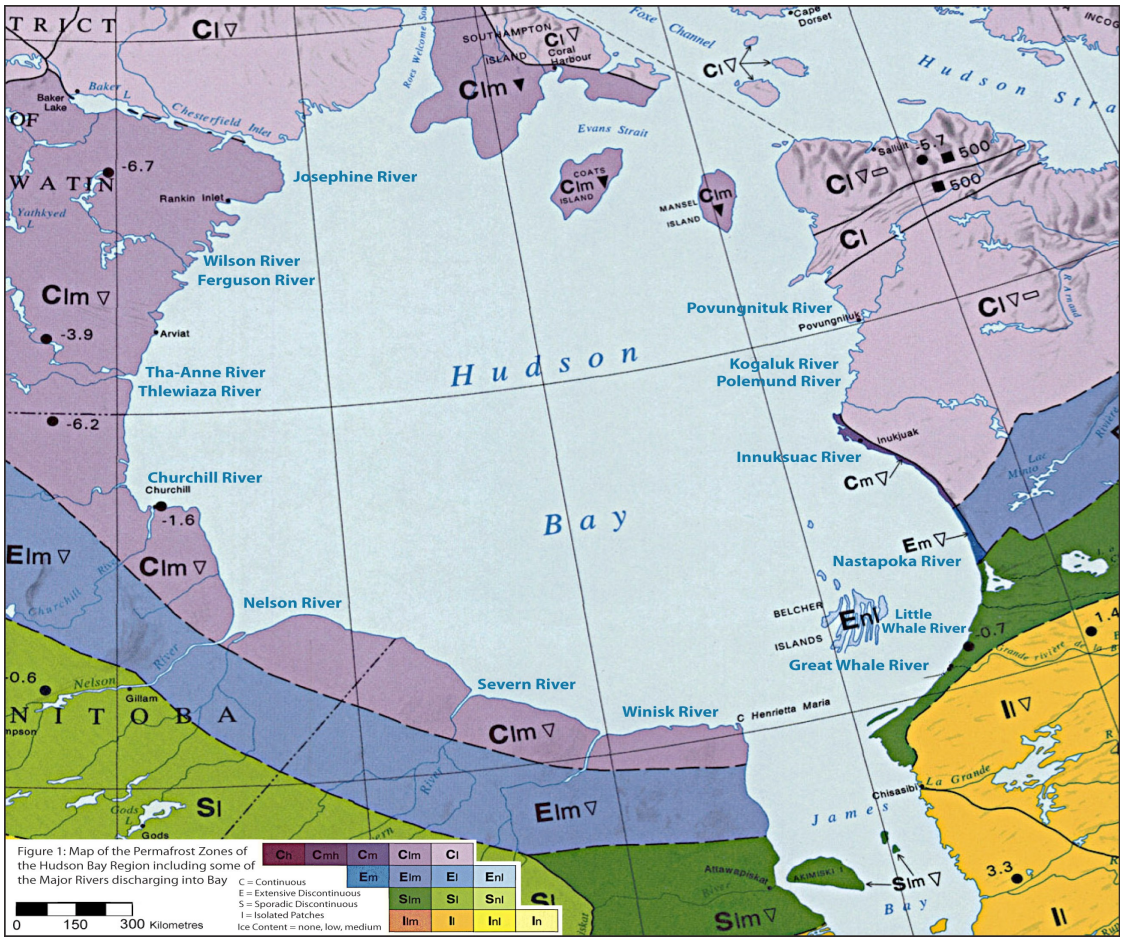

Figure 1.2: Map of the Permafrost Zones of Hudson Bay including names of some of the Major Rivers Discharging into the Bay (Natural Resources Canada, 1995).

River-dominated continental shelves in higher latitudes contribute significantly to the global burial of carbon with the efficient transport of terrigenous material by ice-related processes and high seasonality of discharge leading to increased sedimentation

rates (Goni et al, 2005; Stein and Macdonald, 2004). Freshwater discharge entering Hudson Bay not only affects the upper ocean salinity and sea-ice production, but also has the potential to influence the global thermohaline circulation and the North Atlantic Deep Water Formation (ACIA, 2005; Dery et al., 2005). The freshwater balance in Hudson Bay therefore provides a link between the terrestrial inputs and the downstream marine environment. Understanding the composition and pathways of OC in the marine environment should provide insight into the effect of permafrost degradation on OC cycling within Hudson Bay and, as such, the feedback to the climate system inherent in the release of old, archived carbon.

1.1.3 Terrestrial Organic Carbon Sources in Hudson Bay

The OC in Hudson Bay includes both marine organics produced in the ocean (autochthonous carbon) and carbon supplied from the drainage basin *via* rivers (allochthonous carbon). Terrestrial OC originates from vascular plants, soils, and ancient sedimentary rocks while marine OC is produced by primary productivity. Terrestrial inputs of DOC and POC, transported by freshwater discharge, contribute 8.1% of the global OC flux from rivers to the Arctic Ocean annually (Kuzyk et al., 2008). Recent estimates suggest that annual DOC export from Hudson Bay (~5.1 Tg C $yr^{-}1$) may represent as much as 23% of total riverine DOC export into the Arctic Ocean (Mundy et al., 2010). By quantifying the proportions of both marine and terrestrial OC sources in shelf sediments we are able to further understand the carbon burial efficiency and rate over geologic timescales (Berner, 1989; Drenzek et al., 2007). In the Hudson Bay watershed, the hydrological cycle controls the transport of terrestrial OC from many

sources and also affects the distribution of this OC within Hudson Bay. Projected increases in river runoff, coastal erosion and permafrost thaw will likely increase terrigenous OC fluxes to the coastal sea and potentially also affect sea-ice formation (Guo and Macdonald, 2006).

1.1.4 Permafrost Landscapes, Climate Change and Hudson Bay

Permafrost, or cryosolic soils, which represent approximately 80 percent of the soils contained in the Arctic Ocean drainage basin, are defined as subsurface soil that remains below 0°C for at least two consecutive years (Frey and McClelland, 2009). The seasonal cryogenic cycle and climate impact the distribution of permafrost and its thickness at any given site. There are four permafrost zones in the Hudson Bay drainage basin; continuous (90-100%), discontinuous (50-90%), sporadic (10-50%) and isolated patches (0-10%) that are differentiated by the percentage of areal extent of permafrost (Figure 1.2). Approximately 67% of permafrost has low ice content of less than 10% by volume (Zhang et al., 2008). Thickness of permafrost ranges from as much as 800 m in continuous permafrost to as little as 10 m in isolated permafrost zones.

Permafrost soils are major sinks for carbon accounting for approximately 50 percent of the global below-ground OC pool (Tarnocai et al., 2009). There is estimated to be approximately 1672 Pg of carbon (1 Pg = 10^{15} g = 1 billion tonnes) stored within permafrost and frozen soils worldwide (Tarnocai et al., 2009). Although previous studies have suggested that half of the soil OC pool is found in the top 100 cm (Rodionov et al., 2007; Bockheim and Hinkel, 2007; Tarnocai, 2000), new evidence suggests that only

33% is within the first 100 cm with 44% occurring between 100 and 300 cm and the remainder at even greater depths (Tarnocai et al., 2009). An estimated 88% of this soil OC is found in mid-latitude, perennially frozen soils, which are projected to manifest altered soil thermal regimes with Arctic warming (Tarnocai et al., 2009; Schuur et al., 2011).

Permafrost thaw dynamics are influenced by topography, hydrology at the surface and subsurface, vegetation, soil properties and snow creating a local scale micro-topography, which then affects OC fluxes (Jorgenson et al., 2010). Permafrost degradation is most sensitive to surface water from thermokarst development, ALT, and increased precipitation, all of which impact soil moisture and permafrost hydrology (Schuur et al., 2008; Frey and McClelland, 2009). Precipitation events, such as increased rainfall prior to the onset of winter, earlier snowfall, and increased snow accumulation all impact soil moisture and thermal soil response (Iijima et al., 2010). Surface water has the greatest influence on permafrost thaw by increasing thermal conductivity and near-surface air temperatures by approximately 10°C above the mean annual air temperatures (Hinzman et al., 1997; Jorgenson et al., 2010). Surface water, which has low albedo, is controlled by topography resulting in ice distribution that reflects local relief, especially as it affects hydrological movement and the distribution of surface water both of which will change with warming (Jorgenson et al., 2006). Sandy soils drain more efficiently than silty and organic soils, which retain water and have an increased thermal conductivity (Romanovsky and Osterkamp, 1995).

Permafrost degradation will render deep soil OC pools vulnerable to mobilization making it more available for transport (e.g. via rivers) to coastal shelves such as

Hudson Bay. A study conducted in tundra soils of Siberia in 2008, shows that the greater the initial carbon density in tundra soils the larger the amount of carbon that may be potentially released into the system with warming (Tarnocai et al., 2009; Khvorostyanov et al., 2008). Permafrost in the southwest of Hudson Bay is stable where mean annual air temperatures are at or below -3.5°C, but warming will alter the geographical distribution of this boundary, leading to the conversion of peatlands to fens (Dyck and Sladen, 2010). An increase in fens will reduce the insulating capabilities of surface soils resulting in a reduction in the extent of continuous and discontinuous permafrost (Smith and Burgess, 2004). A shift in atmospheric circulation in the Hudson Bay region due to changes in the AO index, will alter precipitation rates and river discharge further impacting the mobilization of OC in this region (Dery et al., 2005). Therefore, the sensitivity of permafrost in Hudson Bay to degradation depends on not only local scale factors, such as topography and vegetation cover, but also large scale changes in terms of precipitation and atmospheric circulation.

1.2 TRACING OC WITH GEOCHEMICAL, ISOTOPIC DATA AND BIOMARKERS

Measuring contemporary pathways and distribution of OC pools in the Hudson Bay Watershed will provide a baseline against which to assess future change, and also provide a better understanding of pathways likely to be altered by climate change. Change in composition of OC from source to sink may be determined by quantifying and identifying OC in permafrost soils, river DOC and POC, and OC in ocean sediments using bulk measurements (TOC), carbon/nitrogen (C/N) ratios, $\delta^{13}C$ and $\Delta^{14}C$ (Drenzek et al., 2007). Arctic rivers provide direct evidence of the quantity and quality of OC

released from terrigenous systems, especially where radiocarbon and isotopic measurements have been made (Gustafsson et al., 2011). In the marine environment, terrigenous POM may be distinguished from marine POM by its low $\delta^{13}C$ and high C/N ratios although identifying endmembers may prove difficult due to the heterogeneity of POM sources (Kuzyk et al., 2010; Hernes et al., 2007).

Age of the OC provides a way of distinguishing between recently fixed OC (e.g., recent plant litter, marine primary production) and old carbon stored in permafrost. Together, the above bulk measures provide the means to infer OC sources and turnover rates in terrestrial and marine environments. Determining whether or not the OC is old, provides the means to infer apparent storage time for the OC in soil, which then indicates the importance of release of OC from permafrost. Although these sorts of measurements may be made in soils, it is in river POC and DOC that the signal of released carbon is most likely to be found, and differences between these two OC components provide direct insight into the processes leading to migration of soil components into the hydrological cycle (Guo et al., 2007). DOC in measured arctic rivers tends to have young ^{14}C ages, representing vegetative dynamics over the past few centuries, whereas POC is several thousand years old, which definitely signals a dis-equilibrium between DOC and POC and, therefore, a different sensitivity to warming (Guo and Macdonald, 2006; Guo et al., 2007; Raymond et al., 2007). For example, POC samples extracted from five Russian Arctic rivers have shown ^{14}C ages ranging from 8600 to 13,600 years BP, which suggests the release of ancient carbon from frozen reservoirs (Gustafsson et al., 2011). In other more temperate rivers, such as those found on the Oregon Coast, ancient (^{14}C depleted) POC is believed to have been

derived from deep soils and/or bedrock (Hatten et al., 2010). POC in rivers is highly variable and not always ^{14}C depleted as is shown in the Amazon River (Eglinton and Repeta, 2004).

Lignin biomarkers provide an incisive indication of terrigenous vascular plant matter. Specific markers and stable carbon isotopic data have the potential to provide direct evidence of entry points and transport routes for terrestrial OC once it enters coastal and shelf systems (e.g., Kuzyk et al., 2008; Goni et al., 2000). Lignin reaction products from vascular plant tissues have distinct isotopic signatures, which differentiate between C3 and C4 sources and reflect biosynthetic pathways (Goni and Eglinton, 1996; Hedges and Oades, 1997). It has been shown in recent studies that lignin phenol ratios of syringyl/vanillyl (S/V) and cinnamyl/vanillyl (C/V) are well correlated with tundra and taiga vegetative proportions (Tesi et al., 2014; Lobbes et al., 2000). Acid to aldehyde ratios are important diagenetic indicators of terrestrial OM and are used to determine "freshness" of samples (Hernes and Benner, 2006). Lignin biomarker information is enriched by combining it with ^{14}C ages; not only to understand the level of degradation of samples but also to determine where they came from (Amon et el, 2012).

1.2.1 Recent Applications in the Hudson Bay

Lignin biomarkers and stable isotopes ($\delta^{15}N$, $\delta^{13}C$) in dated sediment box cores have been used recently to quantify the sources, transport pathways and sinks of terrigenous OM in Hudson Bay (Kuzyk et al, 2008; 2009). These studies showed a decrease in lignin yields with increasing distance from shore, and a decrease in lignin yields from south to north. High lignin yields (1.46 mg/100mg OC) and increased

sedimentation rates (0.25 g cm^{-2} yr^{-1}) in shallow coastal zones along the southwest inner shelf of Hudson Bay indicated deposition of large amounts of riverine detritus, which then declined toward the interior of Hudson Bay. Kuzyk et al. (2008) proposed that the lignin found in the southern part of HB derived from woody and non-woody tissues, angiosperms and gymnosperms, as indicated by S/V and C/V ratios. These sorts of plants reflect boreal forest and extensive peatland vegetation in the surrounding drainage basin.

Ocean sediments in HB show the effects of hydrodynamic sorting in their POC; terrestrial plant debris is found near river mouths, with the exception of the southwest shelf region where terrestrial POC is found up to 30 km offshore. Lignin concentrations suggest that the fine-grained, mineral-associated fraction of terrigenous carbon is being redistributed to the northeastern part of HB and Hudson Strait within the cyclonic coastal circulation (Saucier et al., 2004; Kuzyk et al., 2008). This distribution of lignin and OC has changed in recent years as is reflected in the sediment record. The northwest of HB is showing increased lignin accumulation rates with an increase in non-woody angiosperm sourced material and less degraded plant material (lower [Ad/Al] ratios) over the past 60 years. The southwest coast is showing increased woody gymnosperm sourced carbon in last 40-50 years along with increased lignin yield and accumulation rates, maybe due to the ice climate of HB, distribution of northern coastal waters, or changes to delivery of terrigenous materials from the Churchill River due to water diversion.

The biomarker data, bulk properties and sedimentation rates were used to produce a budget for marine and terrigenous carbon in Hudson Bay (Kuzyk et al.,

2009). The quantified inputs and outputs of sediment and OC led Kuzyk et al. (2009) to conclude that isostatic rebound in western HB created a large resuspension flux from that coast into the interior basins, a process possibly unique to HB. The Kuzyk et al. (2008, 2009) studies make it clear that further sampling and analysis are required to trace terrestrial OM pathways from their origins in the watershed through their subsequent release and dispersal in Hudson Bay.

1.3 DEVELOPMENT OF THIS STUDY

Mid-latitude changes are already occurring as is evident in the recorded increase in global mean surface air temperatures by 0.2°C to 0.3°C in the last 40 years, with even larger increases occurring between 40 and 70°N (IPCC, 2007; Serreze et al., 2000). From 1975 to 2005, there has been a 1.8°C and 1.1°C increase in temperatures at the circumpolar and mid latitudes respectively (Dzyuba and Zekster, 2011). There is also evidence of decreases in daily surface air temperature variability in winter and increased temperature in summer (Prowse et al., 2009). The Hudson Bay region is considered to be highly sensitive to global warming because it lies at the southern margin of the Arctic, and because it is fed by a large terrigenous drainage basin and is projected to undergo shifts in permafrost distribution and decay. Clearly, changes in the sea-ice and permafrost will have many varied effects on the OC cycle. Feedbacks are projected to occur in terrestrial, marine and biological systems, but due to the complex nature of the overall Arctic system, projected changes are very uncertain. Some responses to global change are already occurring in subarctic permafrost environments of the HB watershed especially in discontinuous permafrost (Camill, 2005; Payette et

al., 2004). These include permafrost degradation from thermal stress, alterations to melt water and runoff as more percolation occurs deeper down the soil profile, and regional and local scale changes to vegetative diversity and composition with the expansion of new species farther north (Prowse et al., 2009).

There is, therefore, the vast potential with climate change to release SOC and in particular older SOC from HB soils with increased rates of permafrost thaw. There are definite information gaps pertaining to the Hudson Bay OC cycle and the interactions between terrestrial and marine systems. Permafrost thaw is poorly understood in this region and more information is required on the rate of thaw, composition of what is being released into HBRs, and the amounts and fluxes of OC and lignin entering Hudson Bay. Monitoring changes to permafrost and river hydrology using ^{14}C ages and SOC biomarkers in rivers and ocean sediments will help to ascertain an understanding of permafrost thaw dynamics and vegetation shifts and their influence on OC pools of the terrestrial and marine environments of Hudson Bay (Gustafsson et al., 2011). The objectives of this thesis are three-fold: to determine how OC and lignin concentrations vary between the HBRs, between the dissolved and particulate phases, and within the permafrost soils and their profiles. Secondly, to determine if permafrost is an important source to the OC budget of HB and if we can trace its effects using lignin biomarkers and ^{14}C ages. Lastly, to provide a baseline for understanding the potential impacts of permafrost degradation on OC storage and transport in order to monitor future change within the HB system.

1.4 REFERENCES

ACIA, 2005. Impacts of a Warming Arctic: Arctic Climate Impact Assessment. Cambridge University Press, Cambridge, NY, 1042 pp.

Amon, R.M.W., Rinehart, A.J., Duan, S., Louchouarn, P., Prokushkin, A., Guggenberger, G., Bauch, D., Stedmon, C., Raymond, P. A., Holmes, R.M., McClelland, J. W., Peterson, B.J., Walker, S.A., Zhulidov, A.V., 2012. Dissolved organic matter sources in large Arctic rivers. *Geochimica et Cosmochimica Acta* 94: 217-237.

Berner, R.A., 1989. Biogeochemical cycles of carbon and sulfur and their effect on atmospheric oxygen over Phanerozoic time. *Palaeogeography, Palaeoclimatology, Palaeoecology (Global and Planetary Change Section)* **75**: 97-122.

Bockheim, J.G. and Hinkel, K.M., 2007. The Importance of "deep" organic carbon in permafrost-affected soils of Arctic Alaska. *Soil Science Society of America Journal* **71**: 1889-1892, doi:10.2136/sssaj2007.0070N.

Camill, P., 2005. Permafrost thaw accelerates in Boreal peatlands during late 20th century climate warming. *Climatic Change* **68:** 135–152.

Carmack, E.C. and Wassman, P., 2006. Food webs and physical-biological coupling on pan-Arctic shelves: Unifying concepts and comprehensive perspectives. *Progress in Oceanography* **71**: 446-477.

Dery, S.J., Stieglitz, M., McKenna, E.C. and Wood, E.F., 2005. Characteristics and trends of river discharge into Hudson, James, and Ungava Bays, 1964-2000. *Journal of Climate* **18**: 2540-2557.

Dery, S.J., Mlynowski, T.J., Hernández-Henríquez, M.A., and Straneo, F., 2010. Variability and trends in streamflow input to Hudson Bay. *Geophysical Research Abstracts* **12**: EGU2010-2256.

Drenzek, N.J., Montluçon, D.B., Yunker, M.B., Macdonald, R.W. and Eglinton, T.I., 2007. Constraints on the origin of sedimentary organic carbon in the Beaufort Sea from coupled molecular ^{13}C and ^{14}C measurements. *Marine Chemistry* **103**: 146–162, doi:10.1016/j.marchem.2006.06.017.

Dyke, L.D., and Sladen, W.E., 2010. Permafrost and Peatland Evolution in the Northern Hudson Bay Lowland, Manitoba. *Arctic* **63** (4): 429 – 441.

Dzyuba, A.V. and Zektser, I.S., 2011. Relationships between groundwater in permafrost zone and climate changes. *Water Resources* **38 (**1): 29–38. doi:10.1134/S0097807811010027.

Eglinton, T.I. and D.J. Repeta, 2004. Sediment diagenesis and benthic flux, pp145-180 in: Holland, H.D., Turekian, K.K. (Eds.), *The Oceans and Marine Geochemistry* (ed. H. Elderfield). Elsevier-Pergamon, Oxford.

Frey, K.E. and McClelland, J.W., 2009. Impacts of permafrost degradation on arctic river biogeochemistry. *Hydrological Processes* **23**: 169–182, doi:10.1002/hyp.7196.

Goni, M.A. and Eglinton, T.I., 1996. Stable carbon isotopic analyses of lignin-derived CuO oxidation products by isotope ratio monitoring-gas chromatography-mass spectrometry (irm-GC-MS). *Organic Geochemistry* **24** (6/7): 601-615.

Goni, M.A., Yunker, M.B., Macdonald, R.W. and Eglinton, T.I., 2000. Distribution and sources of organic biomarkers in arctic sediments from the Mackenzie River and Beaufort Shelf. *Marine Chemistry* **71**: 23–51.

Goni, M.A., Yunker, M.B., Macdonald, R.W. and Eglinton, T.I., 2005. The supply and preservation of ancient and modern components of organic carbon in the Canadian Beaufort Shelf of the Arctic Ocean. *Marine Chemistry* **93**: 53–73.

Goryachkin, S.V., Karavaeva, N.A., Targulian, V.O. and Glazov, M.V., 1999. Arctic Soils: Spatial Distribution, Zonality and Transformation due to Global Change. *Permafrost Periglacial Processes* **10**: 235-250.

Guo, L. and Macdonald, R.W., 2006. Source and transport of terrigenous organic matter in the upper Yukon River: Evidence from isotope ($D^{13}C$, $\Delta^{14}C$, and $\delta^{15}N$) composition of dissolved, colloidal, and particulate phases. *Global Biogeochemical Cycles* **20**: GB2011, doi:10.1029/2005GB002593.

Guo, L., Ping, C. and Macdonald, R.W., 2007. Mobilization pathways of organic carbon from permafrost to arctic rivers in a changing climate. *Geophysical Research Letters* **34**: L13603, doi:10.1029/2007GL030689.

Gustafsson, O., van Dongen, B.E., Vonk, J.E., Dudarev, O.V. and Semiletov, I.P., 2011. Widespread release of old carbon across the Siberian Arctic echoed by its large rivers. *Biogeosciences* **8**: 1737–1743, doi:10.5194/bg-8-1737-2011.

Hatten, J.A., Goni, M.A. and Wheatcroft, R.A., 2010. Chemical characteristics of particulate organic matter from a small, mountainous river system in the Oregon Coast Range, USA. *Biogeochemistry* **107**: 43-66. doi: 10.1007/s10533-010-9529-z.

Hedges, J.I. and Oades, J.M., 1997. Comparative organic geochemistries of soils and marine sediments. *Organic Geochemistry* **27** (7/8): 319-361.

Hernes, P.J., and Benner, R., 2006. Terrigenous organic matter sources and reactivity in the North Atlantic Ocean and a comparison to the Arctic and Pacific oceans. *Marine Chemistry* 100: 66-79. doi:10.1016/j.marchem.2005.11.003.

Hernes, P.J., Robinson, A.C., and Aufdenkampe, A.K. 2007. Fractionation of lignin during leaching and sorption and implications for organic matter 'freshness." *Geophysical Research Letters* **34**: L17401, doi:10.1029/2007GL031017.

Hinzman, L.D., Goering, D.J., Kinney, T.C., and Li, S., 1997. Numeric simulation of thermokarst formation during disturbance. *In Disturbance and recovery in Arctic lands: an ecological perspective*. Kluwer Academic Publishers, Dordrecht, The Netherlands.

Iijima, Y., Fedorov, A.N., Park, H., Suzuki, K., Yabuki, H., Maximov, T.C. and Ohata, T., 2010. Abrupt increases in soil temperatures following increased precipitation in a permafrost region, Central Lena River Basin, Russia. *Permafrost and Periglacial Processes* **21**: 30–41, doi:10.1002/ppp.662.

IPCC, 2007. Technical Summary, *Climate Change 2007: The Physical Science Basis. Contribution of Working Group I to the Fourth Assessment Report of the Intergovernmental Panel on Climate Change*. Solomon, S., Qin, D.M., Manning, Z., et al., Cambridge, N.Y: Cambridge University Press, 2007.

Jorgenson, M.T., Shur, Y.L. and Pullman, E.R., 2006. Abrupt increase in permafrost degradation in Arctic Alaska. *Geophysical Research Letters* **33**: L02503. doi:10.1029/2005GL024960.

Jorgenson, M.T., Romanovsky, V., Harden, J., Shur, Y., O'Donnell, J., Schuur, E.A.G., Kanevskiy, M. and Marchenko, S., 2010. Resilience and vulnerability of permafrost to climate change. *Canadian Journal of Forest Research* **40**: 1219–1236, doi:10.1139/X10- 060.

Khvorostyanov, D.V., Ciais, P., Krinner, G., Zimov, S.A., Corradi, C. and Guggenberger, G., 2008. Vulnerability of permafrost carbon to global warming. Part II: sensitivity of permafrost carbon stock to global warming. *Tellus* **60**B: 265–275, doi:10.1111/j.1600- 0889.2007.00336.x.

Kuzyk, Z.A., Goni, M.A., Stern, G.A. and Macdonald, R.W., 2008. Sources, pathways and sinks of particulate organic matter in Hudson Bay: Evidence from lignin distributions. *Marine Chemistry* **112**: doi:10.1016/j.marchem.2008.08.001.

Kuzyk, Z.A., Macdonald, R.W., Johannessen, S.C., Gobeil, C. and Stern, G.A., 2009. Towards a sediment and organic carbon budget for Hudson Bay. *Marine Geology* **264**: 190-208. doi:10.1016/j.margeo.2009.05.006

Kuzyk, Z.A., Macdonald, R.W., Tremblay, J. and Stern, G.A., 2010. Elemental and stable isotopic constraints on river influence and patterns of nitrogen cycling and biological productivity in Hudson Bay. *Continental Shelf Research* **30**: 163–176. doi:10.1016/j.csr.2009.10.014.

Lobbes, J.M., Fitznar, H.P. and Kattner, G., 2000. Biogeochemical characteristics of dissolved and particulate organic matter in Russian rivers entering the Arctic Ocean. *Geochimica et Cosmochimica Acta* **64** (17): 2973–2983.

Margesin, R., 2009. *Permafrost Soils*. Volume 16, Springer, Berlin. doi:10.1007/978-3-540-69371-0. 322 pp.

Mundy, C.-J., Gosselin, M., Starr, M., and Michel, C., 2010. Riverine export and the effects of circulation on dissolved organic carbon in the Hudson Bay system, Canada. *Limnology and Oceanography* **55** (1): 315-323.

Natural Resources Canada, 1995. The Atlas of Canada – 5th Edition National Atlas of Canada. Government of Canada, Canada Centre for Remote Sensing, GeoAccess Division; Ottawa, Ontario. http://apps1.gdr.nrcan.gc.ca/mirage/full_result_e.php?id=205314.

Payette, S., Delwaide, A., Caccianiga, M. and Beauchemin, M., 2004. Accelerated thawing of subarctic peatland permafrost over the last 50 years. *Geophysical Research Letters* **31**: L18208, doi:10.1029/2004GL020358.

Peterson, B.J., Holmes, R.M., McClelland, J.W., Vorosmarty, C.J., Lammers, R.B., Shiklomanov, A.I., Shiklomanov, I.A. and Rahmstorf, S., 2002. Increasing river discharge to the Arctic Ocean. *Science* **298**: 2171–2173.

Prowse, T.D., Wrona, F.J., Reist, J.D., Hobbie, J.E., Levesque, L.M.J., Vincent, W.F., 2006a. General features of the Arctic relevant to climate change in freshwater ecosystems. *Ambio* **35**(7): 330–338.

Prowse, T.D., Wrona, F.J., Reist, J.D., Gibson, J.J., Hobbie, J.E., Levesque, L.M.J. and Vincent, W.F., 2006b. Climate change effects on hydroecology of Arctic freshwater ecosystems. *Ambio* **35**(7): 347–358.

Prowse, T.D., Furgal, C., Wrona, F.J., and Reist, J.D., 2009. Implications of climate change for northern Canada: Freshwater, marine, and terrestrial ecosystems. *Ambio* **38** (5): 282-289. doi: 10.1579/0044-7447-38.5.282

Raymond, P.A., McClelland, J.W., Holmes, R.M., Zhulidov, A.V., Mull, K., Peterson, B.J., Striegl, R.G., Aiken, G.R. and Gurtovaya, T.Y., 2007. Flux and age of dissolved organic carbon exported to the Arctic Ocean: A carbon isotopic study of the five largest arctic rivers. *Global Biogeochemical Cycles* **21**: GB4011, doi:10.1029/2007GB002934.

Rodionov, A., Flessa, H., Grabe, M., Kazansky, O.A., Shibistova, O. and Guggenberger, G., 2007. Organic carbon and total nitrogen variability in permafrost-affected soils in a forest tundra ecotone. *European Journal of Soil Science* **58**: 1260–1272. doi: 10.1111/j.1365-2389.2007.00919.x.

Romanovsky, V. E. and Osterkamp, T. E., 1995. Interannual variations of the thermal regime of the active layer and near-surface permafrost in Northern Alaska. *Permafrost and Periglacial Processes*, 6(4): 313-335.

Sánchez-García, L., Alling, V., Pugach, S., Vonk, J., van Dongen, B., Humborg, C., Dudarev, O., Semiletov, I. and Gustafsson, O., 2011. Inventories and behavior of particulate organic carbon in the Laptev and East Siberian seas. *Global Biogeochemical Cycles* **25**: GB2007, doi:10.1029/2010GB003862.

Saucier, F., Senneville, S., Prinsenberg, S., Roy, F., Smith, G., Gachon, P., Caya, D., Laprise, R., 2004. Modelling the sea ice–ocean seasonal cycle in Hudson Bay, Foxe Basin and Hudson Strait, Canada. *Climate Dynamics* **23**: 303–326.

Schuur, E.A.G., Bockheim, J., Canadell, J.G., Euskirchen, E., Field, C.B., Goryachkin, S.V., Hagemann, S., Kuhry, P., Lafleur, P.M., Lee, H., Mazhitova, G., Nelson, F.E., Rinke, A., Romanovsky, V.E., Shiklomanov, N., Tarnocai, C., Venevsky, S., Vogel, J.G. and Zimov, S.A., 2008. Vulnerability of permafrost carbon to climate change: Implications for the global carbon cycle. *BioScience* **58** (8): 701-714, doi: 10.1641/B580807.

Schuur, E.A.G., Vogel, J.G., Crummer, K.G., Lee, H., Sickman, J.O. and T. E. Osterkamp, T.E., 2009. The effect of permafrost thaw on old carbon release and net carbon exchange from tundra. *Nature* **459**: 556-559, doi:10.1038/nature08031.

Schuur, E.A.G., Abbott, B., Koven, C.D., Riley, W.J., Subin, Z.M., 2011. High risk of permafrost thaw. *Nature* **480**: 32-33. doi: 10.1038/480032a

Serreze, M.C., Walsh, J.E., Chapin III, F.S., Osterkamp, T., Dyurgerov, M., Romanovsky, V., Oechel, W.C., Morison, J., Zhang, T. and Barry, R.G., 2000. Observational evidence of recent change in the northern high-latitude environment. *Climatic Change* **46**: 159–207.

Smith, S.L. and Burgess, M.M., 2004. *Sensitivity of permafrost to climate warming in Canada*. Geological Survey of Canada, Bulletin 579: 24 pp.

Stein, R. and Macdonald, R.W. (Eds.) 2004, XIX. *The Organic Carbon Cycle in the Arctic Ocean*. Berlin, Heidelberg, New York: Springer-Verlag.382 pp.

Stieglitz, M., Dery, S.J., Romanovsky, V.E. and Osterkamp, T.E., 2003. The role of snow cover in the warming of arctic permafrost. *Geophysical Research*

Letters **30** (13): 1721, doi:10.1029/2003GL017337.

Tarnocai, C., 2000. Carbon pools in soils of the arctic, subarctic, and boreal regions of Canada. p. 91–103. *In* R. Lal et al. (ed.) *Global climate change and cold regions ecosystems*. Lewis Publications, Boca Raton, FL.
Tarnocai, C., Canadell, J.G., Schuur, E.A.G., Kuhry, P., Mazhitova, G. and Simov, S., 2009. Soil organic carbon pools in the northern circumpolar permafrost region. *Global Biogeochemical Cycles* **23**: GB2023, doi:10.1029/2008GB003327.

Tesi, T., Semiletov, I., Hugelius, G., Dudarev, O., Kuhry, P., and Gustafsson, O., 2014. Composition and fate of terrigenous organic matter along the Arctic land–ocean continuum in East Siberia: Insights from biomarkers and carbon isotopes. *Geochimica et Cosmochimica Acta* 133: 235-256.

Thompson, D.W.J. and Wallace, J.M., 2001. Regional climate impacts of the Northern Hemisphere Annular Mode. *Science* **293**: 85-89.

Tsuji, L.J.S., Gomez, N., Mitrovica, J.X., and Kendall, R., 2009. Post-glacial isostatic adjustment and global warming in subarctic Canada: implications for islands of the James Bay Region. *Arctic* **62** (4): 458 – 467.

Woo, M., Kane, D.L., Carey, S.K. and Yang, D., 2008. Progress in permafrost hydrology in the new millennium. *Permafrost and Periglacial Processes* **19**: 237–254, doi:10.1002/ppp.613.

Zhang, T., Barry, R.G., Knowles, K., Heginbottom, J.A. and Brown, J., 2008. Statistics and characteristics of permafrost and ground-ice distribution in the Northern Hemisphere. *Polar Geography* **31**(1-2): 47-68. http://dx.doi.org/10.1080/108893708021758.

Chapter 2: Tracing the terrigenous sources of POC and DOC in the Rivers of Hudson Bay using lignin biomarkers, $\delta^{13}C$ and $\Delta^{14}C$

2.1 INTRODUCTION

Permafrost degradation under a changing climate plays an important role in the global OC cycle. Recent estimates suggest that up to 1024 petagrams (Pg, 10^{15}g, 1 billion tonnes) of OC are stored in the upper 300 cm of northern circumpolar soils with almost half in the upper 100 cm (Tarnocai et al, 2009). In some areas of Hudson Bay, rapid permafrost thaw has already been documented with a 69% decrease in permafrost extent between 1957 and 2003 (Frey and McClelland, 2009; Payette et al, 2004). The age of dissolved organic carbon (DOC) entering rivers increases as old soil organic carbon (SOC) is released from deeper soil horizons as active layer thickness (ALT) increases and soil temperatures warm (Guo et al., 2007; Margesin, 2009; Peterson et al, 2002). Between 1985 and 2004, the mobilization of terrestrial ancient carbon in other studied northern rivers has increased by 3 to 6% signaling that the degradation of permafrost is beginning to release old SOC (Feng et al, 2013). It is important to understand not only the age and lability of materials entering Arctic coastal shelves as a measure of change in permafrost regimes but, we also need more extensive regional and local studies to analyze the sensitivity of the Arctic OC cycle to change and the impacts on the terrestrial-marine Arctic system (Frey and McClelland, 2009; McGuire et al, 2009).

Hudson Bay provides a suitable experimental system for investigating the interacting climatic, cryospheric, vegetational and hydrological causes of changes in terrestrial – marine OC biogeochemistry, and for predicting future changes under a warming climate. The Hudson Bay watershed has over 40 rivers representing different

combinations of vegetative communities, permafrost regimes and climatic zones (Dery and Wood, 2004). The amounts of riverine DOC entering Hudson Bay has been estimated at 5.5 teragrams (Tg, 10^{12} g, 1 million tonnes) of C annually representing 23% of all riverine OC draining into the Arctic Ocean making it an important contribution to terrigenous OC entering the Arctic system (Mundy et al, 2010). In this study we present results on terrestrial transport of OC and its sources for 17 Hudson Bay Rivers (HBRs) and show compositional and concentration differences between DOC and POC using lignin reaction product ratios and ^{14}C. Measurement of DOC and POC river

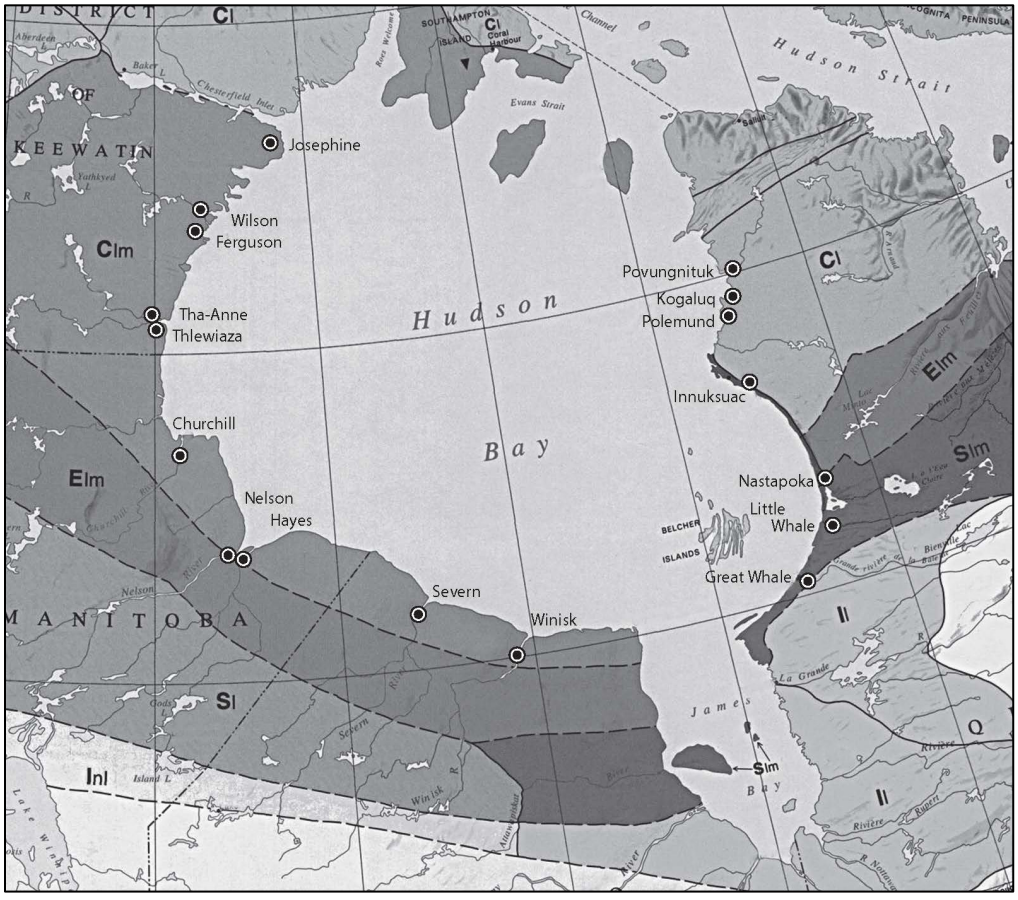

Figure 2.1: Map of Hudson Bay showing sample locations for 17 HBRs and permafrost zonation; Continuous (C), Extensive Discontinuous (E), Sporadic (S) and Isolated Patches (I). Adapted from Natural Resources Canada, 1995).

concentrations, in conjunction with analysis of lignin composition and ^{14}C, provides us with opportunity to better understand terrigenous sources and the role of permafrost degradation in the global OC cycle.

2.2 METHODS

2.2.1 Sample Collection

Samples were collected from the Hudson Bay region in July and August 2010 as part of the Arcticnet-funded CCGS Amundsen expedition. During this cruise, dissolved and particulate samples were collected from freshwater upstream of where 15 major rivers enter the Hudson Bay watershed (Figure 2.1, Table 2.1, Appendix A). These sites were located around the entire Bay and included rivers from differing vegetative, permafrost and latitudinal locations. The Nelson and Hayes River samples were collected during a similar Amundsen cruise in 2005 (Kuzyk et al, 2009; 2008).

2.2.1.1 Dissolved and Suspended Matter

Total suspended solid (TSS) samples were collected from river water using a submersible pump connected by piping to a stainless steel filter holder containing two 142mm GF/F glass fiber filters. The filtered water was collected in 20L collapsible jugs and returned to the ship and filtered again using 47mm GF/Fs. While onboard the Amundsen filters were stored frozen in a freezer at -20°C and the filtrate in a cold room. At the end of the cruise these samples were shipped back to the Freshwater Institute (FWI) in Winnipeg for further processing. Filtered water samples were freeze-dried to isolate the dissolved materials and then weighed. The weight was divided by the volume

of the sample to obtain an estimate of Total Dissolved Solids (TDS, mg/L). TSS weights (mg) were determined by subtracting the average weight of 20 oven-dried GF/F filters (0.0995 ±0.0029 mg) from the weight of the oven-dried sample filter. Concentrations (mg/L) were determined by dividing the total sample weight by the volume of water filtered. Annual flux of OC and lignin was calculated by converting discharge to L/year, multiplying by mg/L, and then converting to Gg/year (1 Gg = 10^9 g). Calculations are presented in Table 2.2 (Appendix A).

2.2.2 Laboratory Analyses

All biomarker analyses of these samples were conducted at the College of Earth, Ocean, and Atmospheric Sciences laboratory at Oregon State University. All samples were analyzed for Total Organic Carbon content (%TOC) and Total Nitrogen (TN) using a NC2500 Elemental Analyzer. Sub-samples were weighed out on a micro scale into silver coated tin boats after which they were exposed to HCl vapor for 24 hours to remove carbonates. %TOC was then used to estimate the amount of lignin in the sample prior to GC/MS analysis. Blank values averaged 2% of the measured values.

Samples were analyzed for lignin-derived phenols and non-lignin by-products such as 3,5-dihydroxybenzoic acid. As previously described, the samples were digested using the microwave/alkaline CuO oxidation method (Kuzyk et al, 2008; Goni and Hedges, 1992). Following oxidation, recovery standards of ethyl vanillin and trans-cinnamic acid were added and samples were centrifuged to separate out any remaining solids. The remaining aqueous product was then acidified to a pH of 1 and extracted twice using ethyl acetate. Extracts were dried under N_2, dissolved in pyridine and then

derivatized using bistrimethylsilyl trifluoroacetamide (BSTFA) and 1% trimethylchlorosilane (TMCS) for 30 minutes at 60 degrees Celsius. Samples were run on the HP6890 Series GC System with DB1 column and the HP5973 Mass Selective Detector. Selective ion monitoring provided quantitative and qualitative fractions of 100 individual CuO products with detection limits of lignin-derived phenols at <10 ng per g sediment (Kuzyk et al., 2008; Goni et al., 2013). Typical precisions for the measurement of individual lignin phenols range from 5-12% of the measured value. Recoveries of individual lignin phenols from spiked matrix samples (n=38) averaged 61% (±11%).

Eight reaction products derived from lignin were measured; the Vanillyl (V-series) phenols, (vanillin, acetovanillone, vanillic acid), syringyl (S-series) phenols (syringaldehyde, acetosyringone, syringic acid), and cinnamyl (C-series) phenols (p-coumaric acid, ferulic acid). Lignin yields were obtained in units of μg/g dry OM and were then converted to units of μgL^{-1} based on the amount of water sample collected and filtered (Table 2.3, Appendix A). For each water sample, dissolved and particulate phase, lignin compositional ratios were calculated using syringyl to vanillyl (S/V), cinnamyl to vanillyl (C/V). Acid to Aldehyde ratios were calculated using the acidic to aldehydic functional groups for vanillyl ([Ad/Al]v) and syringyl ([Ad/Al]s) reaction products and used to determine oxidative lignin degradation associated with the terrestrial environment (Kuzyk et al, 2008; Goni et al 1993).

Stable ($\delta^{13}C$) and radiocarbon analyses ($\Delta^{14}C$) were completed on eight DOC samples (Table 2.2, Appendix A) representing an even distribution across permafrost and vegetation zones on both east and west sides of Hudson Bay. Four rivers were selected each from the east (Povungnituk, Innuksuac, Nastapoka and Little Whale) and

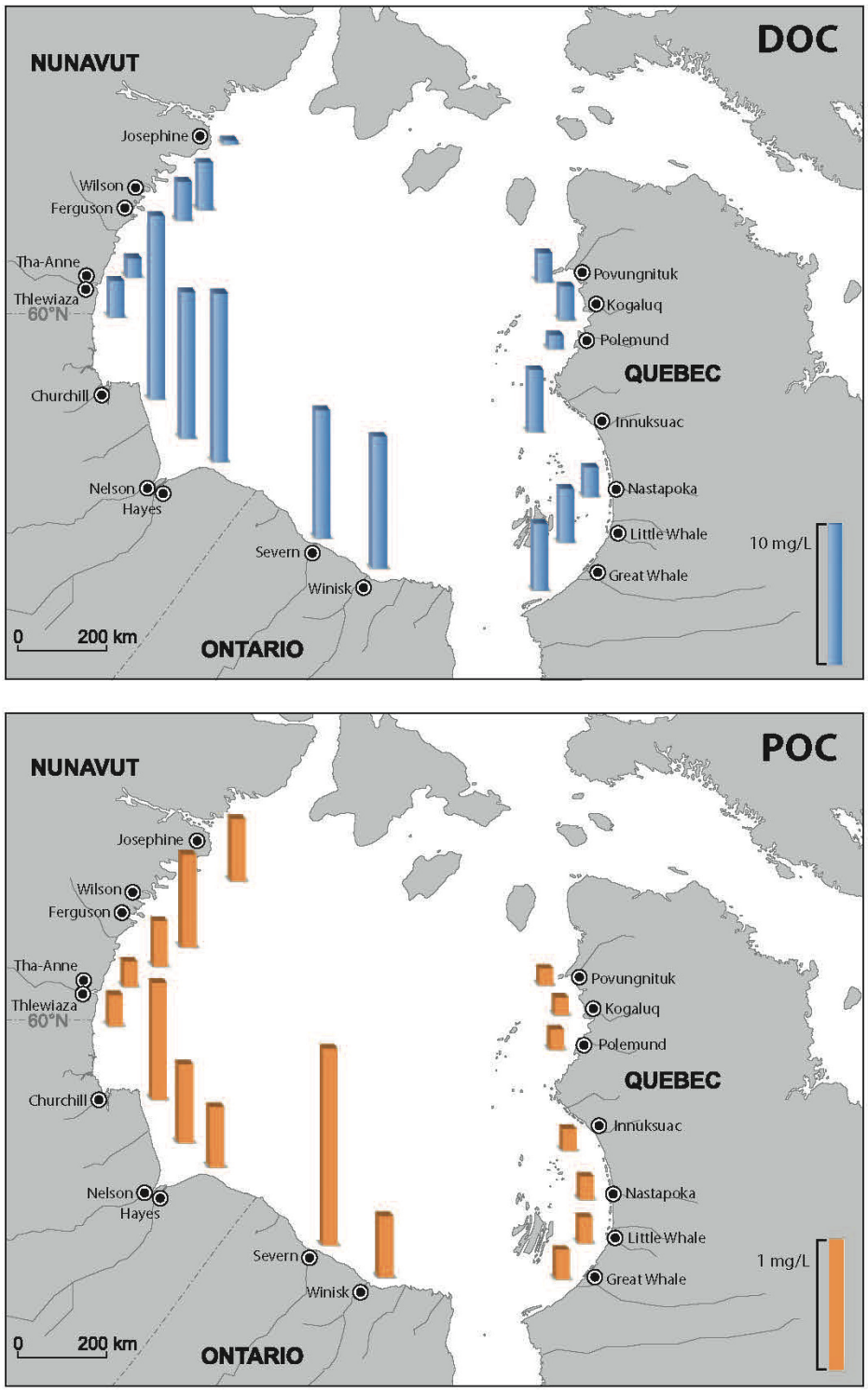

Figure 2.2: Concentration Map of Organic Carbon (mg/L) for 17 HBRs for both Dissolved (blue) and Particulate (orange) Phases.

west (Josephine, Thlewiaza, Churchill and Winisk). The samples were pre-acidified and analyzed at the National Ocean Science Accelerator Mass Spectrometry (NOSAMS) facility at Woods Hole Oceanographic Institution (Vogel et al, 1987; Goni et al., 2013). Radiocarbon ages were not corrected to calendar years based on NOSAMS procedures and modern samples represent post-1950 (>Modern). Errors expressed as fraction of modern ranged from 0.0024 to 0.0035. These errors represent ^{14}C age errors of 20 to 40 years. Particulate samples were not analyzed due to complications with the GF/Fs and their inability to be processed using the methods at NOSAMS.

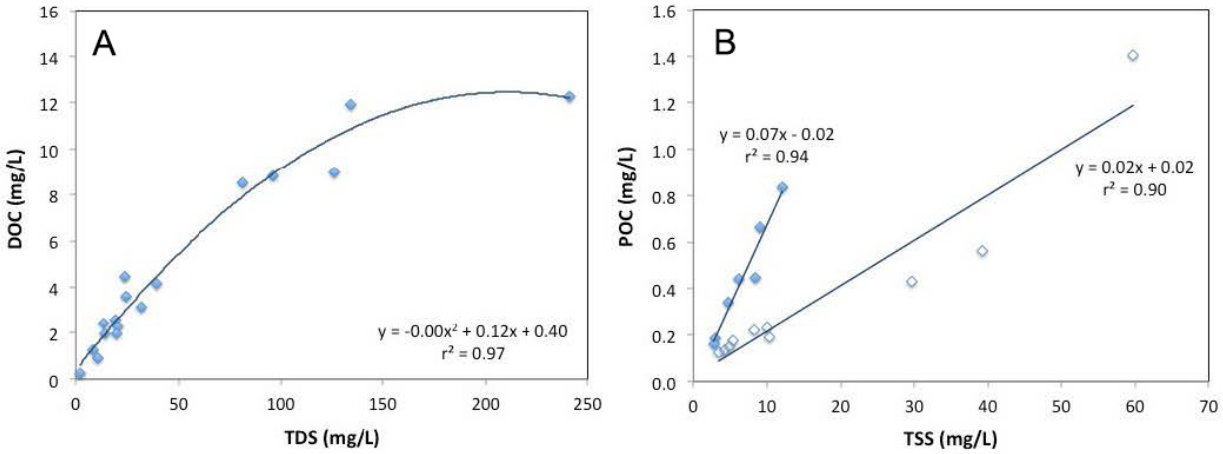

Figure 2.3: Relationship of river sample phases and organic carbon for A) total dissolved solids (TDS) and DOC (mg/L) B) total suspended solids (TSS) and POC (mg/L). *Note differences in scale.

2.3 RESULTS

2.3.1 Dissolved and Suspended Particulate Matter

Concentrations of POC and DOC ranged from 0.13 to 1.41 mg/L and 0.24 to 12.25 mg/L, respectively (Figure 2.2; Table 2.2 in Appendix A). POC and DOC concentrations were weakly correlated with each other (r^2 = 0.35, p = 0.013) and

exhibited the same general spatial pattern, with two- to three-fold higher values in the west than in the east and particularly high values in the southwest. Among the southwest rivers, which include the Churchill, Hayes, Nelson, Severn and Winisk Rivers, POC and DOC concentrations averaged 0.7 and 10 mg/L, respectively, compared to 0.2 and 2.8 mg/L in the eastern HBRs.

Much of the variability in DOC concentrations may be explained by variation in TDS (r^2 = 0.97, p= <0.0001, Figure 2.3A). The southwestern rivers had TDS concentrations greater than 80 mg/L and as high as 241 mg/L (Churchill River), whereas all other rivers had concentrations less than 40 mg/L and DOC concentration did not exceed 12.5 mg/L. Correspondingly, much of the variability in POC may also be explained by variation in TSS with the southwest HBRs having concentrations above 12 mg/L and all other HBRs below 11 mg/L. There appear to be two strong and distinct TSS-POC relationships among the river samples (Figure 2.3B), reflecting relatively high proportions of POC (5-8% of TSS) with TSS concentrations below 12 mg/L in one group of HBRs, including the Churchill and Winisk from the southwest (r^2 = 0.94, p = 0.0002; Table 2.2). The second group reflects relatively low proportions of POC (1-4% of TSS) and includes the other three southwest HBRs, Hayes, Nelson and Severn (r^2 = 0.90, p < 0.0001). DOC does not reflect the same relationship with TDS although the five southwest HBRs have lower proportions of DOC (5-11% of TDS) compared to the remaining rivers on the west coast (10-19% of TDS).

2.3.2 Lignin concentrations and reaction product ratios

Total dissolved and particulate phase lignin concentrations (Σ8 µg/L) are listed in

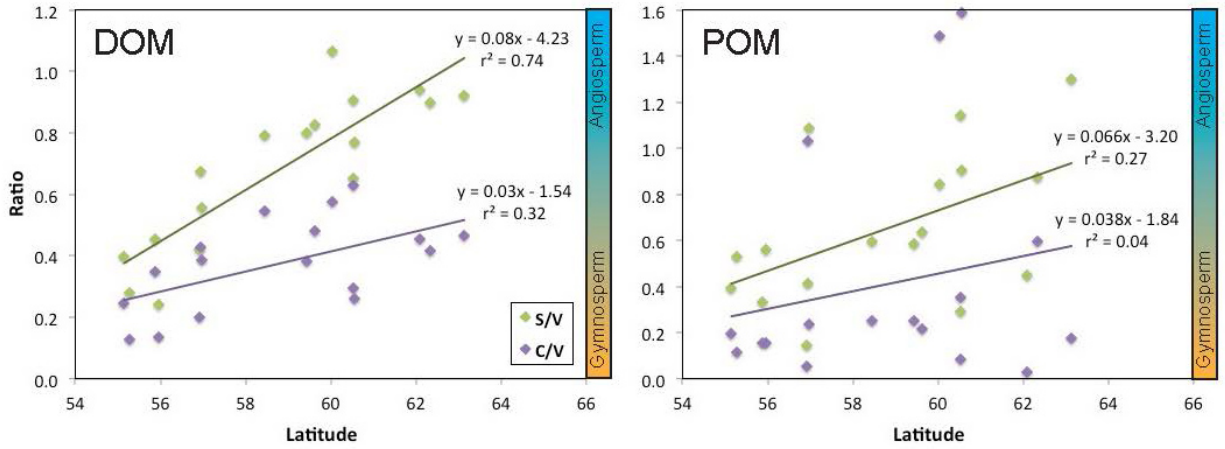

Figure 2.4: Lignin product reaction ratios, Syringyl/Vanillyl (S/V) and Cinnamyl/Vanillyl (C/V), for DOM and POM of 17 HBRs samples and corresponding relationship to latitude *Note the differences in scale.

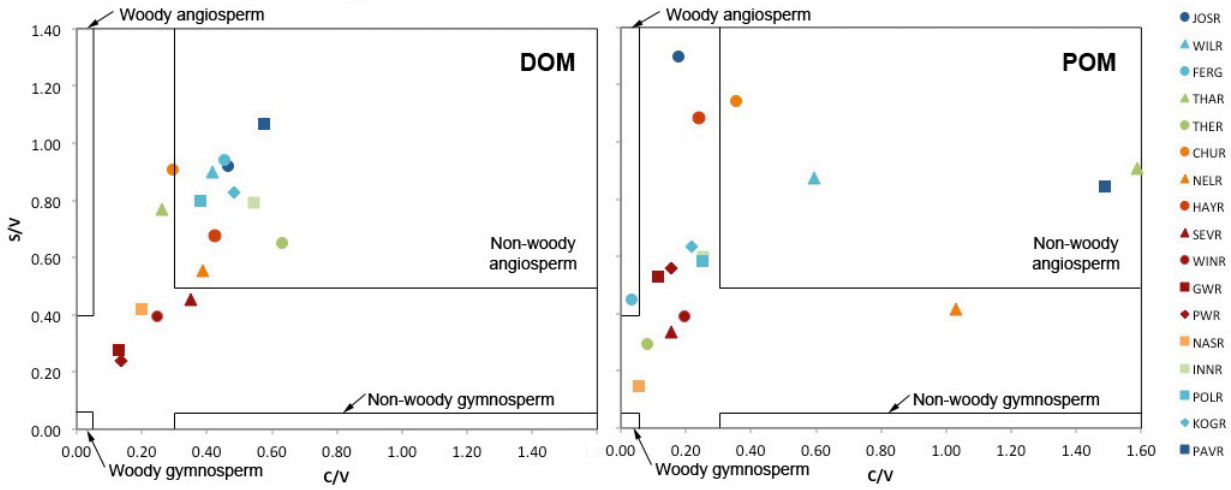

Figure 2.5: Lignin Product ratios, S/V and C/V, for DOM and POM samples of 17 Hudson Bay River samples and corresponding relationship to vegetative species. Rivers are ranked from northwest around to northeast HB with colors representing north (blue/green) and south (red/orange).

Table 2.3 (Appendix A). For both phases, lignin concentrations were highest in the southwestern rivers. Particulate lignin concentrations varied from 6.1 to 9.5 µg/L among four of the five southwestern rivers (Churchill, Nelson, Hayes and Severn), compared to 0.26-1.75 µg/L in the remaining HBRs (including the Winisk from the southwest).

Dissolved lignin concentrations varied from 20 to 102 µg/L among the southwest rivers, compared to 0.8-23 µg/L in the remaining HBRs. When lignin and OC concentrations are compared using linear regression, there is a statistically significant relationship in both the dissolved (r^2 = 0.57, y = 4.56x - 1.57, p = 0.0005) and particulate (r^2 = 0.54, y = 7.19x - 0.36, p = 0.0008) phase.

Syringyl to Vanillyl (S/V) and Cinnamyl to Vanillyl (C/V) ratios in DOM and POM show a distinct increasing gradient with increasing latitude (Figure 2.4, Table 2.3). The S/V and C/V relationship to latitude is much more distinct in the dissolved phase especially the S/V (Figure 2.4, r^2 = 0.74, p < 0.0001) compared to the particulate phase (r^2 = 0.27, p = 0.0315). The increase in S/V and C/V ratios indicates a shift from woody gymnosperm to non-woody angiosperm as you move farther north (Figure 2.5). In the dissolved phase, S/V ranges from as low as 0.24 (Little Whale River) in the south to 1.07 (Povungnituk) in the north (SD±0.3, n=17). The Cinnamyl/Vanillyl (C/V) ratio shows a similar gradient in DOM, although more variation among rivers is present (r^2 = 0.32, p = 0.0197). C/V in DOM ranges from 0.13 (Great Whale) in the south to 0.63 (Thlewiaza) in the north (SD±0.2, n=17). There is no significant latitudinal trend in C/V in POM.

Acid to Aldehyde ratios for vanillyl products ([Ad/Al]v) and syringyl products ([Ad/Al]s) were very highly correlated in both DOM (r^2 = 0.74, p = <0.0001) and POM (r^2 = 0.90, p = <0.0001). [Ad/Al]v ranged from 0.42 to 2.46 ±0.5 for particulates and 0.73 to 2.91 ±0.6 for the dissolved phase. [Ad/Al]s ranged from 0.13 to 2.67 ±0.6 in the particulate phase (average 0.76) and from 0.70 to 1.93 ±0.3 in the dissolved phase (Table 3, SD, n=17).

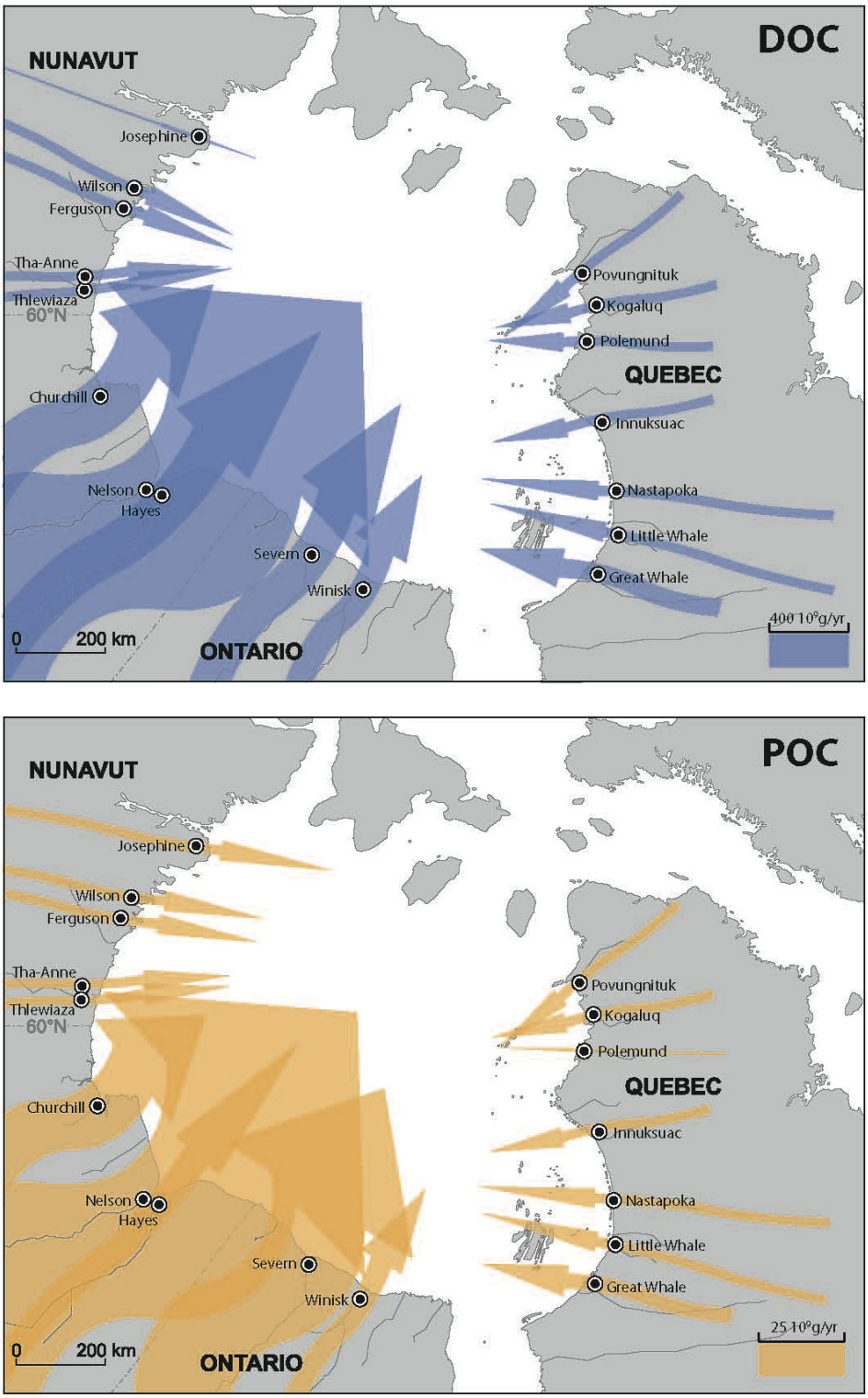

Figure 2.6: Annual Flux map with arrow thickness representing the contributions of organic carbon from the dissolved and particulate phase for 17 HBRs. Note the scale differences between the particulate and dissolved phase.

2.3.3 Stable and Radiocarbon Isotopic Composition

$\delta^{13}C$ and $\Delta^{14}C$ are reported in Table 2.2. $\delta^{13}C$ ranged from -26.1‰ to -27.9‰ (± 0.6‰) and the ages, inferred from the $\Delta^{14}C$, ranged from modern (post-1950) to 2840 (±28) years before present (Table 2.2). There are no obvious spatial patterns in the radiocarbon ages. The Churchill and Nastapoka Rivers were the oldest samples at 2840 (±40) years, followed by the Povungnituk at 715 (±30) years, and the Josephine at 215 (±20) years, with the remaining samples being modern (<50 YBP).

2.3.4 Annual Fluxes in Hudson Bay Rivers

Annual OC fluxes, estimated based on the concentration data obtained in this study and mean annual river discharges (Table 2.1 and 2.2, Figure 2.6), range from 0.2 to 53 Gg/yr (n=17, SD±14) in the particulate phase and 0.6 to 842 Gg/yr (n=17, SD±207) in the dissolved phase. Consistent with its dominance in terms of river discharge, the Nelson River has the highest estimated annual POC and DOC fluxes. Lignin fluxes parallel the POC and DOC fluxes, with the Nelson dominating in both the dissolved and particulate phases, followed by the Churchill in the dissolved phase and the Severn River in the particulate phase.

Despite the distinct lignin compositional trends from south to north (decreasing vanillyl phenol contributions northward), the fluxes of individual lignin phenols show only subtle spatial differences compared to the total lignin flux. In the dissolved phase, Vd fluxes were dominated by the Nelson, followed by the Churchill at approximately half as much (Figure 2.7). Fluxes of Vd from northern rivers, especially in the west, are almost negligible. For Sd, the Nelson dominates but Churchill (83%) is a close second.

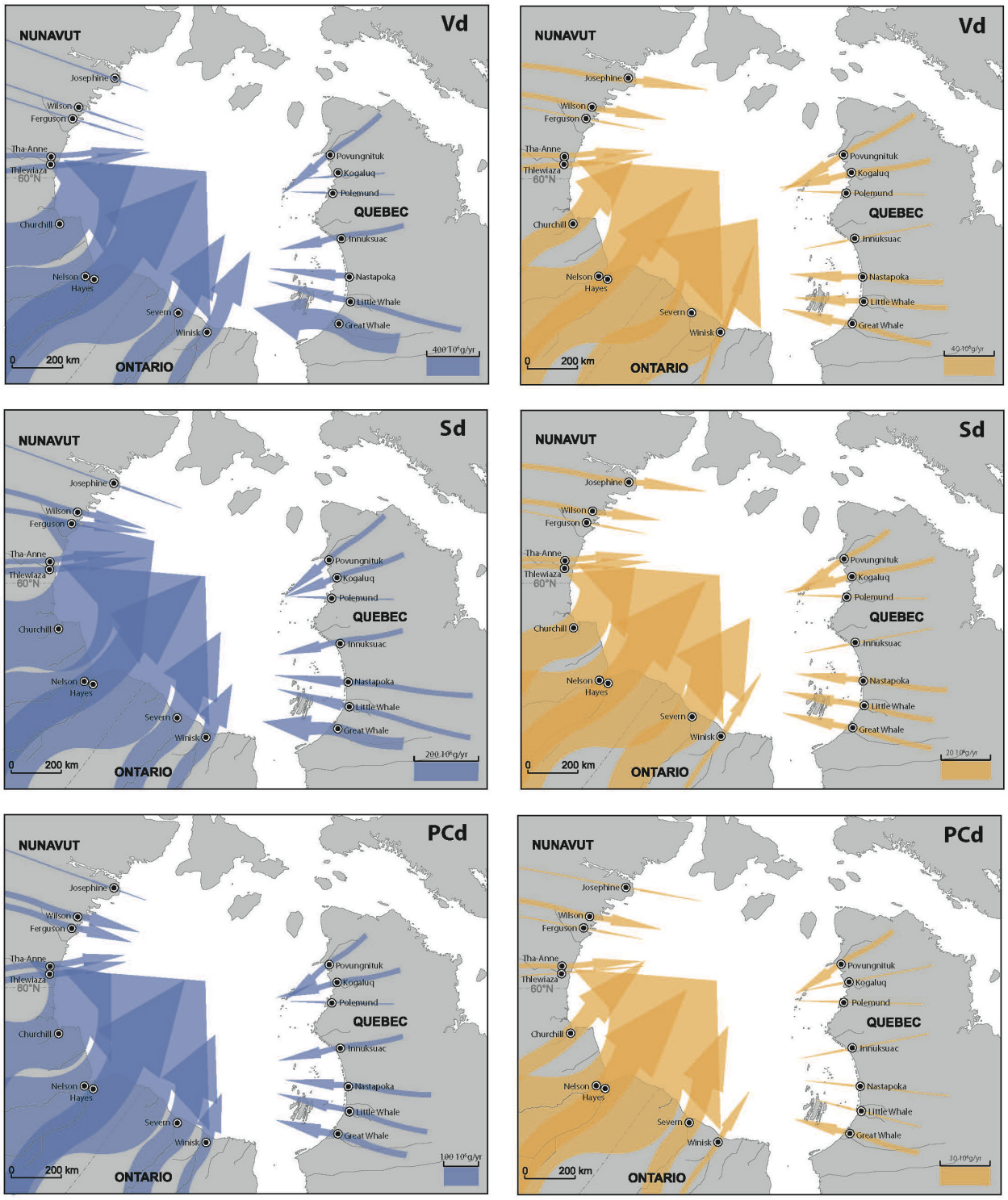

Figure 2.7: Annual flux map with arrow thickness representing the contributions of three different lignin biomarker acids (Vd, Sd, and PCd) in the dissolved (blue) and particulate (orange) phase for 17 Hudson Bay Rivers. Note the scale differences between the phases.

Northern rivers also have proportionately larger fluxes of Sd. In the particulate phase, the Nelson dominates the fluxes of both Vd and Sd with the next highest fluxes from the Severn and Churchill.

2.4 DISCUSSION

2.4.1 Spatial trends in concentrations of particulate and dissolved material

All the parameters measured in HBRs; TSS, TDS, POC, DOC and lignin phenols, exhibit the highest concentrations in the southwest part of HB (Table 2.2 in Appendix A; Figure 2.2). This pattern can be attributed to the southern extent of this region and its increased vulnerability to permafrost degradation due to the thin coastal band of continuous permafrost and extensive discontinuous permafrost on moving inland. Further impacting the high levels of sediments and OC in the rivers is their location within the peat OM-rich Hudson Plains Ecozone and the large catchments of the southwest HBRs extending down into southern latitudes (Dyke and Sladen, 2010; Smith and Burgess, 2004). This southwest region, including the Prairies and northwestern Ontario, represents 47% of the entire HB watershed with double the concentrations of TOC (mg/L) compared to the average of all HBRs (Table 2.2).

Vegetation cover along with deposits of marine and glacial sediments, post-glacial isostatic rebound, and shallow topography of the region contribute to these high concentrations of DOC and the increased supply of fresh and preserved biomass (Hudon et al, 1996). In fact, the DOC contributions of the Nelson River alone make up 41% of the annual TOC contributions for the entire Hudson Bay. The dominance of dissolved phase OC and lignin in the southwest HBRs may be attributed to the

extensive peatlands and bogs that are part of the Hudson Bay Lowland Ecoregion and which constitute the largest wetland in North America. These dominant DOC concentrations are typical of Arctic environments where peat and permafrost are present (Maybeck 1982; Raymond et al, 2007; Benner et al, 2005). Lignin contributions of the southwest HBRs are also reflected in the sediment box core data by Kuzyk et al., 2008, which show that cores representing the southwest HBRs, just offshore of the Winisk River, had the highest lignin yields of all of Hudson Bay. The influence of more woody species, such as dwarf birch and willow, and the location of the treeline along the southwest coast to just north of Churchill may account for these large DOC concentrations compared to elsewhere in the HB region.

Permafrost in the southwestern HBRs is continuous at the coast and becomes more discontinuous and sporadic farther inland (Figure 2.1). The extensive regional peat plateau development and wetland environment may explain the increased risk of permafrost thaw and degradation with warming in the southwest Hudson Bay (Raymond et al, 2007; Smith and Burgess, 2004; Dyke and Sladen, 2010). Dyke and Sladen (2010) suggest that any thawing at a plateau edge may result in thermokarst subsidence and erosion increasing the thermal conductivity of the soil and the transition of peat plateau to fen. In permafrost dominated watersheds, there is an increase in DOC and lignin concentrations compared to other watersheds as overland and subsurface flow coupled with increased peat content decreases the mineral soil exchange of DOC causing its release into rivers (Onstad et al, 2000; Carey, 2003).

Although the southwest HBRs have the highest concentrations of OC in both the dissolved and particulate phase, the Nelson and Hayes have the lowest %POC

compared to the TSS of all HBRs (Table 2.2). The Churchill River has a higher than average %POC (6.94). There may be other factors such as surficial geology, mineralization of OC and soil characteristics contributing to %OC contained in both the dissolved and suspended phase solids.

2.4.2 Composition of POM and DOM and inferences about watershed sources

The clearest trend in DOM and POM composition is the latitudinal increase in S/V and C/V ratios from a transitional mixed forest-tundra environment in the south to a more barren, sparsely vegetated tundra in the north (Figure 2.4). Lower S/V and C/V ratios indicate the presence of relatively more woody gymnosperm species, such as white spruce and tamarack, which are indicative of forest tundra and in northern latitudes, an increase in non-woody angiosperm sources, such as herbs and mosses, replace the gymnosperm species resulting in higher S/V and C/V ratios (Figure 2.5).

The S/V and C/V ratios are also distinctly different in terms of sources between the particulate and dissolved phase (Figure 2.5). The dissolved phase shows a strong distinction between vegetative composition and latitude similar to other studies (Kuzyk et al, 2008; Guo et al 2007). The particulate phase on the other hand, is dominated by lower C/V ratios representing woody vegetation sources and S/V ratios that do not correlate strongly to latitude. The Povungnituk and Tha-Anne Rivers are outliers with unusually high C/V ratio that likely reflect high non-woody sources in the region due to either the fractionation of lignin phenols resulting in sorption of leachates back into the soils such as the selective sorption of vanillyl (Hernes et al., 2007; Woods et al., 2011).

The average S/V and C/V ratios found in HBRs are double those observed in

other Arctic Rivers (Russia and Canada: 0.65 compared to 0.39 (POM), 0.68 compared to 0.40 (DOM) (Lobbes et al, 2000; Amon et al, 2012)). HBRs and other major Arctic Rivers influenced by tundra vegetation show an increase in S/V and C/V ratios as expected. Of all the major Arctic rivers, the Ob River is closest to HBRs in terms of having the highest S/V and C/V ratios of DOM (Table 2.4, Appendix A). This may be due to its mild climate, variable vegetation cover and its location within the largest peat bog system in the world (Amon et al, 2012), features similar to southwest HBRs. The higher latitudinal location of river catchments in Russian Arctic Rivers are likely to be influenced by more northern vegetation, climate and drainage resulting in lower S/V and C/V ratios compared to southwest HB. A similar DOC dominant concentration of 82% has also been reported for Russian Arctic Rivers further showing the importance of dissolved phase in OC terrestrial contributions (Lobbes et al, 2000).

2.4.3 Acid Aldehydes and $\Delta^{14}C$

The degradation state of both POM and DOM are inferred from [Ad/Al] ratios. and are used to determine source specific information regarding dissolved and particulate OM entering rivers with lower ratios representing fresher (less degraded) plant tissues and increasing oxidation and degradation with higher ratios (Goni and Hedges, 1992; Opsahl and Benner, 1998). Most of the POM and DOM samples collected have [Ad/Al] ratios over 0.5 and are therefore not fresh with the dissolved phase more degraded than the particulate phase suggesting that most material has undergone some level of decomposition (Table 2.3). There are exceptions such as the Povungnituk and Tha-Anne Rivers, which contain highly degraded POC indicated by

their high [Ad/Al] ratios compared to samples from other rivers (Table 2.3). The Thlewiaza and Little Whale Rivers are located in forest tundra transitional environments and may be undergoing more intense microbial degradation and mineralization due to increased warming (Schaphoff et al, 2013).

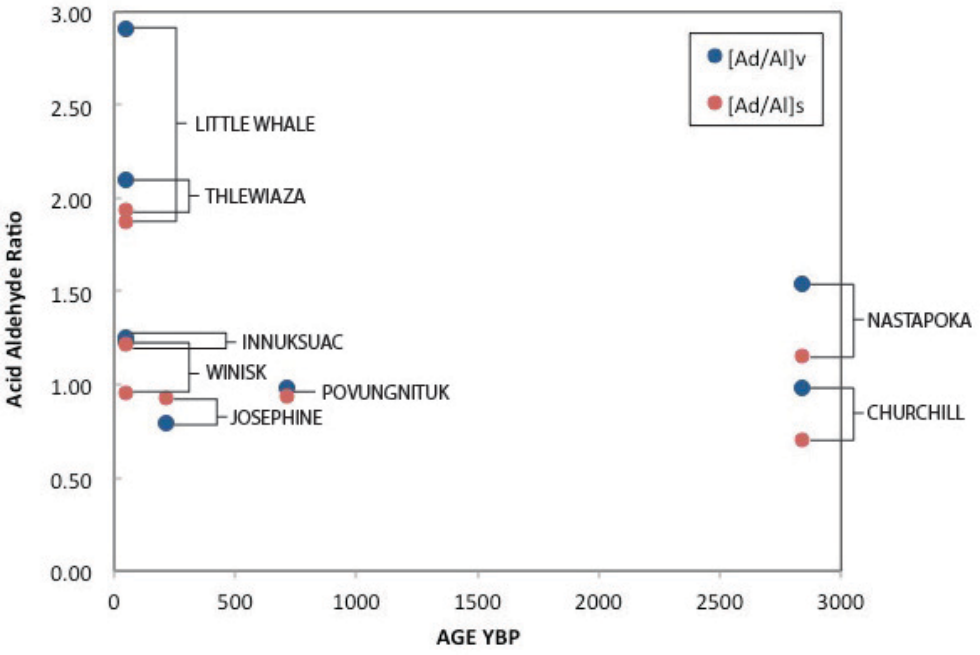

Figure 2.8: Acid to Aldehyde ratios, [Ad/Al]v and [Ad/Al]s, and ^{14}C ages (years before present, YBP) for the dissolved phase of eight HBRs.

Distinct carbon isotopic signatures have been found in lignin reaction products from different classes of vascular plants (Lobbes et al, 2000; Goni and Eglinton, 1996; Hedges and Oades, 1997). [Ad/Al] ratios and $\Delta^{14}C$ ages for DOM samples (Figure 2.8) indicate that most samples are modern and moderately degraded (between 0.54 and 1.54), with the Churchill and Nastapoka Rivers being significantly older (2840 YBP) but similarly degraded and the Thlewiaza and Little Whale Rivers being modern and highly degraded (ratios >1.8). Much of the DOM in the HBRs is young and moderately

degraded and may be derived from the higher terrestrial primary production of boreal regions such as the forest tundra ecotone under processes such as microbial alteration (Guo et al, 2007; Lobbes et al, 2000). Age of these samples indicates that, with the exception of the Churchill and the Nastapoka Rivers, the older dissolved phase OC is not being released into the majority of HBRs, as has been found in other Eurasian and North American Rivers (Benner et al, 2004; Amon et al., 2012).

The Churchill and Nastapoka River DOM is oldest with samples dated to 2840 ybp but the [Ad/Al] ratios are similar or lower and therefore fresher than expected compared to the modern samples, especially DOM from the Thlewiaza and Little Whale Rivers. The Churchill and Nastapoka river samples are located in the forest tundra ecotone, one on the east and one on the west coast (Table 2.1, Appendix A). The forest tundra ecotone is undergoing transition with vegetation shifting northward and permafrost thawing due to its southern extent and the current location of the treeline. The older ages and lower than expected [Ad/Al] ratios of these two samples may reflect the fact that the terrain is undergoing more intense erosion causing older deeper SOC to be released into the rivers. The freshness of the SOC is likely due to preservation within permafrost until their recent release with thawing, which has also been shown in Russian Arctic Rivers (Gustafsson et al, 2011; Vonk et al, 2010).

2.4.4 Annual Fluxes of DOC and POC in Hudson Bay Rivers

The high influx of OC and lignin into the southwest region of Hudson Bay, in particular from the Nelson River, dominates the overall influx of OC and lignin from all HBRs, which is consistent with other studies (Granskog et al., 2007). The high influx in

this region is due to 47% of the Hudson Bay basin draining from the prairies and northwestern Ontario of the southwest and the relatively high river flows dominating from the southwest HBRs (Prinsenberg et al, 1987; Dery et al, 2005). The southwest HB basin, which stretches as far west and south as Alberta and North Dakota, is dominated by land use patterns including dams, diversion and agriculture. The OC flux of the Nelson River is possibly being elevated by the upstream diversion of the Churchill River into the Nelson in 1977 (Dery et al., 2005). This region is the warmest of the Hudson Bay drainage basin and the OC being released is influenced by the southern permafrost-free soils and warmer climates. Thus, the dominant influx of OC and lignin in the southwest of Hudson Bay may be attributed to increased biodiversity and vegetation cover, permafrost distribution and recent warming.

While the annual discharge of HBRs, like the Nelson River, is small in comparison to other Arctic rivers, the annual DOC and lignin fluxes are almost equal to larger rivers like the Mackenzie (Table 2.4, Appendix A). Arctic Rivers with high discharge are likely to release more OC and lignin into coastal seas; however, the southern extent of the Nelson River Drainage Basin, permafrost coverage and the regional vegetation contribute significantly to the concentrations and influx of OC and lignin in the Nelson River. Another example is the Hayes River, which is ranked fifth in discharge for all the sampled HBRs, but fourth in the annual flux of OC and lignin (Table 2.1 to Table 2.3). Therefore, while the discharge of HBRs may be lower compared to other Arctic Rivers, contributions of OC and lignin from Hudson Bay are important when considering the response of other Arctic drainage basins to the thawing of permafrost and the shifting vegetation composition associated with future warming scenarios.

2.4.5 DOC versus POC

The majority of OC (93%) is in the dissolved phase in all HBRs except for the Josephine River. The Josephine is distinct in that the particulate phase dominates OC contributions (65%) with only 0.6 Gg POC/yr to Hudson Bay, which is far below the HBRs average of 108 Gg POC/yr. Barren tundra with rocky outcrops, low vegetation cover and under developed soils dominate the Josephine River, located in the northwest region of Hudson Bay. The lack of soil development, ice-rich environment and slow degradation of plant detritus may account for this reversed ratio between POC and DOC and may lead to the preservation of OC within soil profiles.

The average TOC in HBRs contains a relatively higher proportion of DOC (93%) than is found in Arctic Russian rivers (83%, Lobbes et al., 2000), and the total Arctic Ocean riverine inputs (82%, Stein and Macdonald, 2004). DOC concentrations are influenced by vegetative biomass within the soil and vegetation cover of the region while POC is more representative of mineral soil and permafrost contributions (Guo et al, 2007). The Hudson Bay Basin has the majority of its annual freshwater flux drain through southern latitudes which have a higher vegetative biomass compared to northern latitudes. The HB system contributes approximately 23% of the riverine flux of DOC entering into northern seas (Mundy et al., 2010). Therefore, changes in permafrost distribution leading to changes in vegetation have the potential to produce significant effects on these DOC fluxes both for HB and for the wider Arctic.

2.5 CONCLUSIONS

Analysis of the 17 HBRs indicate that the majority of OC is coming from the

southwest region, especially the Nelson River DOC, which contributes 41% of the total annual OC inputs into the Hudson Bay. The southwestern extent of the Hudson Bay Drainage Basin, the strong influence of the extensive peatlands of the Hudson Bay Lowlands and the increased vegetative biomass of the south are making this region a dominant OC source for the Bay. There is also a significant correlation between S/V and C/V ratios and latitude in DOM that reflects the regional vegetative sources of OC from boreal forest in the south to tundra in the north providing a necessary step in interpreting the influence of vegetation on the OC influx into the Hudson Bay. S/V and C/V ratios, when combined with [Ad/Al] ratios and ^{14}C ages, inform us of the state of degradation and the release of old SOC, formerly locked in permafrost. The mobilization of terrestrial ancient carbon is underway in some of the HBRs as is reflected in the ^{14}C ages of the Nastapoka and Churchill Rivers, indicating that the degradation of permafrost is beginning to release old SOC, although the lower [Ad/Al] ratios suggest that the OM is “fresher” than expected and is being preserved by the permafrost.

Climate modeling in this region predicts as much as a 7 to 8 °C warming by the end of the 21st century resulting in an estimated loss of 53 to 66 percent in near surface permafrost areal extent (Schuur et al, 2011). This warming will enhance surface runoff and, coupled with active layer thickening, increases the potential for DOC and POC export into the HB. As permafrost shifts from continuous to discontinuous we may see a shift in not only the ^{14}C ages of DOM but also the S/V and C/V ratios reflecting the changes associated with regional warming and permafrost degradation. It may be complicated to calculate this shift in the release of older SOC due to it being underestimated and masked by the subsequent increase in the transport of young

surface OC associated with enhanced river runoff (Feng et al., 2013). In this study, we find that the quantities and composition of lignin in both the POM and DOM of HBRs is pertinent information to understanding the transport of OC into the HB, especially in terms of permafrost degradation which influences the mobilization of SOC, and any potential changes to the vegetative sources of OC.

2.6 APPENDIX A

Table 2.1: Sampling Locations and Permafrost zonation with Hydrological and Ecological Site Characteristics of Hudson Bay Rivers (HBRs). Rivers sorted by coastal location and ranked from north to south.

Rivers	Latitude	Longitude	Drainage Basin (km^2)	Annual Q[1] (km^3/yr)	Permafrost Zone[2]	Eco Zone[3]	Vegetation	Eco Region Code[4]
East								
Povungnituk	60.05	77.22	28000	11.9	Continuous	S Arctic	Shrub Tundra	47
Kogaluq	59.61	77.48	11300	5.0	Continuous	S Arctic	Shrub Tundra	47
Polemund	59.43	77.30	N/A	1.5*	Continuous	S Arctic	Shrub Tundra	47
Innuksuac	58.46	78.08	11200	3.3	Continuous	S Arctic	Tundra	47
Nastapoka	56.92	76.43	12500	8.0	Extend-Dis	S Arctic	Forest Tundra	47, 73
Little Whale	55.97	76.67	11700	3.7	Sporadic-Dis	Taiga Shield	Forest Tundra	73
Great Whale	55.27	77.57	43200	19.8	Sporadic-Dis	Taiga Shield	Forest Tundra	72
Northwest								
Josephine	63.13	90.98	N/A	2.5*	Continuous	S Arctic	Shrub Tundra	45
Wilson	62.33	93.13	N/A	2.6*	Continuous	S Arctic	Shrub Tundra	45
Ferguson	62.08	93.35	12400	2.6	Continuous	S Arctic	Shrub Tundra	45
Tha-Anne	60.55	94.92	29400	6.3	Continuous	SA/TS	Shrub Tundra	45, 70
Thlewiaza	60.52	95.02	27000	6.9	Continuous	SA/TS	Shrub Tundra	45, 70
Southwest								
Churchill	60.52	95.02	288880	20.6	Continuous	Hudson Plains	Forest Tundra	215, 71
Nelson	56.94	92.80	1125520	94.1	Continuous	Hudson Plains	Forest Tundra	215, 216
Hayes	56.97	92.37	103000	18.6	Continuous	Hudson Plains	Forest Tundra	215, 216
Severn	55.87	87.82	94300	21.3	Continuous	Hudson Plains	Forest Tundra	215, 216
Winisk	55.15	85.30	54710	14.7	Continuous	Hudson Plains	Forest Tundra	215, 216

*Estimated discharge based on nearby rivers discharge and size.
[1]Annual Q discharge from HYDAT data, average from 1964-2000 from McClelland, 2006 (Auxiliary Table S1).
[2]Permafrost zonation based on percent of land underlain by permafrost; Continuous = 90-100%, Extend-Dis = Extensive discontinuous 50-90%, Sporadic discontinuous 10-50%, Isolated patches 0-10%; from Natural Resources Canada, 1995. Also displayed in Figure 1.
[3]Vegetation Ecozones; SA= Southern Arctic, TS = Taiga Shield; Smith, 2010.
[4]Ecoregion codes; 45 = Maguse River Upland, 47 = Central Ungava Peninsula, 70 = Kazan River Upland, 71 = Selwyn Lake Upland, 72 = La Grande Hills, 73 = Southern Ungava Peninsula, 215 = Coastal Hudson Bay Lowland, 216 = Hudson Bay Lowland; Ecological Stratification Working Group, 1995.

Table 2.2: Concentrations, fluxes and isotopic properties of dissolved and particulate organic carbon in HBRs. Rivers are separated into east, northwest and southwest and then listed in order from north to south.

	Particulate Phase				Dissolved Phase						Total Phases	
Rivers	TSS[1] (mg/L)	%POC[2] (of TSS)	POC[3] (mg/L)	POC Flux[4] Gg/yr	TDS[5] (mg/L)	%DOC[2] (of TDS)	DOC[3] (mg/L)	DOC Flux[4] Gg/yr	$\delta^{13}C$ ‰	^{14}C ages[6]	TOC mg/L	TOC Flux Gg/yr
Povungnituk	3.4	3.7	0.13	1.5	20	10	1.95	23	-26.39	715	2.1	25
Kogaluq	4.2	3.2	0.13	0.7	20	11	2.26	11	--	--	2.4	12
Polemund	4.9	3.1	0.15	0.2	11	8.8	0.93	1.4	--	--	1.1	1.6
Innuksuac	2.7	6.0	0.16	0.5	39	11	4.17	14	-26.1	Mod	4.3	14
Nastapoka	5.3	3.3	0.17	1.4	14	14	1.98	16	-27.69	2840	2.2	17
Little Whale	10	1.9	0.19	0.7	24	15	3.59	13	-27.23	Mod	3.8	14
Great Whale	8.2	2.7	0.22	4.4	24	19	4.43	88	--	--	4.7	92
Mean	**5.6**	**3.4**	**0.17**	**1.4**	**22**	**13**	**2.76**	**24**	**--**	**--**	**2.9**	**25**
Josephine	8.4	5.3	0.45	1.1	1.8	13	0.24	0.6	-26.52	215	0.7	1.7
Wilson	9.0	7.4	0.67	1.7	32	10	3.15	8.2	--	--	3.8	9.9
Ferguson	4.7	7.3	0.34	0.9	19	14	2.59	6.7	--	--	2.9	7.6
Tha-Anne	3.1	6.2	0.19	1.2	8.2	16	1.28	8.1	--	--	1.5	9.2
Thlewiaza	10	2.3	0.23	1.6	13	19	2.44	17	-27.17	Mod	2.7	18
Mean	**7.0**	**5.7**	**0.37**	**1.3**	**15**	**14**	**1.94**	**8.1**	**--**	**--**	**2.3**	**9.4**
Churchill	12	6.9	0.84	17	241	5.1	12.3	252	-27.86	2840	13	270
Nelson	39*	1.4	0.56	53	126	7.1	8.95***	842	--	--	9.5	895
Hayes	30**	1.4	0.43	8.0	134	8.9	11.9****	222	--	--	12	230
Severn	60	2.4	1.41	30	81	11	8.52	181	--	--	9.9	211
Winisk	6.2	7.0	0.44	6.5	96	9.2	8.81	130	-27.41	Mod	9.3	136
Mean	**29**	**3.8**	**0.73**	**23**	**136**	**8.1**	**10.1**	**326**	**--**	**--**	**11**	**350**
Total Mean (SD±)	**13** (16)	**4.2** (2.2)	**0.39** (0.3)	**7.7** (14)	**53** (64)	**12** (3.8)	**4.68** (3.9)	**108** (207)	**--**	**--**	**5.1** (4.1)	**116** (220)

[1]Total suspended solids TSS mg/L calculated based volume of water filtered through GF/Fs and total weight of particulates.
[2]%DOC and %POC based on the amount of OC present in the total sample weight analyzed.
[3]DOC and POC concentration per liter based on the total amount of sample divided by the total water sampled either filtered or freeze-dried prior to analysis. [4]Annual flux of DOC and POC in Gigagrams (Gg, 10^9 g) per year calculated from Table 1 data, and other data represents HYDAT data, average from 1964-2000 from McClelland, 2006.
[5]Total dissolved solids TDS mg/L calculated based on volume of water freeze-dried and total weight of remaining dissolved material.
[6]$\Delta^{14}C$ ages in years before present (YBP); Mod = Modern represents post-1950
*August based on n=5, **Aug based on n=13, ***DOC is average based on n=5. ****DOC is average based on n = 2.

Table 2.3: Lignin product reaction ratios, total lignin concentrations and fluxes of dissolved and particulate phases of HBRs. Rivers are separated into east, northwest and southwest and then listed in order from north to south.

	Particulate Phase						Dissolved Phase					
Rivers	S/V[1]	C/V[1]	[Ad/Al] v[2]	[Ad/Al] s[2]	Σ8[3] µg/L	Σ8 Flux[4] Mg/yr	S/V[1]	C/V[1]	[Ad/Al] v[2]	[Ad/Al] s[2]	Σ8[3] µg/L	Σ8 Flux[4] Mg/yr
East												
Povungnituk	0.85	1.49	1.38	1.65	0.64	7.58	1.07	0.58	0.98	0.93	7.46	88.8
Kogaluq	0.63	0.22	0.53	0.54	0.53	2.67	0.83	0.48	0.88	0.95	5.65	28.3
Polemund	0.58	0.25	0.60	0.45	1.17	1.76	0.80	0.38	0.98	0.85	3.83	5.75
Innuksuac	0.60	0.25	0.60	0.44	0.26	0.87	0.79	0.55	1.25	1.22	17.8	58.8
Nastapoka	0.15	0.05	0.48	0.82	0.54	4.33	0.42	0.20	1.54	1.15	7.87	63.0
Little Whale	0.56	0.15	0.67	0.69	0.66	2.45	0.24	0.14	2.91	1.87	20.7	76.7
Great Whale	0.53	0.12	0.95	0.70	0.81	16.1	0.28	0.13	1.62	1.23	22.9	453
Mean	**0.56**	**0.36**	**0.74**	**0.75**	**0.66**	**5.11**	**0.63**	**0.35**	**1.45**	**1.17**	**12.3**	**111**
Northwest												
Josephine	1.30	0.18	0.66	0.46	1.26	3.14	0.92	0.46	0.79	0.93	0.78	1.94
Wilson	0.87	0.59	0.49	0.43	1.21	3.16	0.90	0.42	0.73	0.82	10.1	26.3
Ferguson	0.45	0.03	0.60	0.13	0.34	0.87	0.94	0.45	0.94	1.06	9.63	25.0
Tha-Anne	0.91	1.59	2.46	2.67	1.75	11.1	0.77	0.26	1.25	0.89	7.24	45.6
Thlewiaza	0.29	0.08	0.42	0.52	0.90	6.22	0.65	0.63	2.10	1.93	16.0	111
Mean	**0.76**	**0.49**	**0.93**	**0.84**	**1.09**	**4.89**	**0.84**	**0.45**	**1.16**	**1.13**	**8.75**	**41.9**
Southwest												
Churchill	1.14	0.35	0.74	0.54	6.10	126	0.91	0.29	0.98	0.70	102	2106
Nelson	0.41	1.03	0.59	0.50	7.05	663	0.67	0.43	1.73	1.15	32.7	3075
Hayes	1.08	0.24	0.29	0.17	9.42	175	0.56	0.39	1.29	1.07	63.3	1178
Severn	0.33	0.15	0.85	0.71	9.54	203	0.45	0.35	1.24	1.41	35.4	753
Winisk	0.39	0.20	0.66	0.57	1.27	18.7	0.40	0.25	1.23	0.96	19.7	475
Mean	**0.67**	**0.39**	**0.63**	**0.50**	**6.68**	**237**	**0.60**	**0.34**	**1.30**	**1.06**	**53.2**	**1518**
Total Mean (SD±)	**0.65** (0.3)	**0.41** (0.5)	**0.76** (0.5)	**0.71** (0.6)	**2.56** (3.2)	**73.3** (165)	**0.68** (0.3)	**0.38** (0.2)	**1.32** (0.6)	**1.12** (0.3)	**23.3** (26)	**504** (866)

[1] S/V and C/V ratios are the ratios between lignin reaction product categories Vanillyl (V) to Cinnamyl (C) and Syringyl (S).
[2] [AD/Al] = Acid aldehydes product ratios reflecting ratio between acid and aldehydes of Vanillyl (Vd/Vl) and Syringyl (Sd/Sl) groups.
[3] Σ8 µg/L = the sum of eight lignin reaction products calculated from hydrological data from Table 1; Vanillyl, Syringyl, and Cinnamyl* groups;
*Ferulic acid (Fd) in Cinnamyl group was estimated based on low yields for some particulate samples of rivers and they were given an estimation based on the average ratio between Fd and p-coumaric acid (P-Cd) another Cinnamyl reaction product.
[4] Annual flux of Σ8 in Megagrams (Mg, 10^6 g) was calculated using the hydrological data from Table 1 and Σ8 ug/L.

Table 2.4: Comparison of DOC and lignin fluxes and ratios of the Southwest HBRs (Nelson and Churchill Rivers) and other Arctic Rivers.

Arctic River DOM Worldwide Comparison								
Arctic Rivers	Nelson[1]	Churchill[1]	Mackenzie	Yukon	Lena	Ob	Yenesei	Kolyma
Discharge (km^3 yr^{-1})	94.1	20.6	298	208	581	427	636	111
DOC (Tg yr^{-1})*	0.84	0.25	1.20	1.75	6.47	3.04	5.08	0.71
% of total DOC (8 rivers)	4.34	1.29	6.21	9.05	33.45	15.72	26.27	3.67
Lignin Σ8 (Gg yr^{-1})*	3.08	2.11	3.60	14.7	91.6	21.5	54.3	6.16
S/V	0.67	0.91	0.33	0.47	0.28	0.48	0.31	0.41
C/V	0.43	0.29	0.10	0.14	0.08	0.14	0.07	0.10
Ad/Al_v	1.73	0.98	0.84	0.87	1.16	1.13	1.03	1.03
Ad/Al_s	1.15	0.70	0.60	0.65	0.79	0.82	0.72	0.71

[1] River data for the Nelson and Churchill Rivers from this Appendix (Table 2.1 to 2.3). All other data obtained from Amon et al, 2012 reflecting the sampled means from 2003-2007.

*Annual flux calculated using DOC (mg/L) and lignin concentrations (µg/L) from Amon et al., 2012 and converting to DOC (Tg yr^{-1}) and Σ8 (Gg yr^{-1}).

2.7 REFERENCES

Amon, R.M.W., Rinehart, A.J., Duan, S., Louchouarn, P., Prokushkin, A., Guggenberger, G., Bauch, D., Stedmon, C., Raymond, P. A., Holmes, R.M., McClelland, J. W., Peterson, B.J., Walker, S.A., Zhulidov, A.V., 2012. Dissolved organic matter sources in large Arctic rivers. *Geochimica et Cosmochimica Acta* **94**: 217-237.

Benner, R., Benitez-Nelson, B., Kaiser, K., and Amon, R.M.W., 2004. Export of young terrigenous dissolved organic carbon from rivers to the Arctic Ocean. *Geophysical Research Letters* **31**: L05305. doi:10.1029/2003GL019251

Benner, R., Louchouarn, P., and Amon, R.M.W., 2005. Terrigenous dissolved organic matter in the Arctic Ocean and its transport to surface and deep waters of the North Atlantic. *Global Biogeochemical Cycles* **19**: GB2025. doi:10.1029/2004GB002398

Carey, S.K., 2003. Dissolved organic carbon fluxes in a discontinuous permafrost subarctic alpine catchment. *Permafrost and Periglacial Processes* **14**: 161–171. doi: 10.1002/ppp.444

Dery, S.J. and Wood, E.F., 2004. Teleconnection between the Arctic Oscillation and Hudson Bay river discharge. *Geophysical Research Letters* **31**; L18205, doi:10.1029/2004GL020729.

Dery, S.J. Stieglitz, M., McKenna, E.C. and Wood, E.F., 2005. Characteristics and trends of river discharge into Hudson, James, and Ungava Bays, 1964-2000. *Journal of Climate* **18**: 2540-2557.

Dyke, L.D., and Sladen, W.E., 2010. Permafrost and Peatland Evolution in the Northern Hudson Bay Lowland, Manitoba. *Arctic* **63** (4): 429 – 441.

Ecological Stratification Working Group, 1995. A National Ecological Framework for Canada. Agriculture and Agri-Food Canada, Research Branch, Centre for Land and Biological Resources Research and Environment Canada, State of the Environment Directorate, Ecozone Analysis Branch, Ottawa/Hull. Report and national map at 1:7500 000 scale.

Feng, X., Vonk, J.E., van Dongen, B.E., Gustafsson, O., Semiletov, I.P., Dudarev, O.V., Wang, Z., Montluçon, D.B., Wacker, L., and Eglinton, T.I., 2013. Differential mobilization of terrestrial carbon pools in Eurasian Arctic river basins. *PNAS, Proceedings of the National Academy of Sciences*, **110** (35): 14168–14173. doi/10.1073/pnas.1307031110.

Frey, K.E. and McClelland, J.W., 2009. Impacts of permafrost degradation on arctic river biogeochemistry. *Hydrological Processes* **23**: 169–182, doi:10.1002/hyp.7196.

Goni, M.A. and Eglinton, T.I., 1996. Stable carbon isotopic analyses of lignin-derived CuO oxidation products by isotope ratio monitoring-gas chromatography-mass spectrometry (irm-GC-MS). *Organic Geochemistry* **24** (6/7): 601-615.

Goni, M.A., and Hedges, J.H., 1992. Lignin dimers: structures, distribution and potential geochemical applications. *Geochimica et Cosmochimica Acta* **56**: 4025-4043.

Goni, M.A., Nelson, B., Blanchette, R.A., and Hedges, J.I., 1993. Fungal degradation of wood lignins: geochemical perspectives from CuO-derived phenolic dimers and monomers. *Geochimica et Cosmochimica Acta* **57**: 3985-4002.

Goni, M.A., Yunker, M.B., Macdonald, R.W. and Eglinton, T.I., 2005. The supply and preservation of ancient and modern components of organic carbon in the Canadian Beaufort Shelf of the Arctic Ocean. *Marine Chemistry* **93**: 53–73.

Goni, M.A., O'Connor, A.E., Kuzyk, Z.A., Yunker, M.B., Gobeil, C., and Macdonald, R.W., 2013. Distribution and sources of organic matter in surface marine sediments across the North American Arctic margin. *Journal of Geophysical Research: Oceans* 118; 1–19. doi:10.1002/jgrc.20286

Granskog, M.A., Macdonald, R.W., Mundy, C.-J., and Barber, D.G., 2007. Distribution, characteristics and potential impacts of chromophoric dissolved organic matter (CDOM) in Hudson Strait and Hudson Bay, Canada. *Continental Shelf Research* **27**: 2032–2050. doi:10.1016/j.csr.2007.05.001

Guo, L., Ping, C. and Macdonald, R.W., 2007. Mobilization pathways of organic carbon from permafrost to arctic rivers in a changing climate. *Geophysical Research Letters* **34**: L13603, doi:10.1029/2007GL030689.

Gustafsson, O., vanDongen, B.E., Vonk, J.E., Dudarev, O.V., and Semiletov, I.P., 2011. Widespread release of old carbon across Siberian Arctic echoed by its large rivers. *Biogeosciences* 8: 1737-1743. doi:10.5194/bg-8-1737-2011

Hedges, J.I. and Oades, J.M., 1997. Comparative organic geochemistries of soils and marine sediments. *Organic Geochemistry* **27** (7/8): 319-361.

Hernes, P.J., Robinson, A.C., and Aufdenkampe, A.K. 2007. Fractionation of lignin during leaching and sorption and implications for organic matter 'freshness." *Geophysical Research Letters* **34**: L17401, doi:10.1029/2007GL031017.

Hudon, C., Morin, R., Bunch, J., and Harland, R., 1996. Carbon and nutrient output from the Great Whale River (Hudson Bay) and a comparison with other rivers around Quebec. *Canadian Journal of Fisheries and Aquatic Sciences* **53**: 1513-1525.

Kuzyk, Z.A., Goni, M.A., Stern, G.A. and Macdonald, R.W., 2008. Sources, pathways and sinks of particulate organic matter in Hudson Bay: Evidence from lignin distributions. *Marine Chemistry* **112**: 215-229. doi:10.1016/j.marchem.2008.08.001

Kuzyk, Z.A., Macdonald, R.W., Johannessen, S.C., Gobeil, C. and Stern, G.A., 2009. Towards a sediment and organic carbon budget for Hudson Bay. *Marine Geology* **264**: 190-208. doi:10.1016/j.margeo.2009.05.006

Lobbes, J.M., Fitznar, H.P. and Kattner, G., 2000. Biogeochemical characteristics of dissolved and particulate organic matter in Russian rivers entering the Arctic Ocean. *Geochimica et Cosmochimica Acta* **64** (17): 2973–2983.

Margesin, R., 2009. *Permafrost Soils*. Volume 16, Springer, Berlin. doi:10.1007/978-3-540-69371-0. 322 pp.

Maybeck, M., 1982. Carbon, nitrogen, and phosphorus transport by world rivers. *American Journal of Science* **282**: 401-450.

McClelland, J.W., Dery, S.J., Peterson, B.J., Holmes, R.M., and Wood, E.F., 2006. A pan-arctic evaluation of changes in river discharge during the latter half of the 20th century. *Geophysical Research Letters* **33**: L06715. doi:10.1029/2006GL025753.

McGuire, A.D., Anderson, L.G., Christensen, T.R., Dallimore, S., Guo, L., Hayes, D.J., Heimann, M., Lorenson, T.D., Macdonald, R.W., and Roulet, N., 2009. Sensitivity of the carbon cycle in the Arctic to climate change. *Ecological Monographs* **79** (4): 523-555.

Mundy, C.-J., Gosselin, M., Starr, M., and Michel, C., 2010. Riverine export and the effects of circulation on dissolved organic carbon in the Hudson Bay system, Canada. *Limnology and Oceanography* **55** (1): 315-323.

Natural Resources Canada, 1995. The Atlas of Canada – 5th Edition National Atlas of Canada. Government of Canada, Canada Centre for Remote Sensing, GeoAccess Division; Ottawa, Ontario. http://apps1.gdr.nrcan.gc.ca/mirage/full_result_e.php?id=205314.

Onstad, G.D., Canfield, D.E., Quay, P.D., and Hedges, J.I., 2000. Sources of particulate organic matter in rivers from the continental USA: Lignin phenol and stable carbon isotope compositions. *Geochimica et Cosmochimica Acta* **64** (20):

3539–3546.

Opsahl, S., and Benner, R., 1998. Photochemical reactivity of dissolved lignin in river and ocean waters. *Limnology and Oceanography* **43** (6): 1297–1304.

Payette, S., Delwaide, A., Caccianiga, M. and Beauchemin, M., 2004. Accelerated thawing of subarctic peatland permafrost over the last 50 years. *Geophysical Research Letters* **31**: L18208, doi:10.1029/2004GL020358.

Peterson, B.J., Holmes, R.M., McClelland, J.W., Vorosmarty, C.J., Lammers, R.B., Shiklomanov, A.I., Shiklomanov, I.A. and Rahmstorf, S., 2002. Increasing river discharge to the Arctic Ocean. *Science* **298**: 2171–2173.

Prinsenberg, S.J., Loucks, R.H., Smith, R.E., and Trites, R.W., 1987. Hudson Bay and Ungava Bay runoff cycles for the period 1963 to 1983. *Canadian Technical Report of Hydrography and Ocean Sciences*, No. **92**. Physical and Chemical Sciences Branch. Department of Fisheries and Oceans.

Raymond, P.A., McClelland, J.W., Holmes, R.M., Zhulidov, A.V., Mull, K., Peterson, B.J., Striegl, R.G., Aiken, G.R. and Gurtovaya, T.Y., 2007. Flux and age of dissolved organic carbon exported to the Arctic Ocean: A carbon isotopic study of the five largest arctic rivers. *Global Biogeochemical Cycles* **21**: GB4011, doi:10.1029/2007GB002934.

Schaphoff, S., Heyder, U., Ostberg, S., Gerten, D., Heinke, J., and Lucht, W., 2013. Contribution of permafrost soils to the global carbon budget. *Environmental Research Letters* **8**: 014026. doi:10.1088/1748-9326/8/1/014026.

Schuur, E.A.G., Abbott, B., Koven, C.D., Riley, W.J., Subin, Z.M., 2011. High risk of permafrost thaw. *Nature* **480**: 32-33. doi: 10.1038/480032a

Smith, S.L. and Burgess, M.M., 2004. *Sensitivity of permafrost to climate warming in Canada*. Geological Survey of Canada, Bulletin 579: 24 pp.

Stein, R.S., and Macdonald, R.W. (Eds.) 2004, XIX. The organic carbon cycle in the Arctic Ocean. Berlin, Heidelberg, New York: Springer-Verlag. 382 pp.

Tarnocai, C., Canadell, J.G., Schuur, E.A.G., Kuhry, P., Mazhitova, G. and Simov, S., 2009. Soil organic carbon pools in the northern circumpolar permafrost region. *Global Biogeochemical Cycles* **23**: GB2023, doi:10.1029/2008GB003327.

Vogel, J. J., Southon, J.R., and Nelson, D.E., 1987, Catalyst and binder effects in the use of filamentous graphite for AMS. *Nuclear Instruments and Methods in Physics Research*, Sect. B, **29**: 50–56.

Vonk, J. E., Sanchez-Garcıa, L., Semiletov, I., Dudarev, O., Eglinton,T., Andersson,A., and Gustafsson,O, 2010. Molecular and radiocarbon constraints

on sources and degradation of terrestrial organic carbon along the Kolyma paleoriver transect, East Siberian Sea. *Biogeosciences* **7**: 3153–3166. doi:10.5194/bg-7- 3153-2010.

Woods, G.C., Simpson, M.J., Pautler, B.G., Lamoureux, S.F., Lafreniere, M.J., and Simpson, A.J., 2011. Evidence for the enhanced lability of dissolved organic matter following permafrost slope disturbance in the Canadian High Arctic. *Geochimica et Cosmochimica Acta* **75**: 7226–7241. doi:10.1016/j.gca.2011.08.013

Chapter 3: Hudson Bay soil profiles and the potential linkages of permafrost degradation and lignin biomarkers on the OC cycle of Hudson Bay

3.1 INTRODUCTION

Longer growing seasons, due to changes in soil thermal dynamics, have enhanced the sequestration of carbon in high latitude environments such as the Hudson Bay (Ping et al., 2008). The southern margins of Hudson Bay's drainage basins, located in discontinuous and sporadic zones of permafrost, are most susceptible to thermal and physical degradation due to their being within 1 or 2 degrees of thawing temperature (Woo, 1986; IPCC, 2007; Schuur et al., 2013). This degradation has now been documented in the discontinuous permafrost in the boreal peatlands of northern Manitoba and the east coast of HB in northern Quebec (Camill, 2005; Payette, et al., 2004). The increase in summer temperatures and precipitation in northern latitudes (Arndt et al., 2010; Wu et al., 2005) has resulted in permafrost degradation manifested as thermokarst development, a thickening of the active layer, and increased percolation of OM down the soil profile potentially increasing the release of deep, older SOC (Jorgenson et al, 2006; Gubin and Lupachev, 2008). Wetter and warmer soils will alter hydrologic flow paths and water storage causing the movement of groundwater into deeper soil horizons potentially influencing SOC storage and seasonal discharge of SOC to coastal shelves like Hudson Bay (McClelland et al., 2004; Iijima et al., 2010; Jorgenson et al., 2013). Upon thaw, sorption processes and microbial decomposition will further alter the storage and release of SOC (Schuur et al., 2013).

SOC pools in Arctic soils have been underestimated in past studies (Rodionov et al., 2007) and based on 139 frozen soils of the North American Arctic, 38% of the SOC is below the permafrost table (Ping et al., 2008; Tarnocai, 2009). The location of SOC in

the soil profile may prove useful in understanding the consequences of active layer (AL) thickening, including increased cryoturbation and altered hydrology of the landscape with permafrost thaw (Ping et al., 2008). The type of soil determines the variability and sensitivity to active layer thickness due to its response to surface temperatures and moisture (Woo et al, 2008; Smith et al, 2009). There have been few measurements of lignin composition in Arctic soils until recently and no soils have previously been measured for OC and lignin in the HB region. This chapter will discuss the composition of lignin and OC down the profile of six sampled permafrost soils collected from the Hudson Bay coastal lands and consider the impacts of permafrost degradation and active layer thickening on the distribution and potential release of SOC. We consider the influences of soil type, moisture content, vegetation and the potential for degradation of these soils using lignin reaction products and their ratios to make inferences about the potential release of SOC with future warming.

3.2 METHODS

3.2.1 Site Description

All samples were collected from the Hudson Bay region using the Canadian Coast Guard Ship *Amundsen* as a base while accessing sites by helicopter during Leg 1a of the 2010 expedition (July-August). Six sites in different vegetation and permafrost zones were selected and sampled from around the Hudson Bay watershed based on the CCGS Amundsen cruise track (Figure 3.1; Table 3.1, Appendix B). Weather and time constraints did not allow for sampling to occur on the southwest coast of HB.

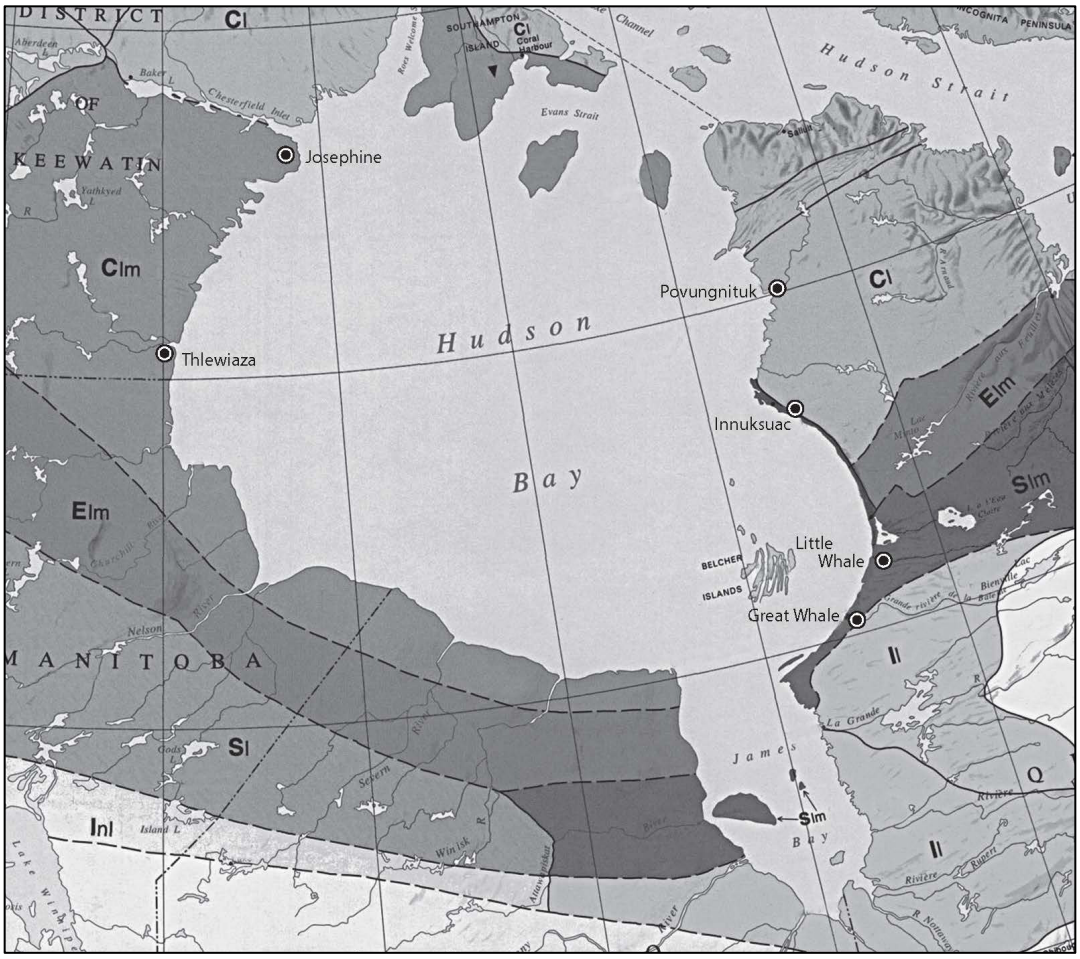

Figure 3.1: Site map for the soil sampling locations and permafrost zonation; Continuous (C), Extensive Discontinuous (E), Sporadic (S) and Isolated Patches (I). Adapted from Natural Resources Canada, 1995.

The Josephine River (63.13°N, -90.98°W), in the northwest coast of the HB, is located in the barren, low arctic ecoclimate of the Southern Arctic ecozone, with continuous permafrost and a landscape dominated by granitic tills and hummocky bedrock (Ecological Stratification Working Group, 1995). Mean annual temperature ranges from between -8°C to -11°C with a mean summer average of 6°C. Vegetation on site was typical of the Maguse River Upland ecoregion with sparse and low-lying shrub tundra, mainly herbaceous species (70%), with a small percent of lichen (3%), moss

(17%), and exposed rock (10%). Soil samples were taken from a site located approximately 20 km inland from the Josephine River mouth, 560 m from the riverbank at an altitude of 103 m above sea level (ASL). Soil was a Gleysolic Static Cryosol with a high percentage of clay and high pore ice content with a shallow AL within 6 cm of the surface. Permafrost table was not reached during the time period allotted for sampling.

The Thlewiaza River (60.52°N, -95.01°W) is located on the western coast of Hudson Bay and runs through the Southern Arctic ecozone near the coast to the Taiga Shield further inland. Mean annual temperature is approximately -8°C with a mean annual summer temperature between 6°C to 8°C, and the ecoclimate ranges from low arctic near the coast to high subarctic inland. Vegetation conforms to the Kazan River Upland ecoregion consisting of shrub tundra dominated by herbaceous cover (70%), including arctic willow, bilberry and Labrador tea, sphagnum moss (29%) and sedge/grass (1%). The soil sample was collected from the center of a polygon development approximately 0.7 m high from the fen edge located approximately 70 m from the riverbank and 7 km from the river mouth at about 40 m ASL. Permafrost is continuous in the region with hummocky bedrock, granitic tills, and polygon development. Soil consisted of Regosolic Cryosol with organic rich upper soil horizons and a 20 cm AL.

The Great Whale River (55.28°N, -77.76°W) is located in the southeast corner of HB in the Taiga Shield ecozone in the La Grande Hills ecoregion. The mean annual temperature is -4°C with a summer mean of 8.5°C and the region is considered to have a low subarctic ecoclimate. The vegetation consisted of forest tundra with open coniferous forests and/or tree islands transitioning to tundra shrub vegetation to the

north. This site was located in an upland region with no trees and an extremely high percent of moss (90%), mainly sphagnum, with only 7% herb and 3% grass. Soil was sampled approximately 1.1 km from riverbank at a distance of 2 km from the river mouth at an altitude of 9 m ASL. The soil was a Humic podzol: no ice found within the top meter of the surface, the depth sampled within the time allotted for sampling.

The Little Whale River (56.01°N, -76.54°W) is located on the southeastern shoreline of the HB in the Taiga Shield ecozone. It borders the region between low arctic to high subarctic ecoclimate with a mean annual temperature ranging from -4°C to -6°C. Average summer temperatures range from 6°C to 8.5°C. The sampling site was located in a forest tundra landscape between the La Grande Hills and the Southern Ungava Peninsula ecoregions, within a glacially scoured valley consisting of flagged spruce tree islands and polygonal peat plateaus. Vegetation was distributed between moss (50%), herbaceous cover (49%) and one small dwarf birch. Soil samples were collected from the center of a large palsa development approximately 7 km from riverbank and approximately 14 km from the river mouth at an altitude of 37 m ASL. The soil was an organic cryosol with a very high peat and OC content visible throughout the profile and a 29 cm AL.

The Innuksuac River (58.46°N, -78.02°W) is located on the northeastern shoreline of HB in the Southern Arctic ecozone. This region is considered a low arctic ecoclimate with a mean annual temperature of -7°C with a summer mean of 3.5°C. The site was consistent with its location within the Central Ungava Peninsula ecoregion consisting of low arctic shrub tundra with almost entirely herbaceous cover (90%) of Labrador tea, *Dryas spp*. with some moss (7%) and grass (3%). Soil sample was

collected 2.4 km from the riverbank approximately 4.5 km from the river mouth at an elevation of 49 m ASL. The soil was a regosolic static cryosol with high organic content in the upper soil horizon decreasing with an increasing sand content. The depth of the AL was only 15 cm to the permafrost table.

The Povungnituk River (60.05°N, -77.22°W) is located on the northeast coast of HB in the Southern Arctic bordering on the Northern Arctic ecozone. Vegetation was consistent with its location in the low arctic ecoclimate with shrub tundra consisting of mostly herbaceous cover (60%) followed by moss (37%) and grass (3%). The river itself also runs through the nearby Northern and Central Ungava Peninsula ecoregions. Mean annual temperature averages at -7°C with a summer mean of 3.5°C. Post-glacial marine beach deposits dominate the region, which was evident in the high sand content of the soil. The soil, which was sampled from the middle of a palsa development, was a static cryosol with high sand content in the lower soil horizons and the AL was 26 cm to the permafrost table.

3.2.2 Permafrost and soil samples

Soil sites were selected in relative proximity to the river sampling sites. Due to terrain and issues with landing, some sites were farther from the water-sampling site but within the same drainage system. We tested the top meter of the soil for the permafrost table using a 1.5 m metal rod. Soil pits were dug to classify soil type and determine active layer thickness when ice was present. Soil was sub-sampled from each soil horizon for further lab analysis. Either the entire active layer or in the case of soil, the profile, was sampled at 1 cm intervals and bagged for analysis. This was done by

cutting soil into a square of approximately 7 cm by 7 cm using a stainless steel saw knife and slicing each centimeter starting at the top and working down to bottom of profile or until permafrost table was reached. Once the permafrost table was reached, samples were collected with a coring auger with a Stihl 4308 model powerhead and a 7.6 cm diameter stainless steel core barrel that was supplied by the Geological Survey of Canada. Samples were then stored in ziploc bags and frozen until they were brought back to the laboratory on the Amundsen for slicing. Permafrost cores were sliced while frozen using a sawsall at 1 cm intervals but switching to 2 cm intervals further down the profile and then stored for analysis.

Vegetative analysis was completed at each site by randomly selecting a 10 m by 10 m vegetative plot close to the soil-sampling pit. A photograph was taken and percentage of ground cover between herb, moss, lichen, tree and grass was determined by bird's-eye view. Only one site had a dwarf tree (Little Whale) but, due to time constraints, the vegetative plot was not increased. Basic site characteristics were recorded with no time for samples and/or genus and species identification. All soil samples, except for the Great Whale, were taken from on top of a palsa or polygon development.

3.2.3 Laboratory Analyses

Soil and permafrost samples were shipped to the College of Earth, Ocean, and Atmospheric Sciences laboratory at Oregon State University (OSU) for chemical analysis. Every second sample was selected for analysis starting from the top layer and also those samples located above and below a soil horizon interface were selected.

These samples were analyzed for Total Organic Carbon (%TOC) and Total Nitrogen (TN) using a NC2500 Elemental Analyzer, and for lignin-derived phenols and non-lignin byproducts such as 3,5-dihydroxybenzoic acid using the alkaline CuO oxidation method to microwave digest samples. A complete description of these methods may be found in Chapter 2. In order to obtain OC content down the soil profile including cumulative OC, bulk density was calculated for each sample (g sediment/cm^3) and then converted to grams OC per cm^2 using OC% and then finally to gOC/m^2 per cm depth (Table 3.2, Appendix B). Cumulative OC content (gOC/m^2) was calculated for the entire soil profile depth of each soil and averaged into gOC/m^2 per cm depth.

Eight reaction products derived from lignin were measured; the Vanillyl (V-series) phenols, (vanillin, acetovanillone, vanillic acid), syringyl (S-series) phenols (syringaldehyde, acetosyringone, syringic acid), and cinnamyl (C-series) phenols (p-coumaric acid, ferulic acid). Lignin yields were obtained in units of ng of compound in total extract and then converted to C-normalized values in mg of compound/100mgOC based on the OC content and further converted to mg/m^2 per cm of depth (Table 3.2). Cumulative lignin content (mg/m^2) was calculated for the entire soil profile depth of each soil and averaged into mg/m^2 per cm depth. Lignin compositional ratios were calculated using syringyl to vanillyl (S/V), cinnamyl to vanillyl (C/V). Acid to Aldehyde ratios were calculated using the acidic to aldehydic functional groups for vanillyl ([Ad/Al]v) and syringyl ([Ad/Al]s) reaction products (Refer to methods in Chapter 2).

Stable and radiocarbon isotopic analysis was performed on the top layer of the six soil samples representing an even distribution across permafrost and vegetation zones on both east and west sides of Hudson Bay. Samples were pre-acidified and

analyzed for both $\Delta^{14}C$ (uncalibrated ages) and $\delta^{13}C$ at the National Ocean Science Accelerator Mass Spectrometry (NOSAMS) facility at Woods Hole Oceanographic Institution (WHOI).

3.3 RESULTS

3.3.1 Organic carbon and physical soil properties

Soil profiles depths ranged from 30 cm in the Innuksuac to 57 cm in the Little Whale (Figure 3.2). The Great Whale is the only soil where the permafrost table was not reached and therefore was not considered in the calculation of AL depths. The Josephine soil had ice in the pores starting at 6 cm but was not considered as part of the permafrost table as it was partially thawed. AL depths ranged from 15 cm in the

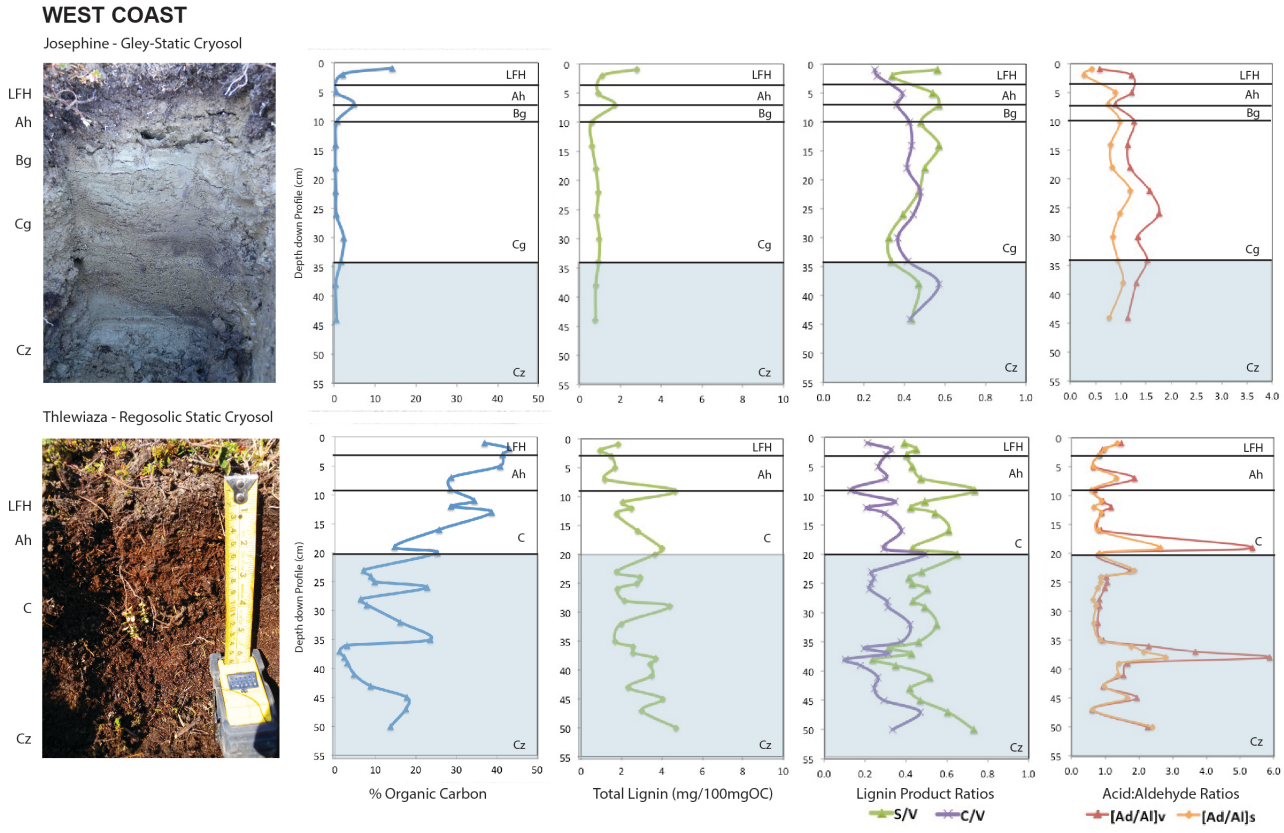

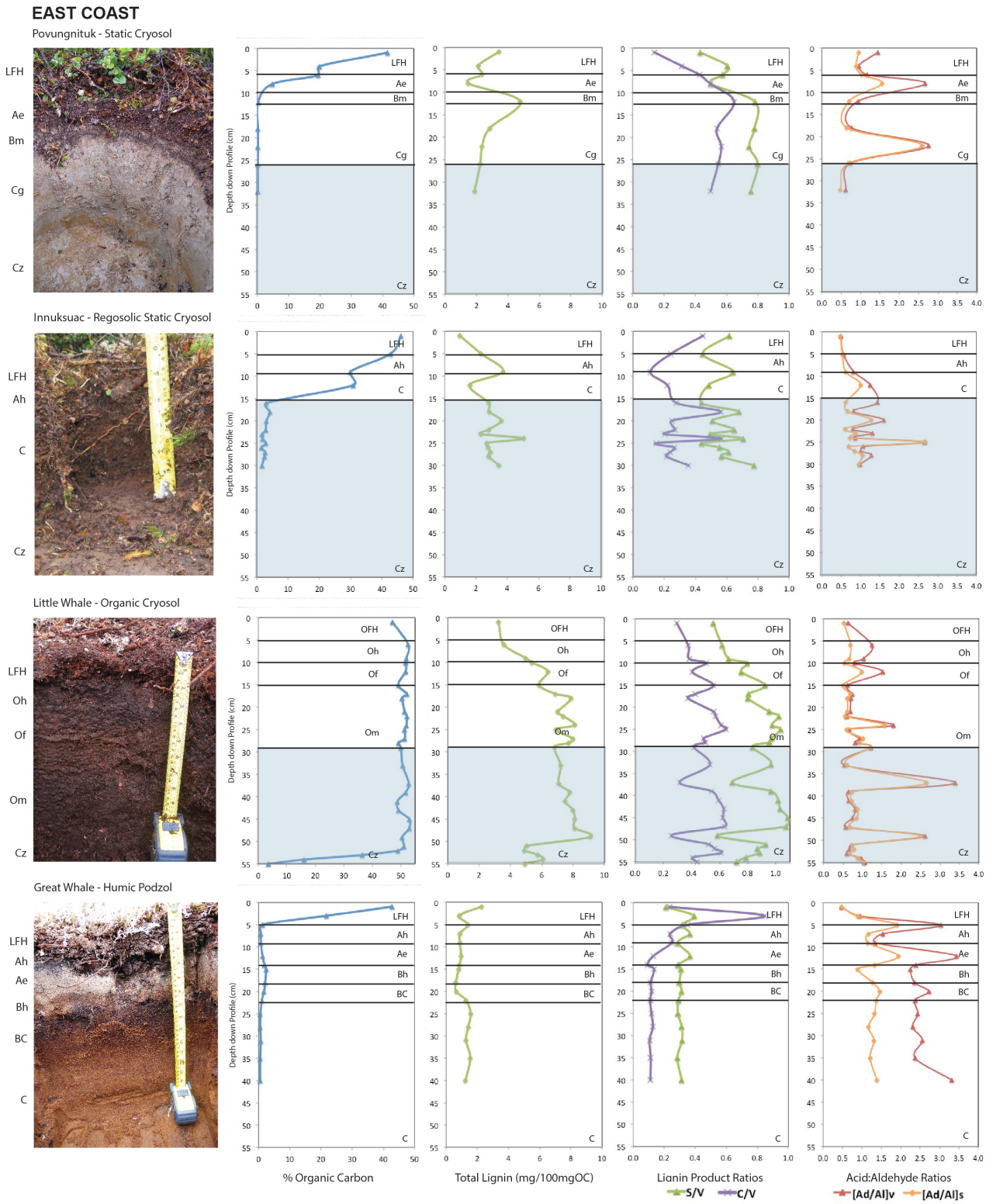

Figure 3.2: Six soil profiles of the HB with profile and horizon information on OC%, Total Lignin (mg/100mgOC), S/V and C/V ratios and [Ad/Al] ratios. Shaded horizon indicates the frozen layer (Cz) with the top being the permafrost table.

Innuksuac to 34 cm in the Josephine with an average of 19 cm for all six soils.

The average organic carbon content of soil by weight is 21% with each soil profile ranging from an average of 2.2% at the Josephine to 48% at the Little Whale (Table 3.1, Appendix B). All soils have high OC in the upper LFH and A horizons and decreased with depth, with the exception of the Little Whale soil profile that has high OC down the entire profile, and the Thlewiaza that has high OC down to the permafrost table (Figure 3.2). All soils, on average, have almost double the OC in the AL compared to the frozen Cz horizon although 30% of OC in all six soils is in the Cz horizon.

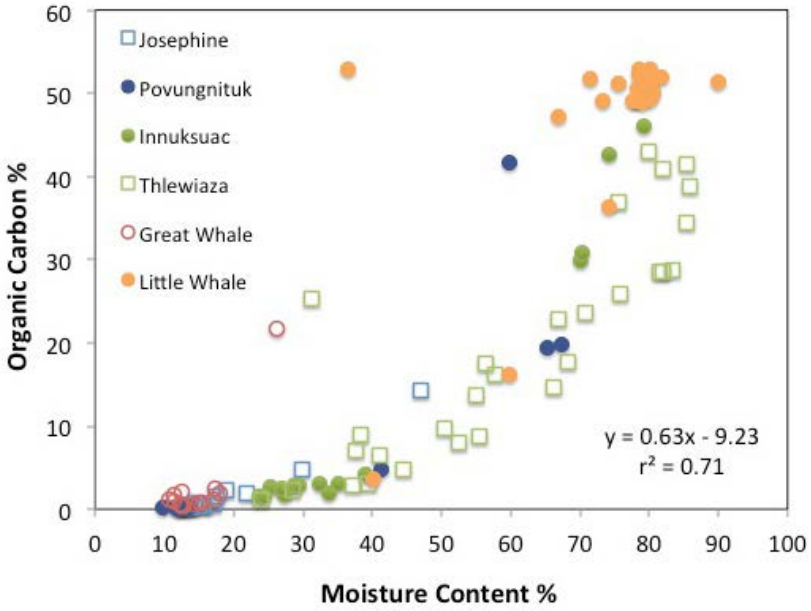

Figure 3.3: Relationship between organic carbon (OC%) and moisture content (MC%) for all samples collected from six soils, and the distribution of all six soils and their samples in relation to OC% and MC%. Color-coded by site ranging from blue in the north, then green, orange and red in the south.

Variation in OC down each soil profile (%RSD) ranged from 24% to as much as 241% in the Innuksuac, which has 29 times the OC in the LFH horizon compared to the bottom

of the Cz horizon. OC% is not well correlated to individual lignin reaction products and ratios. The strongest relationship, which was, nevertheless, weak, is found between OC% and total lignin, ∧8 (r^2 = 0.48, $p < 0.0001$). OC% is well correlated with % moisture content (MC%, Figure 3.3, r^2 = 0.71, $p \leq 0.0001$) with the Great Whale having the lowest OC% and MC% and the Little Whale having the highest.

On average, OC storage per cm depth in all six soils is 0.7 gOC/m^2 ranging from a profile average per cm of 0.30 gOC/m^2 for the Josephine to 1.27 gOC/m^2 for the Little Whale (Table 3.2, Appendix B). Cumulative OC content down each soil profile ranged from 7.5 gOC/m^2 in the Josephine (44 cm depth) to 52.2 gOC/m^2 in the Little Whale (57 cm depth). All soils, on average, have slightly higher OC content in the Cz horizon (0.8 gOC/m^2 per cm) compared to the AL (0.7 gOC/m^2 per cm). The average OC content in the Cz horizon is skewed by the high OC content in the Cz horizon of the Little Whale soil (1.5 gOC/m^2/cm), and if we exclude this sample, the average is only 0.5 gOC/m^2 per cm. Cumulative OC content in the AL averaged 10.6 gOC/m^2 with an average AL depth of 19 cm and ranged from 6.0 gOC/m^2 in the Josephine (34 cm AL depth) to 28.7 gOC/m^2 in the Little Whale (29 cm AL depth).

3.3.2 Lignin Yields of Soil Profiles

Total OC-normalized lignin yields (∧8) ranged from 0.59 to 9.10 mg/100mgOC (Table 3.2). The highest lignin concentrations were found in the Little Whale soil profile with an average of 6.63 mg/100mgOC and the highest value of 9.1 mg/100mgOC at 49 cm in the Cz horizon. The lowest concentrations were in the Josephine soil samples with an average of 1.1 mg/100mgOC. Variation in lignin concentrations down each soil

profile (%RSD) ranged from 22% to 56%: for example, the Josephine had 3 times the lignin in the LFH horizon compared to the Cz horizon. All frozen soils, excluding the Josephine samples, had an increase in lignin yields with depth with the highest values in the Cz horizon representing 52% of total lignin on average. The Great Whale had a high yield in both the LFH and the C horizon. The organic cryosol at Little Whale, and the regosolic static cryosols at Thlewiaza and Innuksuac, ranged from 33% to 49% lower lignin concentrations in the LFH compared to the average for each profile with the majority of lignin occurring at greater depths (Table 3.2, Figure 3.2). Lignin values correlated to %Nitrogen (r^2 = 0.62, $p \leq 0.0001$) and also to moisture content % (r^2 = 0.35, $p \leq 0.0001$).

Total lignin content per cm depth within all six soils averaged 39.2 mg/m^2 ranging from 8.58 mg/m^2 in the Josephine to 103 mg/m^2 in the Little Whale (Table 3.2). Cumulative lignin content down each soil profile ranged from as low as 112 mg/m^2 at the Josephine (44 cm depth) to 2871 mg/m^2 for the Little Whale (57 cm depth). All soils, on average, have slightly higher lignin content in the AL (39.0 mg/m^2 per cm) compared to the Cz horizon (31.9 mg/m^2 per cm), although the average does not reflect the high lignin content in the Cz horizon of the Little Whale (116 mg/m^2 per cm). Cumulative lignin content in the AL, of all six soils, averaged 396 mg/m^2 with an average of 19 cm depth and ranged from 98.6 mg/m^2 in the Josephine (34 cm AL depth) soil profile to 1245 mg/m^2 in the Little Whale soil profile (29 cm depth).

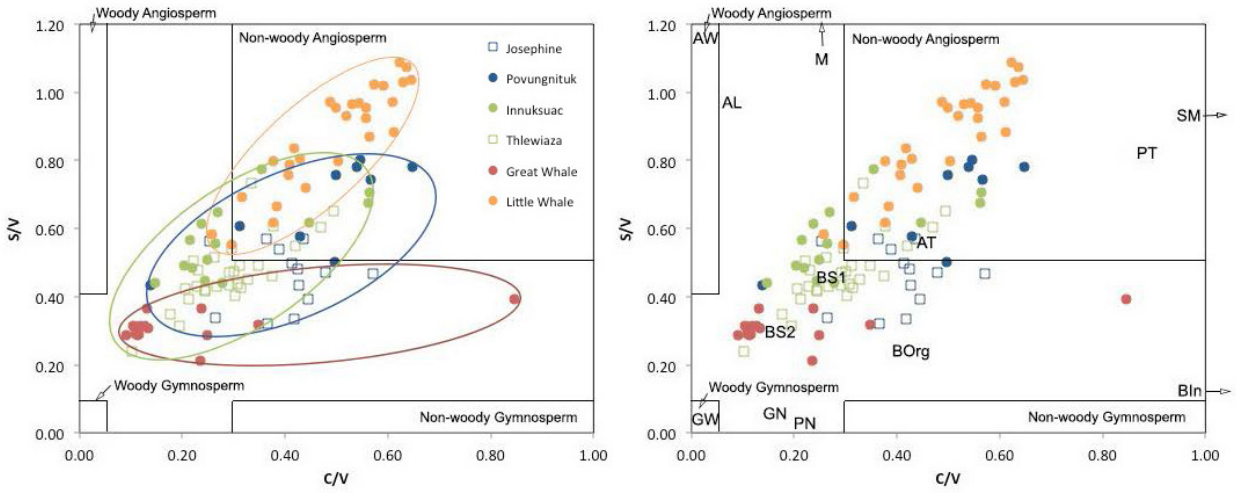

Figure 3.4: S/V and C/V ratios for the six soil profiles with A) circles representing the ranges of S/V and C/V ratios and coinciding vegetative properties and, B) the soil profiles in relation to previous ratios described by Amon et al., 2012 and Spencer et al., 2008). AT (alpine tundra), AL (angiosperm leaves), AW (woody angiosperm), BS (boreal soils), Borg (boreal organic soil), BIn (boreal inorganic soil), GN (gymnosperm needle), GW (woody gymnosperm), M (mosses), PN (*picea* needles), PT (peat), SM (sphagnum moss).

3.3.3 Lignin Composition

Four lignin product reaction ratios were calculated for this study: Syringyl to Vanillyl (S/V), Cinnamyl to Vanillyl (C/V), acid to aldehydic ratios for Vanillyl ([Ad/Al]v) and Syringyl ([Ad/Al]s). All ratios are shown down the entire soil profile (Table 3.2, Figure 3.2). S/V ratios ranged from 0.21 to 1.09 and C/V ratios ranged from 0.09 to 0.65. For both the S/V and C/V ratios, the soil profile average was the highest for the Little Whale (0.87, 0.49) and lowest for the Great Whale (0.31, 0.20). All soils S/V and C/V ratios were indicative of a non-woody angiosperm signal (high S/V and C/V, >0.4) with some samples having a small woody gymnosperm influence, with the exception of the Great Whale, which had a strong woody gymnosperm signal of low S/V ratios (Table 3.2, Figure 3.4). The S/V ratios of the Great Whale, which ranged from 0.2 to 0.4, lay between angiosperm and gymnosperm. Furthermore, the C/V ratio indicates non-woody

OC in the LFH but mainly woody OC (>0.25) as depth increases (Figure 3.2). When comparing the AL horizons to the Cz horizon, S/V ratios were on average higher in the Cz horizon of all soils except for the Josephine and Thlewiaza. The average C/V ratios are higher in the Cz horizon than the AL horizons for all six soil samples.

Acid to aldehyde ratios for Vanillyl ([Ad/Al]v) ranged from 0.48 to 5.87 and Syringyl ([Ad/Al]s) from 0.27 to 2.79. The highest average ([Ad/Al] ratios were for the Great Whale (2.24, 1.27) with the lowest average [Ad/Al]v at Little Whale (1.0) and the lowest average ([Ad/Al]s at the Josephine (0.82). Most soils were mild to moderately degraded with [Ad/Al] ratios >0.5 with some samples being moderately to highly degraded throughout the soil profile. The highest [Ad/Al] ratios and most degraded samples occurred at the 20cm and 38cm depths of the Thlewiaza (5.37, 5.87). All soils, except the Pavungnituk, had higher average [Ad/Al] ratios in the deeper, frozen Cz horizons compared to the AL mainly due to a few very highly degraded samples (>2.5).

3.4 DISCUSSION

3.4.1 Active layer thickening and soil response to OC and Lignin

These six soils contain a total inventory of 80 gOC/m^2 and 2.1 g/m^2 total lignin in the AL (average 19 cm), which undergoes seasonal freeze/thaw dynamics as surface temperatures warm in the spring and summer. The soils were sampled in July so the peak AL depth had not yet been reached. An increase in AL depth in these soils would result in the Cz horizon being exposed to thermal changes and thaw in summer months increasing their potential to release SOC. The Cz horizon in the sampled soils, on average, contains 0.8 gOC/m^2 and 32 mg/m^2 of lignin per cm of depth. Mineral soils,

such as the humic podzol found at the Great Whale, have an average of only 0.3 $gOC/m^2/cm$ below the LFH horizon (below 5cm depth) where the potential for adsorption increases and therefore they are not as likely to increase their release of OC with AL thickening as implied by the findings of Carey (2003) and Petrone et al. (2006). It is more likely that the organic cryosols, such as the Little Whale, will become OC sources with future permafrost degradation and thermokarst development with the potential release of as much as 1.5 gOC/m^2 per cm increase in AL depth. While the peat provides insulation, the increase in moisture and temperature eventually will cause the undecomposed Cz horizon to undergo rapid remobilization of SOC (Routh et al., 2014).

Soil moisture is an important component to permafrost sensitivity and AL depth with wetter sites being more susceptible to warming (Fan et al., 2011). Soil moisture is well correlated to OC% in all six soil samples (Figure 3.3) as was found in Baumann et al. (2009) suggesting that the organic carbon content of permafrost soils is influenced by soil moisture regimes, local topography, drainage and AL depth. Of the six soils, the Little Whale contains the highest OC content with an average of 1.3 gOC/m^2 per cm and 72% moisture content (Table 3.2) due to organic soils having a higher capillary capacity for water compared to mineral soils (Charman et al., 1998). The Little Whale, Thlewiaza and Innuksuac soils contain the highest average moisture content and are the only mineral soils that do not significantly decrease in moisture or lignin content with depth. The Thlewiaza and Innuksuac are both regosolic static cryosols with a lack of horizon development, which may explain the highly variable MC and OC values within the soil profiles. In fact, the Thlewiaza and the Innuksuac were the only mineral soils, where the

lignin content averaged greater than 10 mg/m^2 per cm depth in the Cz horizon (Table 3.2). While moisture content may facilitate heat penetration into the soil, soil type plays a role on how deeply OC is stored and whether it will be released by deepening hydrological flow.

3.4.2 Organic Carbon Storage within the Soil Horizons

The potential for permafrost soils to become a source of CO_2 instead of a sink with future warming scenarios has been modeled in several studies resulting in, for example, increased soil CO_2 efflux to the atmosphere from increased microbial activity due to warming and snow temperatures (Euskirchen et al., 2006) and the release of older SOC from peat soils into rivers such as the Yukon (Aiken et al., 2014). Microbial decomposition and thawing of deeper permafrost soil horizons both increase the probability of permafrost becoming an OC source compared to other scenarios (Schaphoff et al, 2013). With continued surface warming and newly exposed aerobic conditions, these previously undecomposed Cz horizons, would undergo increased microbial activity and thermal decay leading to organic decomposition and the mobilization of OC (Routh et al., 2014; Smith et al., 2009).

The Cz horizon has been shown to be vulnerable to the effects of AL thickening and thermokarst development due to a higher mineralization potential resulting in increased lability of OC (Gillespie et al, 2014). The Little Whale River is significant in that it is an organic, peat-rich cryosol with preserved deep SOC pools containing on average 1.5 gOC/m^2 per cm depth in the Cz horizon, double that of the average of all six soils. The Little Whale contains 41% of the total inventory of OC and 67% of the total

lignin of all six soils combined, with five times the OC and 10 times the lignin compared to mineral soils like the Povungnituk, Innuksuac and Josephine. It also contains the most OC and lignin in the Cz horizon (below permafrost table) compared to all other sites (Figure 3.2; Table 3.2). Therefore, the Little Whale soil has the greatest potential for release of OC with thermokarst development and AL thickening.

Mineral soils, like the ones found in this study, excluding the Little Whale, are also potential OC sinks with AL thickening as a result of increased exposure to deeper mineral horizons and the increased potential for abiotic adsorption of DOC (Parham et al., 2013). The potential release of SOC is influenced by the selective preservation of lignin phenols, the molecular complexity of the organic compounds found in the soil, and freeze/thaw dynamics all of which are controlled by permafrost dynamics such as thermokarst expansion, soil type and drainage (Routh et al, 2014). The soils in this study have a shallow AL containing a cumulative total of 79.7 gOC/m^2 and as the AL thickens and permafrost warms, there are two potential outcomes for OC as it is redistributed deeper within the soil horizons. A mineral soil with high clay content, such as the Josephine, may adsorb OC into the mineral soil matrix due to its high capacity to hold water or a well-drained sandy soil may percolate OC into much deeper soil horizons that may be stored until permafrost degradation allows for drainage of the site. The mineral soils in this study do not contain large amounts of OC in deeper soil horizons and are therefore not a potentially large OC source but rather may become a future storage site for OC as permafrost releases more OC into these mineral horizons.

3.4.3 Vegetative influence on soil profiles and carbon sources

The vegetative influence from the soil surface is reflected in the composition of lignin, in particular the S/V and C/V ratios, which vary among the six soils (Figure 3.4A). The S/V ratios of all six soils indicate angiosperm vegetation sources, although the Great Whale has the strongest indication of gymnosperm sources as reflected by low S/V ratios (<0.5). In their C/V ratios all six soils mainly reflect non-woody sources, although there were a number of individual samples containing lignins from woody sources in the Povungnituk, Thlewiaza and Innuksuac soils (Figure 3.2). Again the Great Whale was distinct from the other soils, exhibiting a wide range of C/V ratios spanning woody and non-woody sources, likely due to its southern location within the forest tundra ecotone and the boreal forest influence of the region. The vegetative composition and S/V and C/V ratios of these soils closely follow the ratios assigned to specific plant species and soils in other studies (Figure 3.4B; Spencer et al., 2008; Amon et al, 2012). The northernmost soils, Josephine and Povungnituk, exhibit alpine tundra ratios, the Thlewiaza and Innuksuac exhibit mixed boreal forest and tundra ratios, and the Great Whale exhibits a strong boreal forest ratio.

The Great Whale soil is a humic podzol, whereas the Little Whale soil is an organic cryosol. The humic podzol of the Great Whale contains the strongest indication of gymnosperm lignins (low S/V) of all the soils, likely due to the boreal forest setting (see, for example, Amon et al., 2012), whereas the organic cryosols of the Little Whale contain the strongest indication of angiosperms/peat (high S/V). Furthermore, the Little Whale soils exhibit the smallest range of C/V ratios indicating a tightly controlled source from non-woody vegetation. In contrast, the Great Whale exhibits a large range of C/V

ratios indicating varied contributions from woody and non-woody sources.. Both sites are in the forest tundra ecotone, but have few or no trees at the sampling site. Great Whale soil, with the highest average [Ad/Al] ratios, is highly degraded, which is typical for a podzol undergoing decomposition, vertical transport and the development of the Ae horizon due to leaching.

3.4.4 Biological alteration and sorption impact on OC composition

Phenolic compounds are found in much greater quantities at high latitudes due to preservation by cold temperatures and reduced microbial activity and decomposition (Roth et al, 2013). Vanillyl is also much more persistent than other phenols. Low S/V and C/V ratios can indicate microbial decomposition (Opsahl and Benner, 1998) and high [Ad/Al] ratios show highly oxidized and degraded OM. There is evidence to support sorption and other processes altering the lignin phenols and their ratios within these soil profiles. The Innuksuac site for example, has one spike of highly degraded sample with an [Ad/Al] ratios > 2.6 in the Cz horizon (Figure 3.2) coupled with very high amounts of Vanillic Acid (Vd) resulting in a decrease in S/V and C/V ratios. Other spikes occur in both the Little Whale and Thlewiaza sites within the Cz horizon. These spikes may be explained by selective sorption or degradation of Syringyl and Cinnamyl, which are more labile, leading to lowered ratios (Hernes et al, 2007; Woods et al, 2011).

The Thlewiaza has the highest [Ad/Al] ratios and therefore most degraded samples located in the C and Cz horizons. Ratios of 4.0 are considered the highest degraded samples according to Opsahl and Benner (1998) and other high ratios have been found in lake sediments (Pautler et al., 2010) and Melville Island watersheds

(Woods et al., 2011). The Thlewiaza has [Ad/Al] ratios over 5.5, which would make them the highest found to date in the Arctic. The Innuksuac, Thlewiaza and Little Whale sites all have peaks in the Cz that may represent a previous AL depth from previous years (Figure 3.2). Our sampling period did not coincide with peak summer temperatures and maximum AL depth that would have occurred somewhere around the end of August. AL depth becomes important when we consider the high mineralization potential of the Cz horizon and its susceptibility to decomposition with a drop in the permafrost table (Gillespie et al, 2014).

3.5 CONCLUSIONS

This study shows that soil type and the distribution of SOC within the soil profile are important factors determining whether soils are a potential sink or source of OC with future warming and increased precipitation. The sensitivity of permafrost soils in Hudson Bay to thermal and physical changes is moderate to high, especially in organic soils such as the Little Whale, with Cz horizons that have been preserved and contain as much as 1.5 gOC/m^2 per cm depth. Mineral soils, on the other hand, have the potential to rearrange the distribution of SOC as it percolates further down the soil profile, becoming buried or adsorbed into the mineral soil matrix. S/V and C/V ratios average 0.58 and 0.35, respectively, indicating non-woody angiosperm sources, typical of tundra. The Great Whale site has the only soil that reflects a strong boreal signal with low S/V ratios indicative of woody gymnosperm influences from the forest tundra ecozone of the southern coast of HB. With increased thermokarst development and migration of the treeline farther north, the surrounding vegetation shifts to a more fen

and an increase in woody gymnosperm species causing a decrease in S/V and C/V ratios in the active layer. Acid to aldehyde ratios, [Ad/Al]v and [Ad/Al]s, in some of these soils greater than 4.0 show very highly degraded SOC in deeper horizons and indicate the maximum thaw depth. With thickening of the AL, these ratios will increase in deeper soil horizons indicating an increase in degradation and potential for SOC release. The decomposition of deep soil OM may occur as much as 70 years after the initial period of warming and may become irreversible once initiated due to the additional heat from microbial activity (Khvorostyanov et al., 2008).

This is a first glimpse into OC and lignin profiles of permafrost soils spanning different ecozones and permafrost zones in the Hudson Bay region. This study provides an important baseline of carbon storage, including that of individual biomarkers found in the permafrost soils of HB. With permafrost thaw, the soils of the Hudson Bay have the potential to either increase the terrestrial inputs of SOC into rivers, with the exposure of deep SOC especially in organic rich cryosols, or to allow percolation and burial of OC deeper down the soil profile. Lignin biomarkers have provided important information of the vegetative sources of OC and shifts in their ratios will not only show us vegetation changes within the drainage basin but will indicate increases in decomposition as the soils are exposed to thermal and physical changes. The comparison of this OC and lignin inventory along with composition will prove useful in looking at riverine OC and lignin to ascertain if the rivers of Hudson Bay are reflecting the changes occurring in permafrost soils. This will have important relevance on future studies looking at river-dominated shelves in terms of OC sources and lignin composition and the terrestrial influence on shelf sediments.

3.6 APPENDIX B

Table 3.1: Permafrost/Cryosol Sampling Locations and Permafrost zonation with Hydrological and Ecological Site Characteristics. Sampling sites sorted by coastal location and ranked by latitude from north to south.

	East Coast				West Coast	
Rivers	**Povungnituk**	**Innuksuac**	**Little Whale**	**Great Whale**	**Josephine**	**Thlewiaza**
Latitude	60.05	58.46	55.97	55.27	63.13	60.52
Longitude	77.22	78.08	76.67	77.57	90.98	95.02
Drainage Basin (km^2)	28000	11200	11700	43200	N/A	27000
Annual Q[1] (km^3/yr)	11.9	3.3	3.7	19.8	2.5*	6.9
Permafrost	Continuous	Continuous	Sporadic-Discontinuous	Sporadic-Discontinuous	Continuous	Continuous
Soil Classification[3]	Static Cryosol	Reg Static Cryosol	Org-Cryosol	Humic Podzol	Gleysolic Static Cryosol	Reg Static Cryosol
Eco Zone[4]	S Arctic	S Arctic	Taiga Shield	Taiga Shield	S Arctic	SA/TS
Vegetation	Shrub Tundra	Tundra	Forest Tundra	Forest Tundra	Shrub Tundra	Shrub Tundra
Eco Region Code[5]	47	47	73	72	45	45, 70

[1] Annual Q discharge from HYDAT data, average from 1964-2000 from McClelland, 2006. *Estimated discharge based on nearby rivers discharge and size.
[2] Permafrost zonation based on percent of land underlain by permafrost; Continuous = 90-100%, Extensive discontinuous 50-90%, Sporadic discontinuous = 10-50%, Isolated patches = 0-10%; from Natural Resources Canada, 1995. Also displayed in Figure 1.
[3] Soil Classification based on Canadian System. Org = Organic; Reg = Regosolic (Scott, G.A.J., 2004).
[4] Vegetation Ecozones; SA= Southern Arctic, TS = Taiga Shield; Smith, 2010.
[5] Ecoregion codes; 45 = Maguse River Upland, 47 = Central Ungava Peninsula, 70 = Kazan River Upland, 71 = Selwyn Lake Upland, 72 = La Grande Hills, 73 = Southern Ungava Peninsula, 215 = Coastal Hudson Bay Lowland, 216 = Hudson Bay Lowland; Ecological Stratification Working Group, 1995.

Table 3.2: Organic carbon (OC) and lignin concentrations and content within the soil profile of six soils in the Hudson Bay region. Lignin product reaction ratios (S/V and C/V) and Acid to aldehyde ratios ([Ad/Al]v and [Ad/Al]s) of all six soils and their profile depths (cm). River sampling sites are separated into east and west coasts and listed in order from north to south.

Soil Profile (Depth in cm)*	%OC[1]	BD[2] (g/cm^3)	OC[3] (g/m^2)	Moisture %[4]	Lignin ∧8 (mg/100mgOC)[5]	Lignin ∧8 (mg/m^2)[6]	S/V[7]	C/V[7]	[Ad/Al]v[8]	[Ad/Al]s[8]
Povungnituk River										
0-2	41.7	0.23	1.94	59.9	3.43	66.6	0.43	0.14	1.44	0.95
4-6	19.9	0.41	1.65	67.3	2.11	34.8	0.61	0.31	0.95	0.89
6-8	19.5	0.82	3.19	65.2	2.35	75.1	0.58	0.43	1.17	1.03
8-10	4.71	2.71	2.55	41.3	1.47	37.7	0.50	0.50	2.67	1.55
12-14	0.25	5.89	0.29	12.7	4.78	14.1	0.78	0.65	0.93	0.70
18-20	0.15	2.68	0.08	9.80	2.84	2.29	0.78	0.54	0.76	0.65
22-24	0.15	3.13	0.09	11.5	2.35	2.21	0.74	0.57	2.76	2.59
26-28	0.12	4.00	0.10	12.1	2.22	2.14	0.80	0.55	0.74	0.69
30-32	0.14	2.13	0.06	13.6	1.87	1.12	0.76	0.50	0.61	0.48
Mean	**9.62**	**2.45**	**0.62**	**32.6**	**2.60**	**26.2**	**0.66**	**0.46**	**1.34**	**1.06**
SD	**±15**	**±1.8**	**±1.2**	**±26**	**±1.0**	**±29**	**±0.1**	**±0.2**	**±0.8**	**±0.7**
Innuksuac River										
0-4	46.1	0.05	0.92	79.2	0.95	8.77	0.62	0.45	0.49	0.47
4-6	42.7	0.18	1.52	74.1	2.32	35.2	0.45	0.24	0.55	0.53
8-10	29.9	0.39	2.31	70.1	3.73	86.1	0.64	0.11	0.82	0.61
11-13	30.9	0.33	2.06	70.4	1.60	32.8	0.48	0.22	1.24	1.00
C15-17	3.01	1.28	0.77	35.2	2.80	21.7	0.44	0.28	1.44	0.61
C17-19	4.24	1.09	0.92	39.0	2.84	26.2	0.68	0.56	0.81	0.65
C19-22	3.00	0.75	0.67	32.4	3.61	24.3	0.51	0.25	1.60	1.27
C22-23	2.81	1.33	0.37	28.7	2.80	10.4	0.65	0.27	0.79	0.59
C23-24	1.72	1.39	0.24	27.3	2.29	5.48	0.49	0.20	1.31	0.87
C24-25	1.85	0.87	0.16	33.7	5.03	8.14	0.71	0.57	0.85	0.72

Table 3.2 Continued…

Soil Profile (Depth in cm)*	%OC[1]	BD[2] (g/cm^3)	OC[3] (g/m^2)	Moisture %[4]	Lignin ∧8 (mg/100mgOC)[5]	Lignin ∧8 (mg/m^2)[6]	S/V[7]	C/V[7]	[Ad/Al]v[8]	[Ad/Al]s[8]
C25-26	2.92	0.96	0.28	29.5	2.69	7.50	0.44	0.15	2.66	2.68
C26-27	1.51	0.95	0.14	23.6	2.76	3.96	0.55	0.26	1.06	0.68
C27-28	2.69	1.17	0.31	25.3	2.92	9.16	0.61	0.24	1.01	0.85
C28-29	2.42	0.79	0.19	26.9	2.79	5.32	0.57	0.21	1.28	1.05
C29-30	1.58	0.87	0.14	24.4	3.47	4.78	0.77	0.35	0.98	0.95
Mean	**11.8**	**0.69**	**0.61**	**41.3**	**2.84**	**19.3**	**0.57**	**0.29**	**1.13**	**0.90**
SD	**±16**	**±0.5**	**±0.7**	**±21**	**±0.9**	**±21**	**±0.1**	**±0.1**	**±0.5**	**±0.5**
Little Whale River										
0-4.5	47.1	0.08	1.52	66.8	3.24	49.3	0.55	0.29	0.62	0.52
6-7	52.6	0.23	3.74	0.60	3.58	134	0.62	0.38	1.24	0.70
9-10	52.0	0.71	2.00	79.8	4.98	99.4	0.67	0.38	1.03	0.66
10-11	51.7	0.31	2.13	71.5	5.37	115	0.80	0.50	0.79	0.54
12-13	51.7	2.95	1.41	79.9	6.39	90.3	0.76	0.41	1.52	0.99
15-16	49.1	2.35	1.44	78.2	5.82	84.0	0.92	0.56	0.61	0.50
17-18	52.1	3.07	1.23	78.5	6.85	84.5	0.81	0.43	0.73	0.69
18-19	50.6	3.61	1.13	78.4	7.87	89.3	0.80	0.38	0.70	0.62
21-22	51.4	2.80	1.62	79.6	7.04	114	0.95	0.56	0.68	0.61
22-23	52.1	2.85	1.32	80.4	7.39	97.4	1.02	0.57	0.60	0.55
24-25	52.0	3.14	0.87	81.8	8.12	70.6	0.97	0.61	1.79	1.57
25-26	51.3	2.57	0.50	90.0	6.90	34.7	1.03	0.65	0.66	0.59
27-28	51.4	3.25	1.24	80.4	7.99	98.9	0.97	0.49	0.92	1.01
28-29	49.1	3.14	1.10	77.7	7.72	85.1	0.96	0.50	0.81	0.91
C29-31	50.0	3.03	0.94	80.7	6.83	64.2	0.83	0.42	1.21	1.21
C33-35	50.7	2.89	1.41	78.8	7.21	101	0.97	0.53	0.53	0.59
C37-39	52.8	3.53	1.38	78.6	7.08	97.8	0.69	0.32	3.39	2.65
C39-41	51.7	3.10	1.54	79.4	7.78	120	0.97	0.54	0.64	0.73

Table 3.2 Continued…

Soil Profile (Depth in cm)*	%OC[1]	BD[2] (g/cm^3)	OC[3] (g/m^2)	Moisture %[4]	Lignin ∧8 (mg/100mgOC)[5]	Lignin ∧8 (mg/m^2)[6]	S/V[7]	C/V[7]	[Ad/Al]v[8]	[Ad/Al]s[8]
C41-43	48.9	2.87	1.20	79.1	7.50	89.8	1.02	0.59	0.65	0.72
C43-45	49.3	3.01	1.49	80.2	8.00	119	1.03	0.63	0.81	0.87
C45-47	53.0	2.99	5.79	36.5	8.11	470	1.09	0.62	0.74	0.85
C47-49	53.0	2.99	1.69	80.2	8.09	137	1.07	0.64	0.56	0.68
C49-51	50.5	4.94	2.14	79.2	9.10	195	0.58	0.26	2.61	2.50
C51-52	51.1	2.06	1.08	75.5	5.05	54.8	0.93	0.52	0.70	0.74
C52-53	49.1	2.00	1.26	73.4	4.88	61.5	0.87	0.56	0.66	0.79
C53-54	36.4	2.30	0.86	74.2	5.74	49.4	0.88	0.61	0.60	0.67
C54-55	16.1	2.77	0.64	59.8	6.08	38.8	0.79	0.41	0.97	0.88
C55-57	3.63	2.29	0.56	40.1	4.95	27.9	0.72	0.44	1.07	1.03
Mean	**47.5**	**2.82**	**1.27**	**72.1**	**6.63**	**103**	**0.87**	**0.49**	**1.00**	**0.91**
SD	**±11**	**±0.6**	**±1.1**	**±18**	**±1.5**	**±80**	**±0.2**	**±0.1**	**±0.7**	**±0.5**
Great Whale River										
0-1	42.9	0.35	1.51	70.9	2.25	33.9	0.21	0.24	0.48	0.47
3-4	21.8	1.62	3.54	26.3	0.85	29.9	0.39	0.85	0.95	0.89
5-6	1.23	2.17	0.27	17.0	1.39	3.71	0.32	0.35	3.03	1.91
7-8	0.71	2.19	0.16	15.4	0.88	1.37	0.36	0.24	1.53	1.17
9-10	0.76	2.13	0.16	15.1	0.87	1.41	0.29	0.25	1.34	1.16
12-13	1.25	3.31	0.41	10.7	0.95	3.93	0.37	0.13	3.44	1.94
14-15	1.95	1.67	0.33	17.9	0.85	2.76	0.29	0.09	2.39	1.32
15-16	2.43	2.60	0.63	17.3	0.80	5.03	0.31	0.13	2.25	0.90
18-19	2.12	2.00	0.42	12.5	0.62	2.65	0.30	0.11	2.36	1.28
20-21	1.76	2.34	0.41	11.3	0.63	2.58	0.31	0.12	2.72	1.46
22-23	1.01	2.03	0.20	11.4	1.28	2.61	0.29	0.11	2.37	1.37
25-26	0.59	1.96	0.12	12.3	1.56	1.80	0.29	0.12	2.44	1.33
28-29	0.49	2.18	0.11	12.7	1.41	1.51	0.31	0.13	2.31	1.17

Table 3.2 Continued…

Soil Profile (Depth in cm)*	%OC[1]	BD[2] (g/cm^3)	OC[3] (g/m^2)	Moisture %[4]	Lignin ∧8 (mg/100mgOC)[5]	Lignin ∧8 (mg/m^2)[6]	S/V[7]	C/V[7]	[Ad/Al]v[8]	[Ad/Al]s[8]
31-32	0.67	2.05	0.14	14.3	1.27	1.75	0.31	0.11	2.56	1.31
34-36	0.48	1.92	0.18	12.6	1.54	2.84	0.29	0.11	2.37	1.21
38-40	0.49	2.43	0.24	12.4	1.24	2.95	0.31	0.11	3.32	1.39
Mean	**5.04**	**1.97**	**0.46**	**18.7**	**1.15**	**6.29**	**0.31**	**0.20**	**2.24**	**1.27**
SD	**±11**	**±0.6**	**±0.7**	**±15**	**±0.4**	**±10**	**±0.04**	**±0.2**	**±0.8**	**±0.4**
Josephine River										
0-1	14.2	1.29	1.83	47.1	2.80	51.2	0.56	0.25	0.58	0.43
2-3	2.00	2.50	0.50	21.8	1.12	5.62	0.34	0.26	1.21	0.27
5-6	0.44	1.28	0.06	15.8	0.90	0.51	0.54	0.39	1.22	0.89
C6-8	4.78	1.18	1.13	29.9	1.72	19.4	0.57	0.36	0.89	0.74
C10-12	0.70	2.34	0.33	14.6	0.59	1.93	0.48	0.42	1.26	0.98
C14-16	0.29	2.86	0.17	12.9	0.61	1.01	0.57	0.44	1.13	0.80
C18-20	0.25	2.36	0.12	13.8	0.79	0.94	0.50	0.41	1.18	0.83
C22-24	0.37	2.94	0.22	13.4	0.90	1.97	0.47	0.48	1.57	1.19
C26-28	0.48	3.18	0.31	15.5	0.84	2.55	0.39	0.44	1.75	0.98
C30-32	2.28	3.07	1.40	18.9	0.97	13.5	0.32	0.37	1.34	0.84
C34-36	1.60	3.19	1.02	17.6	0.93	9.48	0.34	0.42	1.52	0.94
C38-40	0.33	2.46	0.16	13.1	0.78	1.27	0.47	0.57	1.31	1.04
C42-44	0.57	2.43	0.28	17.0	0.78	2.16	0.44	0.43	1.14	0.77
Mean	**2.18**	**1.24**	**0.30**	**19.3**	**1.06**	**8.58**	**0.46**	**0.40**	**1.24**	**0.82**
SD	**±3.8**	**±1.3**	**±0.5**	**±9.5**	**±0.6**	**±14**	**±0.1**	**±0.1**	**±0.3**	**±0.2**
Thlewiaza River										
0-1	37.0	0.40	1.46	75.6	1.85	27.0	0.39	0.21	1.47	1.37
2-3	43.1	0.31	1.34	80.0	0.97	12.9	0.45	0.33	0.92	0.98
3-5	41.5	0.14	1.18	85.5	1.49	17.7	0.40	0.30	0.83	0.82

Table 3.2 Continued…

Soil Profile (Depth in cm)*	%OC[1]	BD[2] (g/cm^3)	OC[3] (g/m^2)	Moisture %[4]	Lignin ∧8 (mg/100mgOC)[5]	Lignin ∧8 (mg/m^2)[6]	S/V[7]	C/V[7]	[Ad/Al]v[8]	[Ad/Al]s[8]
5-6	40.9	0.23	0.93	82.1	1.67	15.6	0.43	0.27	0.66	0.64
7-8	28.8	0.36	1.03	83.3	1.20	12.4	0.48	0.30	1.86	1.34
9-10	28.6	0.24	0.70	81.5	4.68	32.8	0.74	0.13	0.69	0.60
11-12	34.5	0.29	1.01	85.5	2.06	20.9	0.49	0.35	0.93	0.90
12-13	28.6	0.51	1.45	82.0	2.50	36.2	0.42	0.21	1.18	0.65
13-14	38.8	0.29	1.11	85.8	1.75	19.4	0.54	0.30	0.89	0.89
16-17	25.8	0.34	0.88	75.9	2.82	24.5	0.61	0.38	0.86	0.77
C20-21	25.3	1.05	2.67	31.2	3.68	98.1	0.65	0.49	0.83	0.84
C23-24	7.13	1.04	0.74	37.7	1.77	13.2	0.48	0.23	1.72	1.87
C24-25	8.88	1.02	0.91	38.3	2.93	26.5	0.41	0.24	1.03	0.86
C25-26	9.81	0.81	0.79	50.4	2.79	22.1	0.43	0.23	1.05	0.86
C26-27	22.8	0.47	1.07	67.0	1.81	19.4	0.51	0.22	1.00	0.78
C28-29	6.45	1.08	0.70	41.0	2.17	15.1	0.44	0.31	0.82	0.64
C29-30	7.92	0.45	0.36	52.4	4.39	15.6	0.49	0.31	0.83	0.72
C32-33	16.2	0.43	0.69	57.7	2.00	13.9	0.55	0.42	0.77	0.66
C35-36	23.5	0.20	0.47	70.8	1.69	7.95	0.46	0.38	0.93	0.86
C36-37	2.97	0.82	0.24	37.3	2.60	6.36	0.32	0.19	2.28	1.77
C37-38	1.08	1.05	0.11	24.0	2.57	2.91	0.43	0.31	3.68	2.15
C38-39	2.29	0.71	0.16	28.5	3.69	5.97	0.24	0.10	5.87	2.79
C39-41	3.11	0.64	0.40	39.5	3.44	13.6	0.35	0.18	1.66	1.42
C41-43	4.78	0.48	0.46	44.6	3.49	16.0	0.52	0.26	1.54	1.38
C43-45	8.80	0.38	0.66	55.4	2.34	15.5	0.42	0.24	0.95	0.96
C45-47	17.8	0.22	0.80	68.3	4.03	32.2	0.47	0.29	1.94	1.66
C47-49.5	17.5	0.55	2.43	56.4	3.02	73.3	0.61	0.47	0.61	0.61
C49.5-52	13.8	0.39	1.35	55.0	4.70	63.3	0.73	0.33	2.26	2.41
Mean	**19.4**	**0.39**	**0.67**	**60.0**	**2.69**	**24.3**	**0.48**	**0.29**	**1.57**	**1.20**
SD	**±13**	**±0.4**	**±0.6**	**±20**	**±1.1**	**±21**	**±0.1**	**±0.1**	**±1.3**	**±0.6**

Table 3.2 Continued…

Soil Profile (Depth in cm)*	%OC[1]	BD[2] (g/cm^3)	OC[3] (g/m^2)	Moisture %[4]	Lignin ∧8 (mg/100mgOC)[5]	Lignin ∧8 (mg/m^2)[6]	S/V[7]	C/V[7]	[Ad/Al]v[8]	[Ad/Al]s[8]
Total Mean	**20.6**	**0.90**	**0.70**	**43.1**	**3.29**	**39.2**	**0.58**	**0.35**	**1.40**	**1.04**
SD	**±21**	**±1.0**	**±0.9**	**±28**	**±2.3**	**±57**	**±0.2**	**±0.2**	**±1.0**	**±0.5**

*Frozen horizon of the soil profile denoted by C in front of the depth.
[1] Organic Carbon Content % based on the amount of OC present in the total sample weight analyzed.
[2] Bulk density calculated from weight of dry soil divided by total soil volume of 7cm by 7cm soil slices. Depth of sample (cm) used in calculation.
[3] Organic Carbon (OC) in grams per cm^2 calculated from multiplying the fraction of OC% by the bulk density and then multiplying by the number of 1cm slices represented in each of the samples. Then converted to g/m2 by multiplying by 10.
[4] Moisture content % calculated by subtracting the oven-dried sample weight of the sample from the original wet weight (g) and multiplied by 100.
[5] Total sum of eight lignin reaction products from three series (∧8); Vanillyl, Syringyl and Cinnamyl series in mg/100mgOC.
[6] Lignin ∧8 (mg/m^2) calculated by multiplying the number of $100mgOC/m^2$ (divided gOC/m^2 by 0.1) by ∧8 (mg/100mgOC).
[7] S/V and C/V ratios are the ratios between lignin reaction product categories Vanillyl (V) to Cinnamyl (C) and Syringyl (S).
[8] [AD/Al] = Acid aldehydes product ratios reflecting ratio between acid (d) and aldehydes (l) of the Vanillyl and Syringyl groups, v = Vd/Vl and s = Sd/Sl.

3.7 REFERENCES

Aiken, G.R., Spencer, R.G.M., Striegl, R. G., Schuster, P. F., and Raymond, P. A., 2014. Influences of glacier melt and permafrost thaw on the age of dissolved organic carbon in the Yukon River basin. *Global Biogeochemical Cycles* **28**: 525–537. doi:10.1002/2013GB004764.

Amon, R.M.W., Rinehart, A.J., Duan, S., Louchouarn, P., Prokushkin, A., Guggenberger, G., Bauch, D., Stedmon, C., Raymond, P. A., Holmes, R.M., McClelland, J. W., Peterson, B.J., Walker, S.A., Zhulidov, A.V., 2012. Dissolved organic matter sources in large Arctic rivers. *Geochimica et Cosmochimica Acta* 94: 217-237.

Arndt, D.S., Baringer, M.O. and Johnson, M.R., Eds., 2010: State of the Climate in 2009. *Bulletin of the American Meteorological Society* **91** (7): S1–S224.

Camill, P., 2005. Permafrost thaw accelerates in Boreal peatlands during late 20th century climate warming. *Climatic Change* **68:** 135–152.

Carey, S.K., 2003. Dissolved organic carbon fluxes in a discontinuous permafrost subarctic alpine catchment. *Permafrost and Periglacial Processes* **14**: 161–171. doi:10.1002/ppp.444

Charman, P.E.V., and Murphy, B.W., 1998. Soils: their properties and management: a soil conservation handbook for New South Wales. Oxford University: Australia.

Ecological Stratification Working Group, 1995. A National Ecological Framework for Canada. Agriculture and Agri-Food Canada, Research Branch, Centre for Land and Biological Resources Research and Environment Canada, State of the Environment Directorate, Ecozone Analysis Branch, Ottawa/Hull. Report and national map at 1:7500 000 scale.

Euskirchen, E.S., McGuire, A.D., Kicklighter, D.W., Zhuang, Q., Clein, J.S., Dargaville, R.J., Dye, D.G., Kimball, J.S., McDonald, K.C., Melillo, J.M., Romanovsky, V.E. and Smith, N.V., 2006. Importance of recent shifts in soil thermal dynamics on growing season length, productivity, and carbon sequestration in terrestrial high-latitude ecosystems. *Global Change Biology* **12**: 731–750.

Fan, Z., Neff, J.C., Harden, J.W., Zhang, T., Veldhuis, H., Czimczik, C.I., Winston, G.C., and O'Donnell, J.A., 2011. Water and heat transport in boreal soils: Implications for soil response to climate change. *Science of the Total Environment* **409**: 1836–1842. doi:10.1016/j.scitotenv.2011.02.009

Gillespie, A.W., Sanei, H., Diochon, A., Ellert, B.H., Regier, T.Z., Chevrier, D., Dynes, J.J., Tarnocai, C., and Gregorich, E.G., 2014. Perennially and annually

frozen soil carbon differ in their susceptibility to decomposition: Analysis of Subarctic earth hummocks by bioassay, XANES and pyrolysis. *Soil Biology & Biochemistry* **68**: 106-116. http://dx.doi.org/10.1016/j.soilbio.2013.09.021

Gubin, S.V. and Lupachev, A.V., 2008. Soil Formation and the Underlying Permafrost. *Eurasian Soil Science* **41** (6): 574–585.

Hernes, P.J., Robinson, A.C., and Aufdenkampe, A.K., 2007. Fractionation of lignin during leaching and sorption and implications for organic matter ‘‘freshness.’’ *Geophysical Research Letters* **34**: L17401. doi:10.1029/2007GL031017

Iijima, Y., Fedorov, A.N., Park, H., Suzuki, K., Yabuki, H., Maximov, T.C. and Ohata, T., 2010. Abrupt increases in soil temperatures following increased precipitation in a permafrost region, Central Lena River Basin, Russia. *Permafrost and Periglacial Processes* **21**: 30–41, doi:10.1002/ppp.662.

IPCC, 2007. Technical Summary, *Climate Change 2007: The Physical Science Basis. Contribution of Working Group I to the Fourth Assessment Report of the Intergovernmental Panel on Climate Change*. Solomon, S., Qin, D.M., Manning, Z., et al., Cambridge, N.Y: Cambridge University Press, 2007.

Jorgenson, M.T., Shur, Y.L. and Pullman, E.R., 2006. Abrupt increase in permafrost degradation in Arctic Alaska. *Geophysical Research Letters* **33**: L02503. doi:10.1029/2005GL024960.

Jorgenson, M.T., Harden, J., Kanevskiy, M., O’Donnell, J., Wickland, K., Ewing, S., Manies, K., Zhuang, Q., Shur, Y., Striegl, R., and Koch, J., 2013. Reorganization of vegetation, hydrology and soil carbon after permafrost degradation across heterogeneous boreal landscapes. *Environmental Research Letters* **8**: 035017. Doi:10.1088/1748-9326/8/3/035017.

Khvorostyanov*,* D.V., Ciais, P., Krinner, G., Zimov, S.A., Corradi, C. and Guggenberger, G., 2008. Vulnerability of permafrost carbon to global warming. Part II: sensitivity of permafrost carbon stock to global warming. *Tellus* **60**B: 265–275, doi:10.1111/j.1600- 0889.2007.00336.x.

McClelland, J.W., Holmes, R.M., Peterson, B.J., and Stieglitz, M., 2004. Increasing river discharge in the Eurasian Arctic: Consideration of dams, permafrost thaw, and fires as potential agents of change. *Journal of Geophysical Research* **109**: D18102. doi:10.1029/2004JD004583, 2004.

McClelland, J.W., Dery, S.J., Peterson, B.J., Holmes, R.M., and Wood, E.F., 2006. A pan-arctic evaluation of changes in river discharge during the latter half of the 20th century. *Geophysical Research Letters* **33**: L06715. doi:10.1029/2006GL025753.

Natural Resources Canada, 1995. The Atlas of Canada – 5th Edition National Atlas of Canada. Government of Canada, Canada Centre for Remote Sensing, GeoAccess Division; Ottawa, Ontario. http://apps1.gdr.nrcan.gc.ca/mirage/full_result_e.php?id=205314.

Opsahl, S., and Benner, R., 1998. Photochemical reactivity of dissolved lignin in river and ocean waters. *Limnology and Oceanography* **43** (6): 1297-1304.

Parham, L.C., Prokushkin, A.S., Pokrovsky, O.S., Titov, S.V., Grekova, E., Shirokova, L.S., and McDowell, W.H., 2013. Permafrost and fire as regulators of stream chemistry in basins of the Central Siberian Plateau. *Biogeochemistry* **116** (1-3): 55-68. doi: 10.1007/s10533-013-9922-5

Pautler, B.G., Austin, J., Otto, A., Stewart, K., Lamoureux, S.F., and Simpson, M.J., 2010. Biomarker assessment of organic matter sources and degradation in Canadian High Arctic littoral sediments. *Biogeochemistry* **100**: 75–87. doi:10.1007/s10533-009-9405-x

Payette, S., Delwaide, A., Caccianiga, M. and Beauchemin, M., 2004. Accelerated thawing of subarctic peatland permafrost over the last 50 years. *Geophysical Research Letters* **31**: L18208, doi:10.1029/2004GL020358.

Petrone, K.C., Jones, J.B., Hinzman, L.D., and Boone, R.D., 2006. Seasonal export of carbon, nitrogen, and major solutes from Alaskan catchments with discontinuous permafrost. *Journal of Geophysical Research* **111**: G02020. doi:10.1029/2005JG000055,

Ping, C., Michaelson, G.J., Jorgenson, M.T., Kimble, J.M., Epstein, H., Romanovsky, V.E. and Walker, D.A., 2008. High stocks of soil organic carbon in the North American Arctic region. *Nature Geoscience* **1**: 615-619. doi:10.1038/ngeo284.

Rodionov, A., Flessa, H., Grabe, M., Kazansky, O.A., Shibistova, O. and Guggenberger, G., 2007. Organic carbon and total nitrogen variability in permafrost-affected soils in a forest tundra ecotone. *European Journal of Soil Science* **58**: 1260–1272. doi: 10.1111/j.1365-2389.2007.00919.x.

Roth, V.-N., Dittmar, T., Gaupp, R., and Gleixner, G., 2013. Latitude and pH driven trends in the molecular composition of DOM across a north south transect along the Yenisei River. *Geochimica et Cosmochimica Acta* **123**: 93–105. http://dx.doi.org/10.1016/j.gca.2013.09.002

Routh, J., Hugelius, G., Kuhry, P., Filley, T., Tillman, P.K., Becher, M., and Crill, P., 2014. Multi-proxy study of soil organic matter dynamics in permafrost peat deposits reveal vulnerability to climate change in the European Russian Arctic. *Chemical Geology* **368**: 104–117. http://dx.doi.org/10.1016/j.chemgeo.2013.12.022

Schaphoff, S., Heyder, U., Ostberg, S., Gerten, D., Heinke, J., and Lucht, W., 2013. Contribution of permafrost soils to the global carbon budget. *Environmental Research Letters* **8**: 014026. doi:10.1088/1748-9326/8/1/014026

Schuur, E. A. G., Abbott, B.W., Bowden, W.B., Brovkin, V., Camill, P., Canadell, J. G., Chanton, J. P., Chapin III, F. S., Christensen, T. R., Ciais, P., Crosby, B. T., Czimczik, C.I., Grosse, G., Harden, J., Hayes, D.J., Hugelius, G., Jastrow, J.D., Jones, J.B., Kleinen, T., Koven, C.D., Krinner,G., Kuhry, P., Lawrence, D.M., McGuire, A.D., Natali, S.M., O'Donnell, J.A., Ping, C.L., Riley, W.J., Rinke, A., Romanovsky, V.E., Sannel, A.B.K., Schädel, C., Schaefer, K., Sky, J., Subin, Z.M., Tarnocai, C., Turetsky, M.R., Waldrop, M.P., Walter Anthony, K.M., Wickland, K.P., Wilson, C.J., and Zimov, S.A., 2013. Expert assessment of vulnerability of permafrost carbon to climate change. *Climatic Change* **119**: 359–374. doi:10.1007/s10584-013-0730-7.

Smith, S.L., Wolfe, S.A., Riseborough, D.W., and Nixon, F.M., 2009. Active-layer characteristics and summer climatic indices, Mackenzie Valley, Northwest Territories, Canada. Permafrost and Periglacial Processes 20: 201-220. doi:10.1002/ppp.651.

Smith, S. 2011. Trends in permafrost conditions and ecology in northern Canada. *Canadian Biodiversity: Ecosystem Status and Trends 2010*, Technical Thematic Report No. 9. Canadian Councils of Resource Ministers. Ottawa, ON. iii + 22 p. http://www.biodivcanada.ca/default.asp?lang=En&n=137E1147-1

Soil Classification Working Group, 1998. The Canadian System of Soil Classification, 3rd ed. Agriculture and Agri-Food Canada Publication 1646. 187 pp.

Spencer, R.G.M., Aiken, G.R., Wickland, K.P., Striegl, R.G., and Hernes, P.J., 2008. Seasonal and spatial variability in dissolved organic matter quantity and composition from the Yukon River basin, Alaska. *Global Biogeochemical Cycles* **22**: GB4002. doi:10.1029/2008GB003231.

Tarnocai, C., Canadell, J.G., Schuur, E.A.G., Kuhry, P., Mazhitova, G. and Simov, S., 2009. Soil organic carbon pools in the northern circumpolar permafrost region. *Global Biogeochemical Cycles* **23**: GB2023, doi:10.1029/2008GB003327.

Woo, M., 1986. Permafrost hydrology in North America. *Atmosphere-Ocean* **24** (3): 201-234. http://dx.doi.org/10.1080/07055900.1986.9649248.

Woo, M., Kane, D.L., Carey, S.K. and Yang, D., 2008. Progress in permafrost hydrology in the new millennium. *Permafrost and Periglacial Processes* **19**: 237–254. doi:10.1002/ppp.613.

Woods, G.C., Simpson, M.J., Pautler, B.G., Lamoureux, S.F., Lafreniere, M.J., and Simpson, A.J., 2011. Evidence for the enhanced lability of dissolved organic matter following permafrost slope disturbance in the Canadian High Arctic.

Geochimica et Cosmochimica Acta **75**: 7226–7241. doi:10.1016/j.gca.2011.08.013

Wu, P., Wood, R. and Stott, P., 2005. Human influence on increasing Arctic river discharges. *Geophysical Research Letters* **32**: L02703. doi:10.1029/2004GL021570.

Chapter 4: Conclusions and closing remarks

4.1 INTRODUCTION

Recent changes to the hydrological regime of the Arctic, including Hudson Bay (HB), have made us question the influence of permafrost degradation as a mechanism for altered stream flow and organic carbon (OC) flux (Dery et al., 2009; McClelland et al., 2004). The interactions at the terrestrial marine interface provide us with valuable information in terms of the influx of OC from rivers into the HB. Little is understood in the specifics of sources of both dissolved and particulate OC (DOC, POC) entering the Hudson Bay marine environment and the vegetative composition of the OM carried by rivers and hence the potential inputs from permafrost. This chapter summarizes the major findings of the previous chapters and then uses this information to determine the potential linkages between permafrost soil, river DOC and POC, and their overall impact on HB sediments and the OC cycle of HB. PCA analysis using lignin reaction products is used to compare the composition of both dissolved and particulate organic matter (DOM, POM) of Hudson Bay Rivers (HBRs) with permafrost soils.

4.2 SUMMARY OF FINDINGS

4.2.1 The major contributors of OC and lignin in Hudson Bay

Considering all measured parameters (TSS, TDS, POC, DOC and lignin phenols) for all samples, the five southwest HBRs account for ~70% of the total annual discharge of all the sampled rivers combined and have total dissolved and particulate solid concentrations 2.5-fold higher than the mean. In fact, the five southwest HBRs contribute 89% of the total annual flux of OC and lignin into the Bay with 46% coming

from the Nelson River, which is consistent with other studies (Granskog et al., 2007). This high influx is due to the fact that 47% of the Hudson Bay basin drains from the prairies and northwestern Ontario and represents a significant component of the overall discharge into Hudson Bay (Prinsenberg et al, 1987; Dery et al, 2005).

The dominant flux of OC and lignin into the southwest HBRs is due to a combination of the southern extent of the watershed, the influence of upstream vegetation and increased access to carbon pools, permafrost distribution along the coast that decreases farther inland, and increased temperatures and moisture. This region of the HB drainage has more diverse influence from vegetation including mixed boreal forest and prairies from the south, and the treeline extends northward almost to the coast. Also, extensive peatlands and bogs are part of the Hudson Bay Lowland Ecoregion, which influences the influx of OC and lignin into these five southwest HBRs. A small, continuous band of permafrost is located along the coastline but this quickly deteriorates to discontinuous and sporadic permafrost inland due to the reduced cooling effect of the Hudson Bay and an increase in temperatures caused by southern air masses. The overwhelming dominance of the southwest therefore has a major impact in the Hudson Bay on OC cycling and the distribution of lignin and OC within HB ocean sediments, at least in the southern reaches of the Bay.

DOC dominates the concentration (88%) and annual flux (93%) of OC entering the HB from these rivers. The Nelson River DOC contributions alone represent 41% of the total OC annual flux for all HBRs that further validates the importance of the southwest region in terms of OC contributions. A similar DOC concentration contributing 82% of TOC has also been reported for Russian Arctic rivers showing the importance of

the dissolved phase in OC terrestrial inputs (Lobbes et al, 2000). Of all the HBRs, only the Josephine River has a particulate phase dominating the dissolved in terms of concentration and annual flux. This may be explained by the low vegetation cover, which has reduced potential OM sources, coupled with the clay-rich mineral soil and its increased capacity for retaining water. The clay-rich soil in this region of continuous permafrost along with the slow degradation of plant detritus likely limits the production and export of DOC. It has also been shown that rivers of the northeast HB, draining from continuous permafrost, have low DOC concentrations most likely due to the restrictions of continuous permafrost which limit active layer depth and soil moisture resulting in reduced hydrologic flow and the release of DOM into rivers (Granskog et al., 2007; Margesin, 2009).

4.2.2 Organic Cryosols a potential source of OC with a warming climate

Permafrost soils of the Hudson Bay Drainage Basin presently store large amounts of OC, averaging 0.7 g OC/m^2 per cm depth in the active layer and as much as 1.5 g OC/m^2 per cm in deeper Cz horizons of organic cryosols, like the Little Whale. When we consider the size of the Little Whale River drainage basin (11,700 km^2, Table 2.1), and its location within the sporadic/discontinuous permafrost zone, it contains a substantial OC reservoir vulnerable to release with permafrost thaw. As permafrost thaws and water shifts down the soil profile, the AL deepens and with every cm increase in depth results in an increased risk of deeper soil horizons releasing SOC due to microbial decomposition (Frey and McClelland, 2009). What becomes a concern for DOC inputs into the Hudson Bay, is whether permafrost degradation will lead to an

increase or decrease in DOC transport by HBRs. With warming, organic-rich cryosols, such as the Little Whale, are more likely to become OC sources due to their lack of a mineral horizon reducing the potential for sorption and burial of OC.

Mineral soils, like the Povungnituk static cryosol, are more likely to become an OC sink due not only to their low OC content (average 0.5 gOC/m^2 per cm depth) but also soil texture which will determine their potential response to active layer thickening and OC storage or export. Increased percolation adds moisture to deeper soils, which facilitates decomposition of OM and depending on permafrost hydrology and OC storage will influence DOC burial or export. In well drained soils with a high sand content, a deeper active layer would likely release less DOC into rivers and store more OC in deeper mineral soil horizons due to downward percolation (Aiken et al., 2014; Parham et al., 2013). In clay-rich mineral soils, a deepening of the AL as a result of warming will result in the leaching of OC down the profile increasing the potential for mineralization and sorption of DOC (Carey, 2003; Petrone et al., 2006). This may lead to permafrost-degraded soils remaining a sink for OC as SOC is stored in deeper layers over time. However, the increase in soil-water storage capacity over longer periods of time coupled with increased precipitation and warming, will increase subsurface flow to rivers and may expose deeper horizons to DOC export. Increased AL thaw depths over longer periods of time will further increase the potential lability of OC within all soils of the study region resulting in increased potential for OC in upper horizons to be released into rivers.

4.2.3 S/V and C/V ratios reflect regional vegetation in both rivers and soil

The clearest trend in river lignin composition is the increase in S/V and C/V ratios from south to north in both DOM and POM. This trend reflects vegetation, which goes from a transitional mixed forest-tundra environment in the south to a more barren, sparsely vegetated tundra in the north. The higher S/V and C/V ratios on moving northward reflect the shift from woody gymnosperms to non-woody angiosperms typical of tundra vegetation (e.g., see Kuzyk et al, 2008). The particulate phase is dominated by lower C/V ratios representing woody vegetation and S/V ratios that do not correlate with latitude. Selective fractionation of lignin phenols resulting in the sorption of leachates back into the soils such as the selective sorption of Vanillyl may be reflected in the variability in S/V ratios for POM (Hernes et al., 2007; Woods et al., 2011).

The S/V and C/V ratios in the soil profiles reflect either a tundra-dominated landscape or boreal influences from the Forest-Tundra Ecotone. Two soils, the Thlewiaza and Innuksuak, had peaks of woody lignin (low C/V) within the soil profile suggesting some influence from Boreal Forest ecozones nearby while the Povungnituk showed only one such peak in the surface OM horizon (LFH), which may have been a woody plant or possibly a root (Chapter 3, Figure 3.2). The Great Whale soils, which had the strongest gymnosperm (low S/V) signal of all six soils, was located in an ecoregion with closed stands of boreal forest and a transition to open stands and tundra. The Little Whale has a high OC and lignin content with some of the highest S/V ratios (>1.0) indicating a dominance of low shrub tundra with little influence from woody species. While the soils were different types, neither exhibited cryoturbation or significant changes to vegetative sources within the soil profile. The Great Whale is a

typical humic podzol with evidence of leaching down the profile, for which we would expect highly variable S/V and C/V ratios reflecting sorption or degradation processes. Instead, the lignin ratios, especially for S/V, remained constant down the entire profile. These two soils seem to reflect the vegetative influence of the surrounding area rather than soil type or permafrost distribution.

4.2.4 ^{14}C ages and [Ad/Al] ratios show release of old, preserved SOC

The ^{14}C ages of the DOM in HBRs, when coupled with [Ad/Al] ratios, give insight into the complex nature of permafrost hydrology and how freshness of samples does not always indicate young in terms of OC sources. Young DOM found in HBRs, had high [Ad/Al] ratios indicative of high decomposition, possibly microbial, indicating that permafrost soils are not yet releasing older deep Cz horizon OM, with the exception of the Churchill and the Nastapoka Rivers. The Churchill and Nastapoka Rivers were older than the other HBRs (2840 YBP), containing lower [Ad/Al] ratios, which are consistent with fresher plant material, signifying that OM preservation within the Cz horizons is most likely keeping SOM fresh. The Churchill River had a very high lignin content in DOM (µg/L), contrary to the relationship found by Amon et al., (2012) that Arctic rivers with higher lignin concentrations generally have modern DOM. The Churchill River has undergone modification from hydroelectric development with the creation of the Churchill Diversion that may be influencing riverbank erosion resulting in alteration of DOM ^{14}C ages, composition and level of degradation.

The older ^{14}C ages of DOM coupled with the lower than expected [Ad/Al] ratios of DOM in the Churchill and Nastapoka Rivers may indicate that the terrain is undergoing

erosion releasing older and deeper materials to the rivers. Looked at this way, the freshness of the lignins would be due to preservation within permafrost, which is now thawing and releasing them, a phenomenon also shown for Russian Arctic rivers (Gustaffson et al, 2011; Vonk et al, 2010). With warming, the increased release of older SOC may be masked by the simultaneous increase in young surface SOC entering HBRs altering ^{14}C ages of riverine OC (Feng et al., 2013). The ^{14}C ages of DOM is expected to increase with a decrease in soil moisture content as groundwater drains with permafrost thaw and deeper soil horizons become an increasingly more important source of OC (Aiken et al., 2014; Benner et al., 2004). The use of lignin reaction products and ^{14}C ages in determining OC sources in the Arctic show promising results when deciphering the complexity of the terrestrial OC inputs into HB.

4.2.5 Sorption and other soil processes shown by [Ad/Al] ratios

The acid to aldehyde ratios, [Ad/Al]v and [Ad/Al]s, reflected the level of degradation of OC sources in not only HBRs, but also within the soil profiles. The location of peaks in both [Ad/Al] ratios are important indicators reflecting the maximum active layer depth and a historical record of soil OM degradation processes. There were high peaks in [Ad/Al] ratios of the Little Whale, Thlewiaza and Povungnituk soils showing an increase in decomposition at specific depths. In particular, the Cz horizon of the Thlewiaza soil showed very high [Ad/Al] ratios (>5.0) at the 16 cm and 37 cm depths. The [Ad/Al] ratio peaks within the Cz horizon may be a historical record showing periods of years when decomposition rates were higher and over time these former surface OM layers were buried and today constitutes part of the Cz horizon. They may

also represent a previous year thawing depth which would indicate that the maximum active layer depth for the 2010 summer season may not have been reached during the sampling period. Warmer temperatures resulting in increased thermokarst development, AL thickening and moisture content will increase microbial activity and mineralization resulting in higher [Ad/Al] ratios in the Cz horizon, a possible indicator of OC sorption or export of older DOC into HBRs (Kawahigashi et al., 2004; Aiken et al., 2014).

4.3 INTERCONNECTIONS BETWEEN PERMAFROST AND RIVERS

PCA analysis was conducted on six soil sites with a total of 110 individual soil samples and 17 river samples of both DOM and POM (Figure 4.1 and 4.2). The analysis was conducted in Systat using a correlation matrix. The eight lignin phenols are expressed as % contribution to measured total lignin. The first principal component (PC1) explains 39% of variance, PC2 explains 23%, and PC3 explains 13% (thus total variance explained by first 3 components = 75%). Syringyl aldehyde (Sl) has a strong positive loading on PC1 and Vanillyl aldehyde (Vl) has a strong negative loading on PC2 (Figure 4.1A). PC1 also has strong negative loadings of Vanillyl ketones and acids (Vn and Vd) while PC2 has strong positive loadings of Cinnamyl (Fd, PCd) acids and Syringyl (Sd) acids. PC3 has not so strong loadings with a negative Vanillyl acid (Vd) and a positive Syringyl ketone (Sn) (Figure 4.2A).

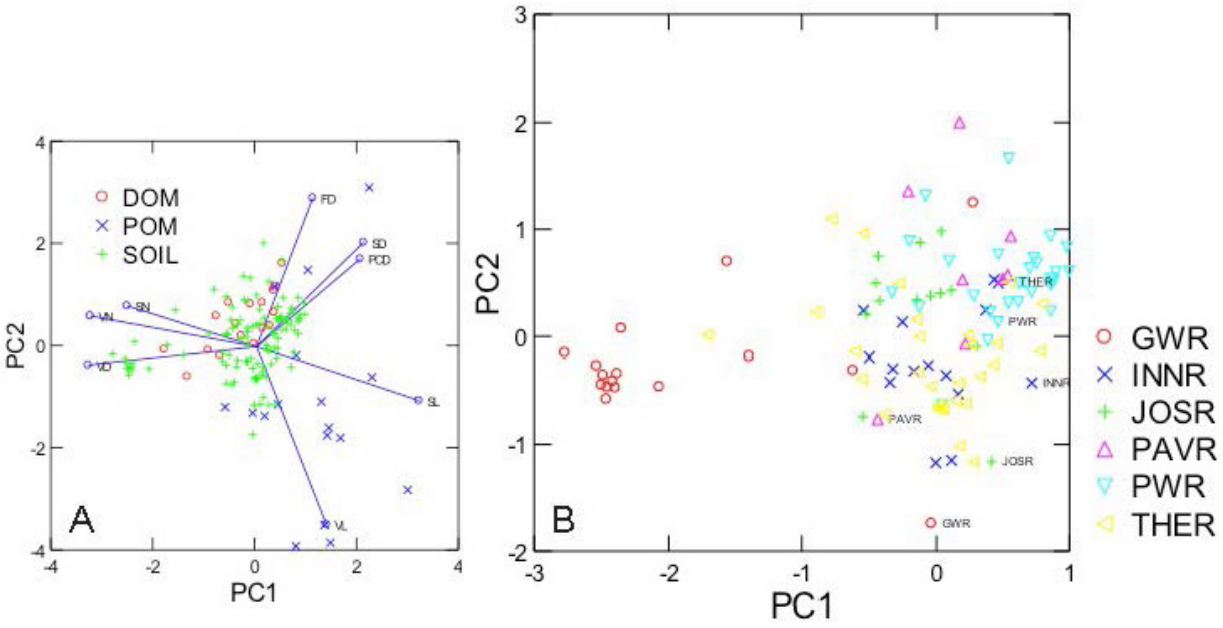

Figure 4.1: PCA analysis on DOM, POM and permafrost soils using lignin reaction products (phenols). Lignin phenols expressed as % of total lignin (∧8). PC1 explains 39% of variance, PC2 explains 23% (Total variance explained 62%). Labelled samples represent the surface layer of each soil.

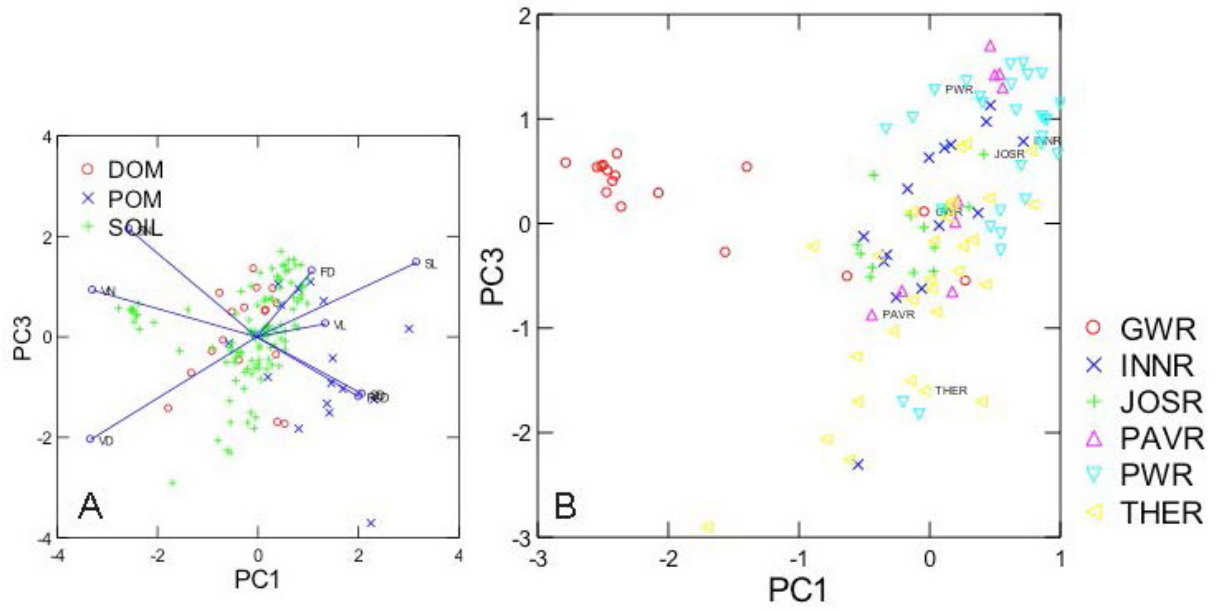

Figure 4.2: PCA analysis on DOM, POM and permafrost soils using lignin reaction products (phenols). Lignin phenols expressed as % of total lignin (V8). PC1 explains 39% of variance, PC3 explains 13% (Total variance explained 52%). Labelled samples represent the surface layer of each soil.

4.3.1 Lignin composition between DOM and POM

Some of the variance in PC1 and PC2 relates to the sample matrix (Figure 4.1A). From the PCA analysis we can see that the DOM and the permafrost soils have similar scores on both PC1 and PC2 but both matrices have significantly lower scores on PC1 and higher scores on PC2 compared to POM (ANOVA, $p<0.05$). The lower scores on PC1 and higher scores on PC2 for DOM and soil reflect much lower Syringyl and Vanillyl aldehydes (Sl and Vl) in these matrices compared to POM. POM has higher proportions of aldehydes (both Sl and Vl) and if we compare this to [Ad/Al] ratios we see that POM has significantly lower [Ad/Al]v ($p<0.001$) and [Ad/Al]s ($p=0.039$). This suggests that POM is less degraded comparatively to DOM and permafrost soils, which have more Vanillyl acids (Vd) and a higher [Ad/Al]v ratio. This further indicates the important differences between POC and DOC fluxes and their sources in terms of environmental controls and drainage basin characteristics. POC fluxes, consisting of unconsolidated materials, undergo mechanical weathering and erosion based on lithology and basin drainage as opposed to DOC fluxes which are more influenced by chemical weathering, vegetation cover and the carbon content of soils (Syvitski and Millman, 2007; Ludwig et al., 1996).

The relationship between DOM and permafrost soils is apparent in the lignin composition as is reflected by the PCA analysis. They have more Vanillyl acids and ketones (Vd, Vn) and more Syringyl ketones (Sn) compared to POM. DOM and soil are more influenced by Vd than is POM, as shown by PC1 and PC3 (Figure 4.2A). POM, unlike DOM and SOM, is more influenced by Syringyl (Sd) and Cinnamyl (PCd) acids. PCA analysis shows the linkages between DOM and SOM in permafrost with increased

Vanillyl acids (Vd) contributing to the higher [Ad/Al]v ratios resulting in more degraded material compared to POM. This may also indicate a solubilization effect from plant litter to leachate associated with an increase in [Ad/Al]v ratios. Similarities in lignin composition between DOM and permafrost soils and their differences to POM make the study of riverine OM an important part of connecting permafrost degradation and hydrological changes to the OC sources in HB.

4.3.2 Lignin composition reflects variation among permafrost soils

While DOM and permafrost soils are not significantly different in terms of lignin composition, the permafrost soils are much more variable and seem to be pulled apart from the DOM especially in terms of PC1 scores (Figure 4.1A, 4.2A). Permafrost soils are mainly dominated by Syringyl aldehydes (Sl) resulting in a strong positive loading in PC1 with the top layer of soil being fresh with higher Vanillyl aldehydes (Vl) compared to acids (Figure 4.1B, 4.2B). The remaining samples have highly variable lignin phenol compositions except for the Great Whale. The Great Whale has relatively low PC1 scores in the deeper horizons of the soil profile below 9 cm caused by a downward shift in the C/V ratio (i.e., more woody) with more Vanillyl acids and ketones (Vd, Vn) in deeper horizons. This supports the low S/V and C/V ratios of the Great Whale soil, which had the strongest influence from gymnosperm and woody sources of all six HB soils. The Little Whale, along with some of the Povungnituk and Thlewiaza samples, have more Syringyl and Cinnamyl acids (Fd, Sd, PCd, Figure 4.1B) compared to the other soils and when coupled with their high [Ad/Al] ratios (Chapter 3, Figure 3.2), further confirms that these samples are more degraded than the other soils of this

study.

Soils appear to be discriminated in PC3, especially the Thlewiaza and the Little Whale, due to the strong positive loadings of Sl and negative loadings of Vd (Figure 4.2B). These soils have highly variable S/V ratios (Figure 3.2, Chapter 3), indicating a lower Sl and/or higher Vd compared to other samples in the profile. These soils also had the highest [Ad/Al] ratios with highly degraded soil layers coinciding with the lowest S/V and C/V ratios. The high Vd and low Sl of these degraded samples indicate that preferential degradation or sorption of Syringyl aldehydes is most likely affecting the ratios. The Little Whale soil is the most degraded sample indicative of high [Ad/Al] ratios, especially at the 37-39 cm and 49-51 cm depths, which plausibly derive from previously exposed surface layers to decomposition. Alternatively, these layers could be hydraulic conduits where the transport of moisture promotes microbial decomposition (Feng et al., 2013). In fact the Thlewiaza has the second highest degraded soil sample at 38-39 cm depth, coupled with lower than average S/V ratios, that suggests a similar decomposition is occurring.

4.4 CONCLUSIONS

For the first time, we have examined rivers and soils distributed widely in the HB for lignin products, total organic carbon and ^{14}C age. This region is unique in its latitudinal span, which encompasses ecosystems from prairies to northern boreal to tundra making it important to create a baseline and to monitor changes in terms of OC sources from vegetation and permafrost degradation. Already, permafrost is thawing and hydrology is changing, both due to the cryospheric changes and due to human

interventions (i.e., dams and reservoirs for hydropower). We have verified the differences in terms of OC and lignin concentrations between the dissolved and particulate phase of 17 HBRs, concluding that the dissolved phase dominates in terms of OC and lignin contributions (93%), is more degraded with higher [Ad/Al] ratios, and is well correlated in terms of latitude and the vegetative sources of OC shown by S/V and C/V ratios. Our findings also show that the five southwest HBRs are the dominant source of OC (89%), especially the Nelson River that contributes high volumes of DOC into the HB annually.

Organic carbon, and in particular, organic biomarkers, have a better potential to identify changes within the Hudson Bay OC cycle than does water flow by itself. The composition of DOM (lignin content, S/V and C/V ratios, ^{14}C ages) in HBRs provides evidence of the sources of this OC, which then permits an evaluation of vulnerability to change in the cryosophere due to warming and anthropogenic influences. PCA analysis has confirmed how lignin phenol composition of DOM and permafrost soils are closely related in terms of vegetative sources compared to POM. Both permafrost soils and DOM reflect the vegetation of their drainage basins, although only DOM is highly correlated to latitude, as is shown by S/V and C/V ratios. Our southernmost location, the Great Whale, is influenced by boreal forest vegetation, as is indicated by its low S/V and C/V ratios in both the soil and DOM, and is an excellent example of how to gauge future vegetative change in the southern HB region.

In summary, this study has been able to address our main objectives and confirm that there are major differences in terms of the quantities and composition of OC and lignin in both the dissolved and particulate phases of HBRs, and within the different soils

sampled in this study. We have also verified the importance of permafrost soils as OC sources, especially the organic cryosols, that have the potential to release as much as 1.5 g OC/m^2 for every cm increase in AL thickness. The transport or burial of OC within the Hudson Bay Drainage Basin is complex as has been shown by the [Ad/Al] ratios showing there are multiple processes at work and interpreting lignin biomarkers may require more understanding of degradation processes within the soil as well as in transport through HBRs. The variations of lignin reaction products and their ratios among HBRs and soils confirm that the use of lignin biomarkers and ^{14}C ages will help in the determination of not only the sources of OC entering the HB but also the processes involved in the release and mobilization of OC in the Hudson Bay terrestrial marine interface.

4.4.1 Future Studies

This study has only begun to address the complexity of organic carbon stored in permafrost of the Hudson Bay Drainage Basin, and links it with OC transported by rivers and sequestered in HB sediments. A continued analysis of the HBRs would be effective in monitoring change in Hudson Bay especially if sampling occurred before, during, and after freshet to reflect seasonality and it may be beneficial to study HBRs impacted by hydroelectric development separately. Using the PARTNERS sampling parameters found in other lignin analytical studies (Raymond et al, 2007; Holmes et al, 2012; Amon et al, 2012), the future study of the HB region would result in more long term and accurate comparisons between these Arctic basins. Radiocarbon dating of both DOM and POM samples in future studies may reveal more information by using ages and

[Ad/Al] ratios to reflect the terrestrial OC sources whether they are from recent vegetation or due to degradation of ancient plant material preserved in permafrost. Lastly, as the climate changes, the monitoring of changes of riverine and permafrost lignin composition will be a useful tool when trying to model the complex HB environment as changes occur in biodiversity, hydrology and permafrost degradation.

4.5 REFERENCES

Aiken, G.R., Spencer, R.G.M., Striegl, R. G., Schuster, P. F., and Raymond, P. A., 2014. Influences of glacier melt and permafrost thaw on the age of dissolved organic carbon in the Yukon River basin. *Global Biogeochemical Cycles* **28**: 525–537. doi:10.1002/2013GB004764.

Amon, R.M.W., Rinehart, A.J., Duan, S., Louchouarn, P., Prokushkin, A., Guggenberger, G., Bauch, D., Stedmon, C., Raymond, P. A., Holmes, R.M., McClelland, J. W., Peterson, B.J., Walker, S.A., Zhulidov, A.V., 2012. Dissolved organic matter sources in large Arctic rivers. *Geochimica et Cosmochimica Acta* 94: 217-237.

Benner, R., Benitez-Nelson, B., Kaiser, K., and Amon, R.M.W., 2004. Export of young terrigenous dissolved organic carbon from rivers to the Arctic Ocean. *Geophysical Research Letters* **31**: L05305. doi:10.1029/2003GL019251.

Carey, S.K., 2003. Dissolved organic carbon fluxes in a discontinuous permafrost subarctic alpine catchment. *Permafrost and Periglacial Processes* **14**: 161–171. doi:10.1002/ppp.444.

Dery, S.J. Stieglitz, M., McKenna, E.C. and Wood, E.F., 2005. Characteristics and trends of river discharge into Hudson, James, and Ungava Bays, 1964-2000. *Journal of Climate* **18**: 2540-2557.

Dery, S.J., Hernandez-Henriquez, M.A., Burford, J.E., and Wood, E.F., 2009. Observational evidence of an intensifying hydrological cycle in northern Canada. *Geophysical Research Letters* **36**: L13402. doi:10.1029/2009GL038852.

Feng, X., Vonk, J.E., van Dongen, B.E., Gustafsson, O., Semiletov, I.P., Dudarev, O.V., Wang, Z., Montluçon, D.B., Wacker, L., and Eglinton, T.I., 2013. Differential mobilization of terrestrial carbon pools in Eurasian Arctic river basins. *PNAS, Proceedings of the National Academy of Sciences*, **110** (35): 14168–14173. doi/10.1073/pnas.1307031110.

Frey, K.E. and McClelland, J.W., 2009. Impacts of permafrost degradation on arctic river biogeochemistry. *Hydrological Processes* **23**: 169–182, doi:10.1002/hyp.7196.

Granskog, M.A., Macdonald, R.W., Mundy, C.-J., and Barber, D.G., 2007. Distribution, characteristics and potential impacts of chromophoric dissolved organic matter (CDOM) in Hudson Strait and Hudson Bay, Canada. *Continental Shelf Research* **27**: 2032–2050. doi:10.1016/j.csr.2007.05.001.

Gustafsson, O., vanDongen, B.E., Vonk, J.E., Dudarev, O.V., and Semiletov, I.P., 2011. Widespread release of old carbon across Siberian Arctic echoed by its large rivers. *Biogeosciences* 8: 1737-1743. doi:10.5194/bg-8-1737-2011.

Hernes, P.J., Robinson, A.C., and Aufdenkampe, A.K. 2007. Fractionation of lignin during leaching and sorption and implications for organic matter 'freshness." *Geophysical Research Letters* **34**: L17401, doi:10.1029/2007GL031017.

Holmes, R.M., McClelland, J.W., Peterson, B.J., Tank, S.E., Bulygina, E., Eglinton, T.I., Gordeev, V.V., Gurtovaya, T.Y., Raymond, P.A., Repeta, D.J., Staples, R., Striegl, R.G., Zhulidov, A.V., and Zimov, S.A., 2012. Seasonal and annual fluxes of nutrients and organic matter from large rivers to the Arctic Ocean and surrounding seas. *Estuaries and Coasts* **35**: 369-382. doi: 10.1007/s12237-011-9386-6.

Kuzyk, Z.A., Goni, M.A., Stern, G.A. and Macdonald, R.W., 2008. Sources, pathways and sinks of particulate organic matter in Hudson Bay: Evidence from lignin distributions. *Marine Chemistry* **112**: 215-229. doi:10.1016/j.marchem.2008.08.001.

Kawahigashi, M., Kaiser, K., Kalbitz, K., Rodionov, A., and Guggenberger, G., 2004. Dissolved organic matter in small streams along a gradient from discontinuous to continuous permafrost. *Global Change Biology* **10**: 1576–1586. doi: 10.1111/j.1365-2486.2004.00827.x.

Lobbes, J.M., Fitznar, H.P. and Kattner, G., 2000. Biogeochemical characteristics of dissolved and particulate organic matter in Russian rivers entering the Arctic Ocean. *Geochimica et Cosmochimica Acta* **64** (17): 2973–2983.

Ludwig, W., Probst, J-L., and Kempe, S., 1996. Predicting the oceanic input of organic carbon by continental erosion. *Global Biogeochemical Cycles* **10** (1): 23-41. doi: 10.1029/95GB02925.

Margesin, R., 2009. *Permafrost Soils*. Volume 16, Springer, Berlin. doi:10.1007/978-3-540-69371-0. 322 pp.

McClelland, J.W., Holmes, R.M., Peterson, B.J., and Stieglitz, M., 2004. Increasing river discharge in the Eurasian Arctic: Consideration of dams, permafrost thaw, and fires as potential agents of change. *Journal of Geophysical Research* **109**: D18102. doi:10.1029/2004JD004583.

Mundy, C.-J., Gosselin, M., Starr, M., and Michel, C., 2010. Riverine export and the effects of circulation on dissolved organic carbon in the Hudson Bay system, Canada. *Limnology and Oceanography* **55** (1): 315-323.

Parham, L.C., Prokushkin, A.S., Pokrovsky, O.S., Titov, S.V., Grekova, E., Shirokova, L.S., and McDowell, W.H., 2013. Permafrost and fire as regulators of stream chemistry in basins of the Central Siberian Plateau. *Biogeochemistry* **116** (1-3): 55-68. doi: 10.1007/s10533-013-9922-5.

Petrone, K.C., Jones, J.B., Hinzman, L.D., and Boone, R.D., 2006. Seasonal export of carbon, nitrogen, and major solutes from Alaskan catchments with

discontinuous permafrost. *Journal of Geophysical Research* **111**: G02020. doi:10.1029/2005JG000055.

Prinsenberg, S.J., Loucks, R.H., Smith, R.E., and Trites, R.W., 1987. Hudson Bay and Ungava Bay runoff cycles for the period 1963 to 1983. *Canadian Technical Report of Hydrography and Ocean Sciences*, No. **92**. Physical and Chemical Sciences Branch. Department of Fisheries and Oceans.

Raymond, P.A., McClelland, J.W., Holmes, R.M., Zhulidov, A.V., Mull, K., Peterson, B.J., Striegl, R.G., Aiken, G.R. and Gurtovaya, T.Y., 2007. Flux and age of dissolved organic carbon exported to the Arctic Ocean: A carbon isotopic study of the five largest arctic rivers. *Global Biogeochemical Cycles* **21**: GB4011, doi:10.1029/2007GB002934.

Syvitski, J.P.M., and Milliman, J.D., 2007. Geology, Geography, and Humans Battle for Dominance over the Delivery of Fluvial Sediment to the Coastal Ocean. *The Journal of Geology* **115**: 1-19.

Vonk, J. E., Sanchez-Garcıa, L., Semiletov, I., Dudarev, O., Eglinton,T., Andersson,A., and Gustafsson,O, 2010. Molecular and radiocarbon constraints on sources and degradation of terrestrial organic carbon along the Kolyma paleoriver transect, East Siberian Sea. *Biogeosciences* **7**: 3153–3166. doi:10.5194/bg-7-3153-2010.

Woods, G.C., Simpson, M.J., Pautler, B.G., Lamoureux, S.F., Lafreniere, M.J., and Simpson, A.J., 2011. Evidence for the enhanced lability of dissolved organic matter following permafrost slope disturbance in the Canadian High Arctic. *Geochimica et Cosmochimica Acta* **75**: 7226–7241. doi:10.1016/j.gca.2011.08.013.